BIO-INSPIRED DESIGN FOR ROBUST POWER SYSTEMS

A Thesis

by

VARUNESWARA REDDY PANYAM

Submitted to the Office of Graduate and Professional Studies of
Texas A&M University
in partial fulfillment of the requirements for the degree of

MASTER OF SCIENCE

Chair of Committee,	Astrid Layton
Committee Members,	Katherine Davis
	Richard Malak
Head of Department,	Andreas A. Polycarpou

December 2019

Major Subject: Mechanical Engineering

ABSTRACT

This thesis deals with redesigning power grids from the ground up to improve their robustness and resilience to various kinds of disturbances. An innovative biologically inspired approach is proposed to achieve this goal. The modern world is highly dependent on an uninterrupted electric power supply, yet extreme weather events and deliberate attacks continue to disrupt power systems. Inherently robust ecological networks present a rich source of robust design guidelines for modern power grids. Analyses of ecosystem networks in literature suggest that this robustness is a consequence of a unique preference for redundant pathways over efficient ones. The structural similarity between these two system-types is exploited here through the application of ecological properties and analysis techniques to long-term power grid design. The level of biological similarity between these two system-types is quantitatively investigated and compared by computing ecological network metrics for a set of synthetic power systems and food webs. The comparison substantiates the use of the ecological robustness metric for optimizing the design of power grid networks. A bio-inspired optimization model is implemented, which restructures the synthetic power systems to mimic ecosystem robustness. The bio-inspired optimal networks are evaluated using N-1, N-2, and N-3 contingency analyses to assess system performance under the loss of 1, 2, and 3 components respectively. The bio-inspired grids all experienced significantly fewer violations in each loss scenario compared to traditional configurations, further supporting the application of the ecological robustness metric for measuring power system robustness. The results provide insights into how ecological robustness and other metrics used in ecosystem analysis can guide the design of power systems for improved infrastructural resilience to better survive disturbances.

DEDICATION

To my mother

ACKNOWLEDGMENTS

I would like to thank my parents, especially my mother for always being there for me. She gives me all my strength and new perspectives needed to sustain as a researcher. I would like to thank Dr. Astrid Layton for mentoring me during my Masters. I would like to thank Hao Huang and Bogdan Pinte for their help with modeling and optimizing power systems in PowerWorld simulator. I would also like to thank Dr. Katherine Davis for helping me with the electrical part of this project.

CONTRIBUTORS AND FUNDING SOURCES

Contributors

This work was supported by a thesis committee consisting of Professors Astrid Layton and Richard Malak of the J. Mike Walker ’66 Department of Mechanical Engineering and Professor Katherine Davis of the Department of Electrical and Computer Engineering.

The data analyzed for Chapter 5 was provided by Professors Astrid Layton and Katherine Davis. The analyses depicted in Chapter 5 were conducted in part by Hao Huang of the Department of Electrical and Computer Engineering.

All other work conducted for the thesis was completed by the student independently.

Funding Sources

My research was supported by startup funds of Dr. Astrid Layton and a seed grant from Texas A&M Energy Institute.

NOMENCLATURE

λ_{max}	Cyclicity
AMI	Average mutual information
ac	Alternating current
ASC	Ascendency
B5	5-bus power grid
B6	6-bus power grid
B7	7-bus power grid
B9	9-bus power grid
B10	10-bus power grid
B14	14-bus power grid
C	Connectance
DC	Development capacity
dc	Direct current
ENA	Ecological network analysis
FCI	Finn cycling index
FW	Food web
H	Shannon index
L	Number of links
L_D	Linkage density
LA	Network modeled with physical links as actors
LE	Network modeled with physical links as edges
MW	Megawatt

N	Number of actors
P_R	Prey to predator ratio
R	Ecological robustness
TSTp	Total system throughput

TABLE OF CONTENTS

Page

LIST OF FIGURES

FIGURE Page

LIST OF TABLES

TABLE Page

1. INTRODUCTION

1.1 Motivation

The U.S. power grid supplies approximately 3,800 terawatt-hours of energy from over 7,000 power plants per year, with over 19,000 individual generators supplying power to almost 160 million consumers [1]. This electric power is the primary source of energy for most sectors of the U.S. economy including crucial ones such as transportation and health care. The widespread dependence of the nation on electricity requires a robust and resilient power grid design that reduces interruptions and quickly recovers from disturbances [12, 13]. Moreover, increases in extreme weather events and malicious attacks from physical and cyber domains have caused millions of power interruption hours in the U.S. in recent years [1] as shown in Figure 1.1. The disturbances to the grid often lead to power outages that can last minutes to weeks, with major blackouts incurring losses of billions of dollars for both power providers and users, sometimes even causing loss of life [14].

The significant cost of power interruptions has resulted in a surge of research on the behavior and management of grids under failure [15, 16, 17, 18, 19]. Transmission networks make up thousands of miles of grid infrastructure and require a large portion of the total grid investments. Disturbances in transmission networks can lead to blackouts [20], so innovative and updated transmission network design is an essential requirement to improve the robustness and resilience of power systems. The transmission network infrastructure also needs renovation and expansion due to reasons like aging components, increasing capacity requirements, and other operational considerations. However, design of the transmission network is not given as much attention as operational enhancements due to high costs and limitations imposed by industrial standards and government policies [21, 22, 23, 24]. Accordingly, the focus of this work is on long-term robust design of power transmission networks using innovative design inspiration from the naturally robust organization of biological food webs (FWs).

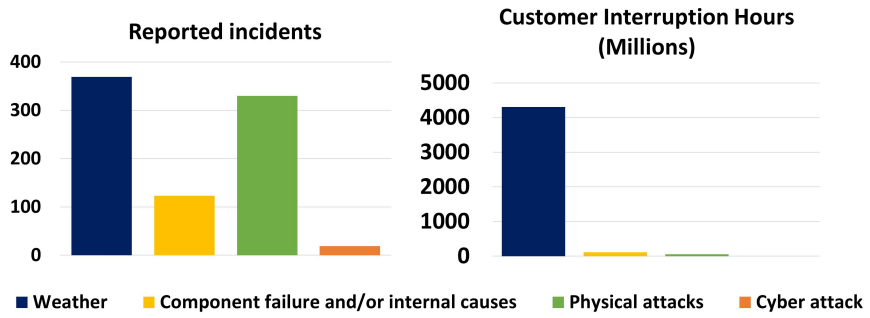

Figure 1.1: Number of power outages and total interrupted customer hours in millions (Data from the Quadrennial Energy Review 2015 report by the US Department of Energy [1]. In the US, extreme weather events, component failures, physical attacks, and cyber attacks were the largest contributors to power outages from 2011-2014. Original figure published in Panyam et al. [2]

1.1.1 Bio-inspired human networks

Similar to how extreme weather events and deliberate attacks can disrupt power system operation, extreme weather events and other variations can disrupt biological ecosystems. In the worst cases, disturbances can cause one or more species to perish, and these effects can cascade, causing the entire system to collapse. Biological ecosystems have structured themselves over millions of years to withstand and survive such disruptions, a characteristic that has inspired the analysis and redesign of structurally analogous industrial networks. A comprehensive analysis of a data set of food webs revealed that FWs maintain a slightly higher redundancy than efficiency in their energy/material interactions [25, 11] to achieve robust structure. $Ecosystem\ robustness$ is defined as the ability of the system to sustain disturbances and continue functioning. This characteristic of food webs is beneficial for power systems as well.

The success of bio-inspired design observed through improvements in human networks, such as industrial resource networks and water distribution networks, motivates the investigation of the analogy between food webs and power systems. As with these other systems, power systems are structurally and functionally analogous to food webs in that they both function to satisfy the requirements of consumers (or predators) and are comprised of components (or species) that process and exchange energy and/or material, as illustrated in Figure 1.2. Both system-types need to con-

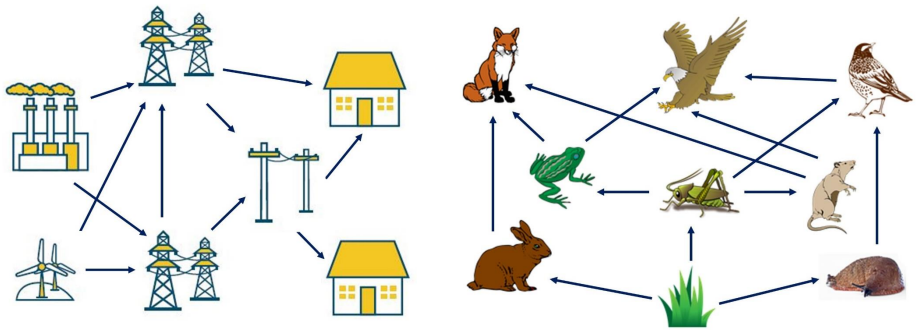

Figure 1.2: A simple illustration of the structurally similar generic topologies of a power grid (left) and a food web (right). Original figure published in Panyam et al. [2]

tinue to function even with negative impacts of disturbances. The ascendency model, a type of ecological network analysis that emphasizes the role of structure and flow organization of the network on its functioning [26], is highly applicable to power systems analysis and design because the structural organization of power systems can have significant ramifications on their robustness and resilience [27, 28].

1.2 Research questions and goals

The overarching goal of this work is to answer the following research question and meet the following research goal:

Research Question: Can ecosystems suggest design changes that improve the robustness of power grids?

Research Goal: Improve the robustness of power grids through the application of ecosystem structure and function to their design.

1.2.1 Secondary research questions and goals

The primary research goal is achieved through a number of smaller questions and goals.

1.2.1.1 Secondary research question 1

Can power grids be modeled as ecosystems?

The following research goals are proposed to address this research question:

- **Research goal 1a)** Generate a food web model that is applicable to power grids.

1.2.1.2 Secondary research question 2

What changes are seen in power grids when we mimic ecosystem structure?

- **Research goal 2a)** Understand the structural and operational changes in power systems brought by mimicking ecosystem structures.

1.2.1.3 Secondary research question 3

Can ecosystem robustness be used as an objective to improve the robustness of power systems against disturbances?

- **Research goal 3a)** Understand the ecological metric "robustness" from an engineering perspective.

- **Research goal 3b)** Establish a relationship between ecological robustness and power system performance.

1.2.1.4 Secondary research question 4

Can ecosystems suggest design changes specifically for newer bi-directional power grid setups to better realize their potential?

- **Research goal 4a)** Identify ecosystem features that mimic and analyze bi-direction network characteristics.

1.3 Contributions

This thesis results in new knowledge of bio-inspired design of power systems and is the first comprehensive development in design and analysis of power grid networks using biological practices and principles. This thesis can be used a guide to further develop guidelines on how ecosystems can aid in designing more robust and resilient power systems.

1.3.1 Primary research contributions

- **A comprehensive understanding of the structural and organizational similarities and differences between food webs and power systems.**

  Evaluating ecological robustness requires the calculation of a number of other ecological flow metrics. This suite of metrics provides a new way to analyze and assess the effectiveness of power systems in multiple aspects. Although the focus of this work is on the robustness of power systems, future work can be extended to include other ecological metrics that have been applied to other types of human systems.

- **A novel optimization approach to improve the ecological robustness of power grid networks**

  Once the ecological robustness of original configurations of the power systems is evaluated, the goal is to try and increase those values to get them as close to food webs as possible. The optimization approach developed as a part of this work modifies power grid configurations to take them closer to food webs.

1.3.2 Secondary research contributions

- **New perspectives on how robustness and resilience of power systems can be analyzed and improved**

  Prior research on power system robustness and resilience has mostly been limited to case-based analyses, where a single system is analyzed and suggestions are provided to strengthen it. The bio-inspired approach presented here is novel and innovative in that it focuses exclusively on the role of *flow path organization* for pre-planning any general transmission network to survive disturbances. This method enables power grid networks to use the robust organization of ecosystems as a benchmark. The process of the bio-inspired method proposed here lends itself well to compare and contrast it with various previously proposed resilience strategies.

1.4 Methodology

The proposed research goals are achieved by performing the following research tasks.

1.4.1 Research goal 1

- **Research goal 1a)** Generate a food web model that is applicable to power grids.

1.4.2 Research task 1

- **Research task 1a)** Create a framework to generate ecosystem models of power grids.
- **Research task 1b)** Identify any limitations of the frame work
- **Research task 1c)** Identify potential solutions to overcome the identified limitations.

1.4.3 Research goal 2

- **Research goal 2a)** Understand the structural and operational changes in power systems brought by mimicking ecosystem structures.

1.4.4 Research task 2

- **Research task 2a)** Collect a data set of food webs and power grids that enable their structures and flows to be fairly compared and contrasted.
- **Research task 2b)** Analyze the level of biological similarity between food webs and power grids using ecological metrics.

1.4.5 Research goal 3

- **Research goal 3a)** Understand the ecological metric "robustness" from an engineering perspective.
- **Research goal 3b)** Establish a relationship between ecological robustness and power system performance.

1.4.6 Research task 3

- **Research task 3a)** Develop an engineering-based understanding of ecological robustness using thermodynamic power cycles.
- **Research task 3b)** Analyze the current level of biological similarity between food webs and power grids using the metric "ecological robustness".
- **Research task 3c)** Based on the results of research task 3b, design an optimization approach to create biologically similar power grids.
- **Research task 3d)** Validate the results of the bio-inspired optimization of 3c using a traditional N-X contingency analysis.

1.4.7 Research goal 4

- **Research goal 4a)** Identify ecosystem features that mimic and analyze bi-direction network characteristics.

1.4.8 Research task 4

- **Research task 4a)** Collect a dataset of power grids with distributed generation and evaluate ecological cycling metrics to identify the current level of cyclic pathways in bi-directional grids.
- **Research task 4b)** Validate the biological similar findings of bi-directional grids using a traditional N-X contingency analysis.

1.5 Thesis layout

This dissertation covers the different aspects of the design and analysis of power grid networks using ecological network analysis principles. Following this introduction, a thorough literature review covers the current state of power grid enhancements and bio-inspired human networks. The literature review shows that there is no prior research analogizing power systems and natural

ecosystems. The third chapter covers the general ENA methodology and the description of structural and flow metrics used. Fourth chapter In the fifth chapter, the level of biological similarity between ecosystems and traditional setup of power systems is first discussed, following which an innovative two-step optimization approach to improve the ecological robustness of power systems is presented. The optimized power systems are then validated using N-X contingency analyses to gauge their capability to survive contingencies. Potential ways to overcome the limitations of using analogy between ecosystems and power systems are presented in the sixth chapter. Seventh chapter covers the potential use of ecosystem cycling metrics to quantify bi-directional characteristics of grids with distributed generation. Finally, the thesis is concluded with a summary of the work done and the findings. Proposed future work stemming from the findings is also presented in the final chapter.

2. LITERATURE REVIEW

2.1 Sustainability of systems

Sustainability of a system can be defined as its ability to maintain function in the present and future, despite fluctuations in inputs, demand, and the surroundings [29]. Many considerations go into defining sustainability of systems, including their social, economic, and environmental aspects [30, 31, 32]. Robustness is an important aspect of sustainability in systems as it can enhance the ability of a system to function effectively under different kinds of disturbances [31, 33]. Designing for robustness is a common goal across many disciplines that deal with systems, for example design theory and methodology. Metrics like Taguchi's signal to noise ratio offer design guidance for dealing with unwanted input variations, the introduction of the signal to noise ratio advanced the way performance was balanced with qualities such as robustness in system designs. Over the years fields such as quality engineering and statistics have spurred variations to Taguchi's methods, as well as other approaches that have lead to improvements in the robustness of systems and products [34, 35]. These approaches are based on optimizing the effect of operational parameters on the performance measures of a system. Currently, there are no standard system level measures of robustness and sustainability for human networks that take into account both the topology and flow organization [6, 36, 4, 2]. Robustness for ecosystems on the other hand is well defined with a detailed quantitative formulation that considers both those attributes [25, 37, 38, 39].

2.2 ENA and its application to human networks

Biological food webs have evolved over millions of years to manage and survive extreme events. These networks have already inspired the redesign of several organizationally analogous human networks: carpet manufacturing networks, water distribution networks, and industrial networks all saw reduced environmental impacts and cost when redesigned to mimic the characteristic structure of food webs [40, 11, 41, 42, 43, 44]. A detailed analysis reveals that the quantitative metric $ecosystem\ robustness$ of a dataset of food webs is maximized through a slightly higher

preference for flexibility and redundancy over efficiency in interactions [11].

$Ecological\ network\ analysis$ (ENA) is a generic term used by ecologists that refers to a collection of tools and techniques to study and quantify the structure and functioning of biological food webs [45, 46, 47, 48, 49]. ENA has been widely used by researchers to analyze various types of networks: Layton *et al.* [41] reported reduced environmental impacts and costs for a carpet manufacturing network and improved energy usage for a set of eco-industrial parks [42, 43] when re-designed after food webs. Bailey *et al.* [50] used ecological input-output modeling to re-design industrial systems with improved environmental impacts. Bodini *et al.* [44] applied ENA to a water network in an Italian city, suggesting modifications to improve sustainability. Kharrazi *et al.* [51, 40] used ecological techniques to define sustainability and resilience of economic and global commodity trade networks. Malone *et al.* [52] used ENA to analyze material flows in the Chinese steel industry since the 1980's and were able to conclude that it was moving in a sustainable direction using ENA. ENA has been used in energy $related$ research for modeling urban energy consumption in Chinese cities [53, 54] and a virtual water network running parallel to Chinese power grid (the focus was on the water network and not the power grid) [55]. The energy-water nexus in China has also been investigated using ENA [56, 57, 58]. However, ENA has not been used to analyze and design the electric power transmission grid.

The literature review on these bio-inspired network analyses and designs suggests that ecosystems may be a rich source of inspiration for improving power grid design as well in a way that has not previously been explored.

2.3 Thermodynamic principles and sustainability

Thermodynamic efficiency represents the efficiency with which the total available energy is used [59]. This definition relates thermodynamic efficiency to sustainability and as a result there have been many studies connecting thermodynamic principles with sustainability [30, 33, 60, 61]. Most of these works however, focus on *qualitative* analyses, with an exception of [61], which quantitatively investigated the ENA structural metric cyclicity using thermodynamic power cycles. The work correlates changes in thermodynamic efficiency to changes in the ecological metric

cyclicity for a group of thermodynamic systems. Their results suggested that increases in thermal efficiency, indicating efficiency improvements in the use of input energy, correlated with higher cyclicity values, a characteristic of biological ecosystems. Cyclicity increases can thus be understood to quantify improvements in how a system uses the materials and energy available. The bio-inspired design of human networks for sustainability has since that work been further developed to use more complex flow-based metrics from ENA as described in the previous section. As a result, there is a need for these flow-based metrics, including robustness, to be investigated and understood in a similar manner.

2.4 Power grid transmission network robustness and resilience

Goals for power systems are often described in terms of their reliability and resilience. Each characteristic represents different aspects of the state and functioning of the system. Achieving these characteristics in new designs can benefit from a multidisciplinary perspective as power grids are complex cyber-physical systems. Various metrics [62, 63, 64, 28, 27, 65] have been proposed to quantify reliability and resilience of power systems, but a $standard$ does not exist, making system comparisons difficult. Modern power systems are generally reliable enough to sustain credible threats, but may not be resilient to major disturbances [66]. Resilient solutions have focused largely on reactive measures, such as enhancing operational resilience, ignoring preventive measures like infrastructural reorganization to improve infrastructure resilience. Panteli *et al.* [67] proposed an algorithm to isolate vulnerable components in power systems and split the network into self-adequate islands to avoid cascading outages during extreme weather emergencies. Li *et al.* [68] proposed networked microgrids' operation during extreme events to enhance resilience. A hierarchical outage management with multi-microgrids for enhancing power system resilience against unexpected disaster events is proposed in [69]. A two-stage stochastic programming approach to the optimal scheduling of a resilient micro-grid against uncertainties is presented in [70]. Davarikia *et al.* [71] established a tri-level defender-attacker-operator interdiction problem to define vulnerability indices and proposed a set of hardening strategies to mitigate the worst-case damages, based on the vulnerabilities. Several techniques have also been proposed to model the cyber-physical

architecture for power systems [72, 73, 74] to provide security assessments for increasing their operational resilience and reliability [75, 76]. These methods provide situational awareness for operators helping them prepare preventive solutions ahead against unexpected events in both cyber and physical domains. While such operational practices and situational awareness measures for power systems are important, they alone may not be sufficient to improve overall resilience. They must be complemented by infrastructural enhancements to maximally enhance the overall resilience. However, few works have looked at defining infrastructural resilience. Panteli *et al.* [77, 78] proposed a set of metrics, collectively named as "$FLEP$," to quantify the operational and infrastructural resilience of power systems against extreme weather, which relies on fragility of each component during extreme contingency.

Robustness for power systems has been defined mostly based on topology. Ellens *et al.* [79] introduce a metric for effective topological resistance based on electrical circuit analysis principles to assess general network robustness to disturbances. The authors do not however explicitly apply the metric to power system models. Koç *et al.* [80] propose an entropy-based metric to quantify the robustness of power grids by calculating each electrical node's robustness and significance under cascading failures. Zhang *et al.* [81] introduce three metrics, the percentage of unserved nodes (PUN), the percentage of non-critical links (PNL), and the node-generator distance (DG) to assess power system robustness. Tu *et al.* [82] then utilize these metrics to optimize power grid network design. Azzolin *et al.* [83] identified a baseline combination of topological factors, including transmission line redundancy and generator layout, to protect power systems against cascading failures. These papers all primarily focus on using component criticality to quantitatively measure grid robustness and security against cascading failures. This method of quantification suffers from a lack of benchmarked standards to guide network modifications and improvements. The bio-inspired approach proposed in this thesis is highly novel in that it focuses exclusively on the role of *flow path organization* for pre-planning transmission networks to survive disturbances. Literature review on robustness of power systems suggests that this grid characteristic is important to current efforts working towards grid resilience.

It can be concluded from the literature review that the definitions of reliability, resilience and robustness in the context of power systems lack clear distinction due to some conceptual overlap. Furthermore, there are no studies that quantitatively investigate the overlap between reliability, robustness and resilience. Resilience is taken here to be the ability of the system to gracefully degrade its function and quickly recover once perturbations cease [84]. Power grid robustness is taken as referred to in [63], the ability of the system to maintain function when exposed to perturbations. Resilience has some dependence on the system structure in the pre-planning stages and therefore infrastructural robustness can be considered a vital feature of a resilient network [27]. This thesis explores that utility of ecological robustness as a generic metric to measure power grid robustness and its quantitative relationship with traditional grid reliability standards to contribute toward improving grid resilience.

2.5 Sustainability of power systems

Sustainability in the context of power systems is not concretely defined, even though it is a priority for grid design and maintenance. Broadly speaking, sustainability for power systems can be defined as their ability to survive and sustain in the long term with changing consumer needs and generation technologies [1, 85, 86]. The following factors are identified as critical to enhancing the sustainability of power systems [1, 87]:

- Power source (renewable energy vs fossil fuel)
- Structural longevity of grid components
- Resilience of the grid to disturbances
- The efficiency of generation and transmission
- Profitability for the service providers
- Environmental impact of grid components

Grid evolution has seen the addition of components that help continuously monitor loads, balance generation and usage, and improve reliability and resilience. These changes are referred to

as "Grid Modernization" [87]. Despite these many improvements, reliability and resilience is still an active area of research for power systems [87]. The U.S. has suffered from several wide-spread blackouts in the past, examples include: the New York City blackout of 1977 (a cost of $1.2 billion in 2017 dollars); the Northeast blackout of 2003 (losses estimated at $ 6 billion) [88] and East coast power outages due to Hurricane Sandy in 2012 (costs estimated at $ 80 billion) [89]. Grid component failures can lead to cascading failures across the grid while natural disasters can knock down lines and components resulting in grid overloads.

The most sustainable grid scenarios include a high use of renewables and nuclear power along with high network resilience [86]. The increasing affordability of renewable power sources has resulted in strong increases in their prevalence [90]. This increase has not yet replaced traditional fossil fuel based power plants, which have a strong negative impact on the environment [91], however it's growth is formative: annual US electricity generation from solar and wind energy increased by a factor of 11 from 2006 to 2016 [90].

2.5.1 Cyclic organization in power systems with distributed generation vs ecosystems

Renewable energy systems installed at consumer locations (for example, solar panels on a home or commercial roofs), allow consumers (also referred to as loads) to use their own power and sell back extra. This two-way exchange of power between the grid and the consumer is known as net-metering. Customer participation in net-metering is becoming more popular every year [3] as seen in Figure 2.1 and public electric utilities in the U.S. are required to offer net metering when requested [92]. These small scale power generating units are known as distributed generation (DG) systems [93] and are changing grid operation. As a result of consumer sell back, the traditionally linear grid is evolving into a complex network with circular pathways reminiscent of the cyclic organization found in ecosystems.

Organisms in a food web are classified as prey and predators (producers and consumers) and the complex interplay between them leads to high amount of cycling [94]. Past research indicates that food webs have evolved to have a highly cyclic organization [95, 96, 97, 98] that results in the efficient use of available resources [99, 100, 101]. Structural cycling in these natural systems

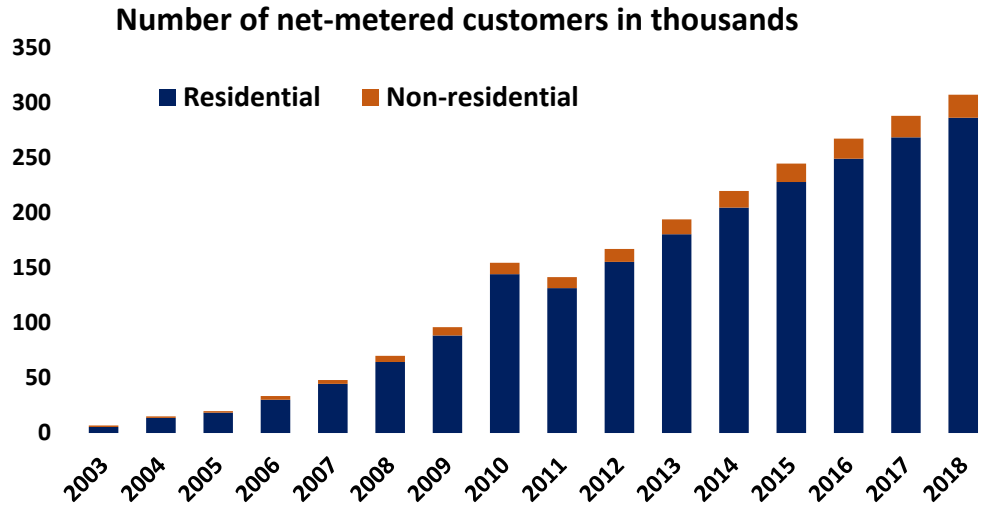

Figure 2.1: The number of net-metered customers in the U.S. Data until 2010 from [3] and a linear forecast suggests a further increase through 2018. Original figure published in [4]

exists primarily due to detritus, waste generated by actors, creating feedback from actors that are traditionally only consumers [98]. Paths that connect actors indirectly (actors that are separated by one or more actor) are another inherent feature of highly cyclical food web networks. Indirect pathways have been found to dominate direct ones, resulting in cycles that impact network stability [102, 103, 104]. Similarly complex indirect pathways exist in power systems, industrial networks, economic networks and other human resource networks. This has inspired studies to look for relationships between ecosystem-like cycling, efficiency, and robustness in industrial and economic resource networks [42, 105, 106] as well as thermodynamic cycles [61]. Improving cycling to promote the efficient re-use of waste and consequently reduce environmental impact has been extensively examined by Layton et al. [41, 43]. Their results show that cyclic design of industrial networks results in economically and environmentally superior networks compared to traditional, less cyclic, design goals. Modern power systems may thus benefit from Nature's rich repertoire of both cyclic and robust organization.

2.6 Limitations of using ecosystem analogy for human systems

Fath $et\ al.$ [45] underscored that there is no single "correct" way to construct an ecosystem network model for food webs. Ecologists have modeled ecosystems as highly aggregated food webs, where even small similarities warranted grouping, all the way down to well articulated food webs, where every individual animal is documented separately [107]. This presents a potential problem as shortcomings of using ecological analogies without proper adjustments have been well discussed in literature: Hesse [108] discussed common issues associated with using analogies between different fields back in the 1970s highlighting the need for proper justification of analogies. Wells [109] pointed out that different interpretations of ecological metaphors for man-made systems can result in different implications for their intended use, a point reiterated by Ehrenfeld[110]. Husar [111] found that ecosystem models of human activities gave little regard to the physical transfer of matter, that is believed to be critical in human activities. Chertow [112] discussed the challenges associated with geographic locations and distances between industries in defining industrial ecosystems. Thus, in the absence of guidelines for the construction of an ecosystem model, literature asserts that sufficient care needs to be taken to understand the needs of the power grid network models while also ensuring that energy exchanges and transfers are accurately accounted.

3. ECOLOGICAL NETWORK ANALYSIS

3.1 Introduction

Ecological network analysis (ENA) is a generic term used by ecologists that refers to a collection of tools and techniques to study and quantify the structure and functioning of biological food webs [45, 46, 47, 48, 49]. The food web and flow matrices are the bases for the structural and flow-based ENA analyses respectively. The matrices and the metrics presented in this chapter are used multiple times in the subsequent chapters. The readers are encouraged to come back to this chapter when ambiguity arises about the origin and formulation of any matrix and/or metric.

3.2 Flow and food web matrices

The flow matrix [**T**] is a square (N+3) x (N+3) matrix, where *N* is the number of actors inside the system boundary, containing the magnitudes of all energy exchanges in the network [113]. The "extra" three entries of the flow matrix represent the system inputs, useful exports and dissipation. The entries in [**T**] are notated as T_{ij} and represent the flow magnitude from node i to node j, or from rows (producers) to columns (consumers). Non-zero values in this matrix represent an interaction, and zeros indicate no interaction. The first column and the last two rows of the flow matrix [**T**], as well as the last two columns of the first row, are permanently zero as these are impossible interactions: the system inputs cannot output, and the system outputs cannot input. The creation of a flow matrix for a hypothetical ecosystem is illustrated in Figure 3.1: the system boundaries and actors are defined, a digraph of 3 nodes is created, and finally a 6 x 6 flow matrix is constructed.

The food web matrix [**F**] is a N x N matrix filled with ones and zeros, where a one represents an interaction and a zero no interaction [4]. [**F**] indicates the presence and direction of the inter-compartmental flows in [**T**]. An element F_{ij} is equal to 1 if there is a flow from i to j and 0 otherwise. The creation of a food web matrix from a corresponding flow matrix is shown in Fig. 3.2.

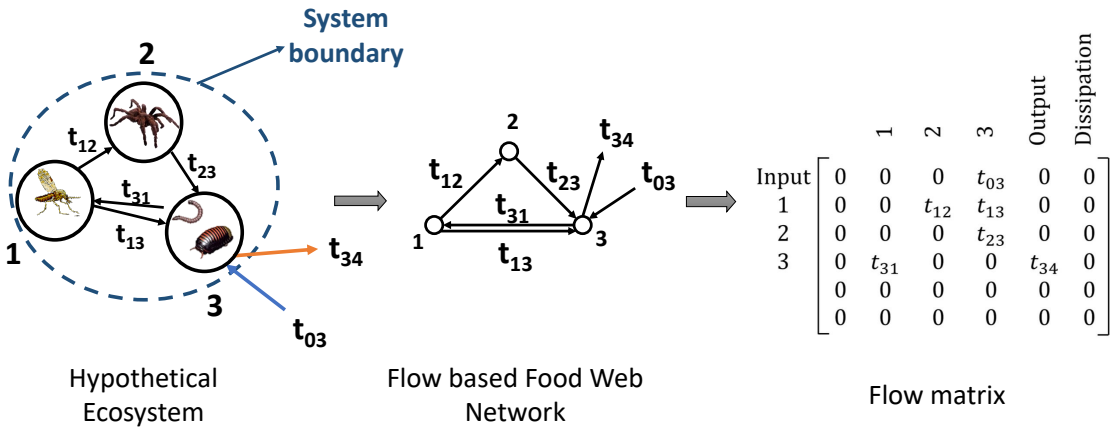

Figure 3.1: The conversion of a hypothetical ecosystem into a digraph and a flow matrix. Original figure published in Panyam et al. [2]

3.3 ENA-structure

Structural ENA has been widely performed on various food webs and industrial networks [43]. The structural metrics: linkage density (L_d), connectance (C) and prey to predator ratio (P_R) are used in this work and are defined below. They are calculated using the food web matrix [F].

Both linkage density and connectance measure complexity in food webs in terms of the number of actors and their links [114]. Prey to predator ratio indicates the relative abundance of actors that provide with respect to those that receive.

3.3.1 Number of actors (N)

The total number of actors or components in the network, equal to the number of rows/columns in [**F**] [99].

3.3.2 Number of links (L)

The total number of connections between any two actors/components in the network, equal to the number of non-zero elements in [**F**] [99].

3.3.3 Linkage density ($\mathbf{L_D}$)

Linkage density is the ratio of number of links to the number of actors in the network [99].

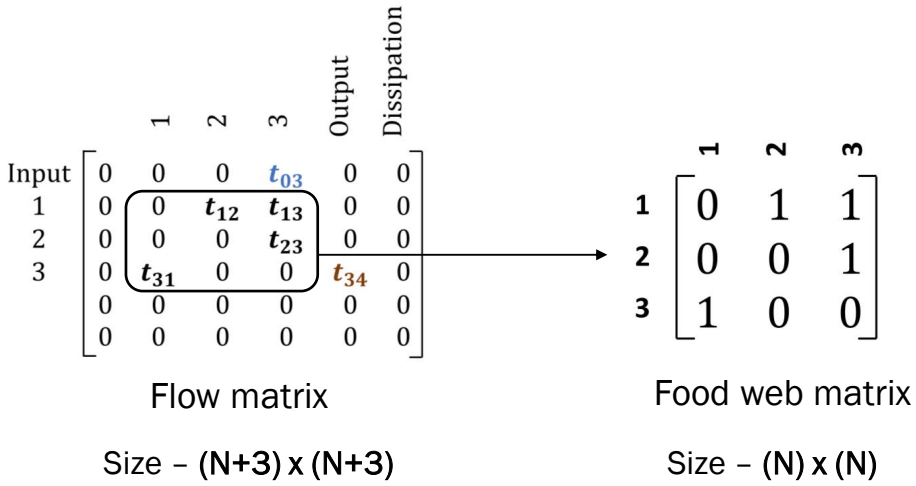

Figure 3.2: The conversion of a flow matrix to food web matrix

$$L_D = \frac{L}{N} \tag{3.1}$$

3.3.4 Connectance (C)

Connectance is the ratio of number of links to the total number of possible connections in the network including cannibalism (equal to N^2).

$$C = \frac{L}{N^2} \tag{3.2}$$

3.3.5 Prey to predator ratio ($\mathbf{P_R}$)

The ratio of number of prey to predators in the network [99]. A component is classified as prey if it sends energy/water to at least one other component and predator if it receives from at least one other component. Components that send and receive energy/water are classified as both prey and predators. Very small or very large values of P_R for a network imply that it is heavily relying on relatively less number of suppliers or receivers respectively, which could reduce robustness levels [115].

$$P_R = \frac{N_{prey}}{N_{predator}} \tag{3.3}$$

3.4 ENA-flow

The ecologists Ulanowicz *et al.* [25] present an information theory perspective to describe long term robust behavior in ecosystems, that results in the origination of the metric "Robustness". Robustness here is a function of two opposing but complementary attributes: unutilized capacity in the system and the system's effective performance. What follows is a brief summary of different flow magnitude dependent metrics used by Ulanowicz *et al.* to formulate ecological robustness.

3.4.1 Surprisal (s)

The formulation of ecosystem robustness is based on the concept of **surprisal**, which is similar to "information" as defined by Shannon [116] and "entropy" as defined by Boltzmann [25]. The surprisal of an event i is the measure of its absence and eq. (3.4) is used as a basis for other metrics presented.

$$s = -log(p) \tag{3.4}$$

where s is surprisal of an event that has probability p of occurrence

3.4.2 Shannon index (H)

Surprisal can be applied to describe the **Shannon Index** (also called indeterminacy) of an event *i* (h_i) as the product of the presence of an event p_i and its surprisal s:

$$h_i = -p_i \times log(p_i) \tag{3.5}$$

The Shannon Index measures the potential for change with respect to an event i, where event i (part of a system) must both be likely enough to occur ($p_i >> 0$) and unlikely enough ($s_i >> 0$), such that it can affect the system functioning ($h_i >> 0$). When an event is almost certainly present

($p_i \approx 1$) or absent ($p_i \approx 0$) there is no indeterminacy.

Low probability events possess a high potential for change but do not occur frequently enough to do so, while high probability events possess a low potential for change because they occur often and therefore the system is accustomed to them [44]. Thus a system's Shannon Index relates to its capacity to withstand change with respect to the set of events in the system:

$$H = \sum_i h_i = -1 \sum_i (p_i \times log(p_i)) \tag{3.6}$$

3.4.3 Total system throughput (TSTp)

While i and j are general events described above, the focus here is on events that are *flows* or *transfers*. This allows the probabilities above to be estimated by the frequencies of occurrence of transfers. Thus, i is now the event of a unit of flow leaving component i, j is the event of a unit of flow entering component j, and T_{ij} equals the units of flow moving from i to j. The probabilities p_{ij} and flows T_{ij} are thus related as follows,

$$p_{ij} = T_{ij}/TSTp \tag{3.7}$$

where system size, measured by the total units of energy circulated, is called the **total system throughput** (*TSTp*):

$$TSTp = \sum_{i=1}^{N+3} \sum_{j=1}^{N+3} T_{ij} \tag{3.8}$$

TSTp is computed by summing all directed transactions in the network, or elements in the flow matrix [**T**] [26].

3.4.4 Development capacity (DC)

The **development capacity** (DC) is the maximum amount of aggregated uncertainty that a network can have, or Shannon Index H scaled by system size $TSTp$ [117],

$$DC = -TSTp \times \sum_{i=1}^{N+3} \sum_{j=1}^{N+3} H_{ij} \tag{3.9}$$

where H_{ij} (3.10) is Shannon Index calculated from flows:

$$H_{ij} = \frac{T_{ij}}{TSTp} \times log\Big(\frac{T_{ij}}{TSTp}\Big) \tag{3.10}$$

3.4.5 Average mutual information (*AMI*)

The **average mutual information** (AMI), also called average mutual constraint X, was presented by Rutledge et al. [118] and updated by Ulanowicz [119]. AMI measures how much the actual surprisal s_{ij} of the joint event ij differs from the maximal surprisal s^*_{ij} that would arise if the two events were independent.

For events i and j, the mutual constraint is defined as follows,

$$\begin{aligned} x_{ij} &= s^*_{ij} - s_{ij} \\ &= [-k \times log(p_i \times p_j)] - [-k \times log(p_{ij})] \\ &= k \times log\left(\frac{p_{ij}}{p_i \times p_j}\right) \end{aligned} \tag{3.11}$$

where x is greatest when actual surprisal is lowest, so it is also called *order*.

The initial measure of uncertainty (H, in (3.10)) can be reduced by updating it with the knowledge of source and end nodes for each actual flow, resulting in the new uncertainty H':

$$H'_{ij} = \frac{T_{ij}}{TSTp} \times log\left(\frac{T_{ij} \times TSTp}{\sum_{m=1}^{N+3} T_{im} \times \sum_{n=1}^{N+3} T_{nj}}\right) \tag{3.12}$$

AMI of a network contains the aggregate amount of uncertainty accompanying each flow, updated with the knowledge of source and end nodes, multiplied by the probability that the flow occurs in the first place:

$$AMI = -1 \times \sum_{i=1}^{N+3} \sum_{j=1}^{N+3} H'_{ij} \tag{3.13}$$

3.4.6 Ascendency (ASC)

Ascendency (ASC) [119] is the scaled mutual constraint that reflects order or the dependence between events:

$$ASC = TSTp \times AMI \tag{3.14}$$

ASC multiplies AMI by $TSTp$ to give a dimensional version of network uncertainty. A higher ASC for the same size system represents a network that has fewer options for pathways for flows moving from any one actor to another, resulting in a network with a lower level of uncertainty. The limiting case, where each node has only one input and one output and all uncertainty about the source of input for a node has been resolved, results in an ASC equal to DC.

3.4.7 Degree of system order (ASC/DC)

The ratio ASC/DC is called the **Degree of System Order** and represents how efficiently a network is connected. A higher ratio, closer to one means the network is more organized (efficient) and the number of options available to travel between any two nodes have been reduced. The extreme case is a perfectly efficient network; each end point can only be reached by one route (equal to one). A low ratio, closer to zero implies a less efficient but highly redundant network with a large number of connections. The extreme case is completely connected network, where every point is connected to every other point (equal to zero).

3.4.8 Robustness (R)

The ecological metric **robustness** R quantitatively measures the potential of ecosystems to sustain changes and disturbances and is thus related to the long-term survival of a network. *R* is defined as the negative of the product of *ASC/DC* and the natural logarithm of *ASC/DC* as seen in Eq. (3.15) [25]. Previous applications of the ecosystem robustness metric to human networks used

a base two logarithm [11]. Changing the base of the logarithm increases/decreases the steepness of the *R* vs *ASC/DC* curve. Users need only ensure that all compared data sets use the same base. Base e is chosen here as it is currently the standard practice in ecology [46]. The negative sign ensures that *R* will be a positive value. A value of *ASC/DC* of zero or one gives a robustness of zero. Biological ecosystems have an *ASC/DC* value clustering around 0.367 or $(1/e)$ [25] known as the "window of vitality", the maximum value signifying a preference for redundancy over efficiency.

$$R = -1 \times \left(\frac{ASC}{DC}\right) \times ln\left(\frac{ASC}{DC}\right) \tag{3.15}$$

4. ECOLOGICAL ROBUSTNESS APPLIED TO THERMODYNAMIC POWER CYCLES

4.1 Introduction

Similar to how ecosystems see an increase in pathway efficiency through maturation, efficiency of thermodynamic cycles can be increased through physical modifications. This provides an opportunity to test the result of well understood network modifications for energy efficiency, on the resultant response of ecosystem metrics. Two basic thermodynamic systems are used here for this purpose: Rankine and Brayton power cycles. These cycles produce power by using energy in the working fluid, water and air respectively, via thermodynamic processes. These transformation and exchange processes are analogous to the prey-predator exchanges in ecosystems. First law efficiency (η_I) measures the net energy output in terms of the total input energy for a thermodynamic system. The relationships between thermodynamic efficiency and four ecological flow metrics, robustness (*R*), *ASC/DC*, *AMI* and *H*, are processed for twenty three Rankine and Brayton cycles (one set of variations was done on the Brayton cycle and two are done for the Rankine cycle). The variations made to the cycles are of increasing complexity and are all done with the goal of increasing η_I. The process is set up to result in the creation of an engineering-based understanding of these ecosystem measures, which can further aid in the bio-inspired design of engineering systems such as power grids and transportation networks.

4.2 Methodology

4.2.1 Thermodynamic power cycles

Seven modifications of the ideal Brayton cycle and fourteen modifications of the ideal Rankine cycle were used in the analysis. These types of cycles are widely used in jet engines (Brayton cycle) and power plants (Rankine cycle). A basic Brayton cycle consists of three components: compressor, combustor and turbine. The compressor draws in air from the atmosphere and compresses it, resulting in an increase in temperature and pressure. The high temperature air is mixed with fuel for combustion and the resulting high temperature gases propel the turbine. Part of the

work output of the turbine is used to power the compressor creating a connection between the two components. A basic Rankine cycle consists of four components: pump, boiler, turbine, and condenser as shown in Fig. 4.1. Water passes through the different components, converting from a liquid state to a vapor state and back. Heat and work are supplied by external sources as required by the boiler and pump respectively. The turbine outputs useful work and any leftover energy in the working fluid is exported in the form of heat by the condenser. Inputs to and outputs from the system are denoted by arrows crossing the boundary (dashed line) in the node diagram of Fig. 4.1. The addition of components such as feed-water heaters (FWHs), reheaters, and intercoolers increases the thermodynamic efficiency of the Rankine and Brayton cycles [120]. These components harness the energy left over in the exhaust gases, usually in the form of waste heat, sending it back to earlier stages in the system where heat is required. These modifications decrease the amount of total heat energy required for system functioning. The source and sink temperatures of each cycle are kept constant across all the variations investigated here to ensure accurate comparisons.

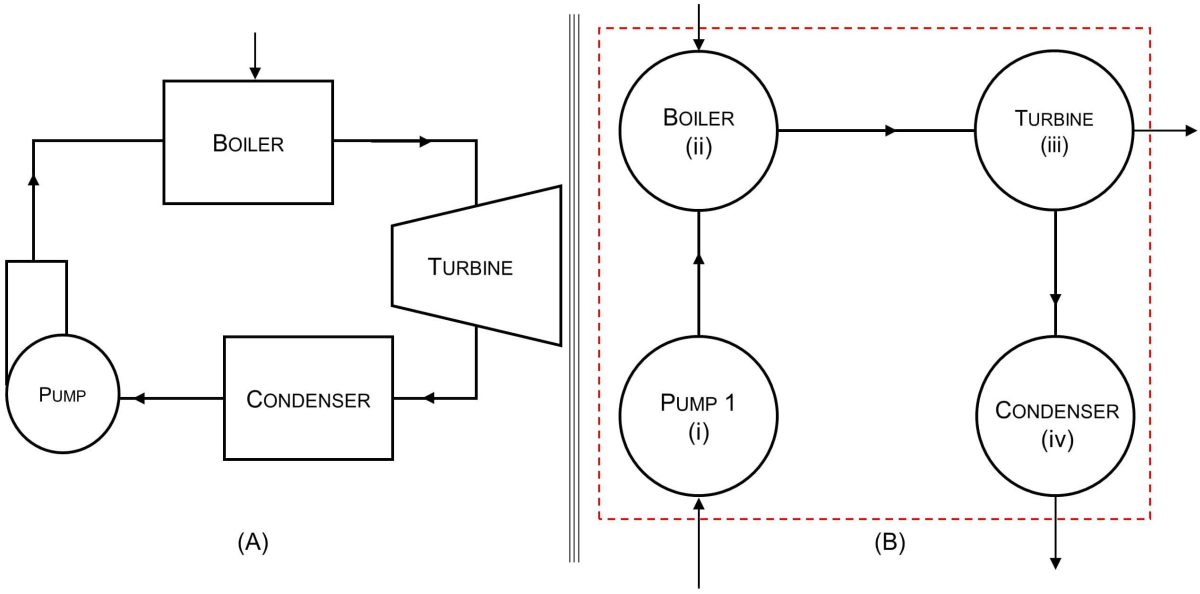

Figure 4.1: (A) An idealized equipment diagram and (B) A node diagram for the simple Rankine cycle. The red dotted square indicates the system boundary.

Rankine cycles - Water	**Brayton cycles - Air**
T_{min}=318.9 K	T_{min}=288.2 K
T_{max}=873.2 K	T_{max}=1273 K
$P_{pump1,input}$=10 kPa	$P_{compressor,input}$=100 kPa
$P_{boiler,input}$=15000 kPa	r_p=10 (pressure ratio)
η_C=0.634	η_C=0.773

Table 4.1: Initial state point data used for the ideal Rankine and Brayton cycles.

The energy exchanges between any two components in the cycle can be calculated using the enthalpy of the working fluid entering and exiting the components. Energy in the form of heat and work input to and output from the system are calculated from Eq. 4.1 - 4.3. The enthalpies, work, and heat for the cycles were calculated using Engineering Equation Solver (EES) version V8.881-3D. State point data for the basic Rankine cycle of Fig. 4.1 is given in Table 4.1. Thermal efficiency calculated using Eq. 4.4 uses the information in Table 4.2. Thermal efficiency is the ratio of total useful output from a cycle to the total energy input (Eq. 4.5). The Carnot efficiency, given by Eq. 4.4 specifies the maximum possible thermal efficiency that can be achieved by a power cycle operating between a given source and sink temperature [120].

$$W_{in,i} = \Big(h_{exit} h_{inlet}\Big)_{compressor,pump} \tag{4.1}$$

$$W_{out,i} = \Big(h_{exit} h_{inlet}\Big)_{turbine} \tag{4.2}$$

$$Q_{in,i} = \Big(h_{exit} h_{inlet}\Big)_{boiler,combustor} \tag{4.3}$$

$$\eta_C = 1 - \frac{T_{min}}{T_{max}} \tag{4.4}$$

$$\eta_I = \frac{\sum_i \left(W_{out,i} + W_{in,i} \right)}{\sum_i \left(Q_{in,i} \right)} \tag{4.5}$$

	T (K)	**h (kJ/kg)**
into (i)	318.9 (Saturated liquid)	191.8
out of (i) and into (ii)	319.5	206.9
out of (ii) and into (iii)	873.2	3582
out of (iii) and into (iv)	318.9 (Saturated vapor)	2114
out of (iv) and into environment	318.9 (Saturated liquid)	191.8

Table 4.2: Energy information (kJ/kg) used to fill in the flow matrix [**T**] for the simple Rankine cycle of Fig. 4.1, calculated using the temperature and pressure information in Table 4.1

.

The ENA of power cycles here considers each component in the thermodynamic cycles an actor. Figure 4.2 shows a flow matrix for the basic Rankine cycle of Fig. 4.1. Energy values (kJ/kg) are from the enthalpy, heat, and work information in Table 4.2.

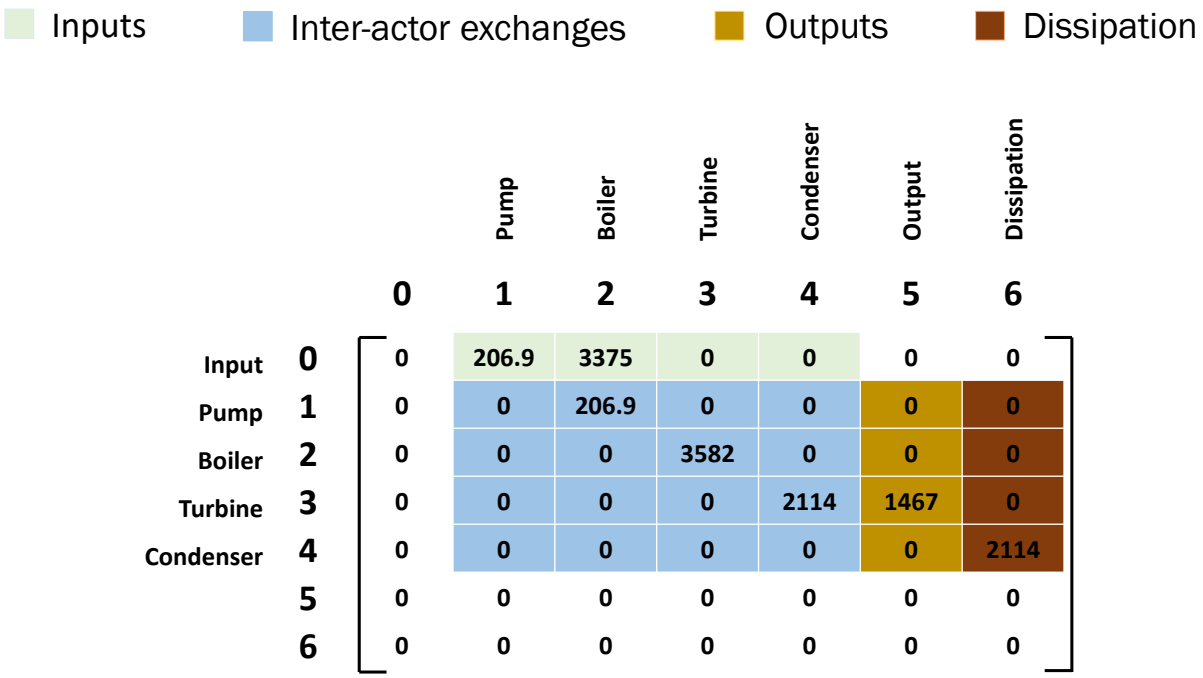

Figure 4.2: Flow matrix [**T**] for the simple Rankine cycle of Fig. 4.1. All the flows are measured in [kJ/kg] of energy. Flow is documented as going from rows to (i) to columns (j). Row 0 is inputs to the system, column 5 contains outputs from the system and column 6 is the dissipation to the outside environment.

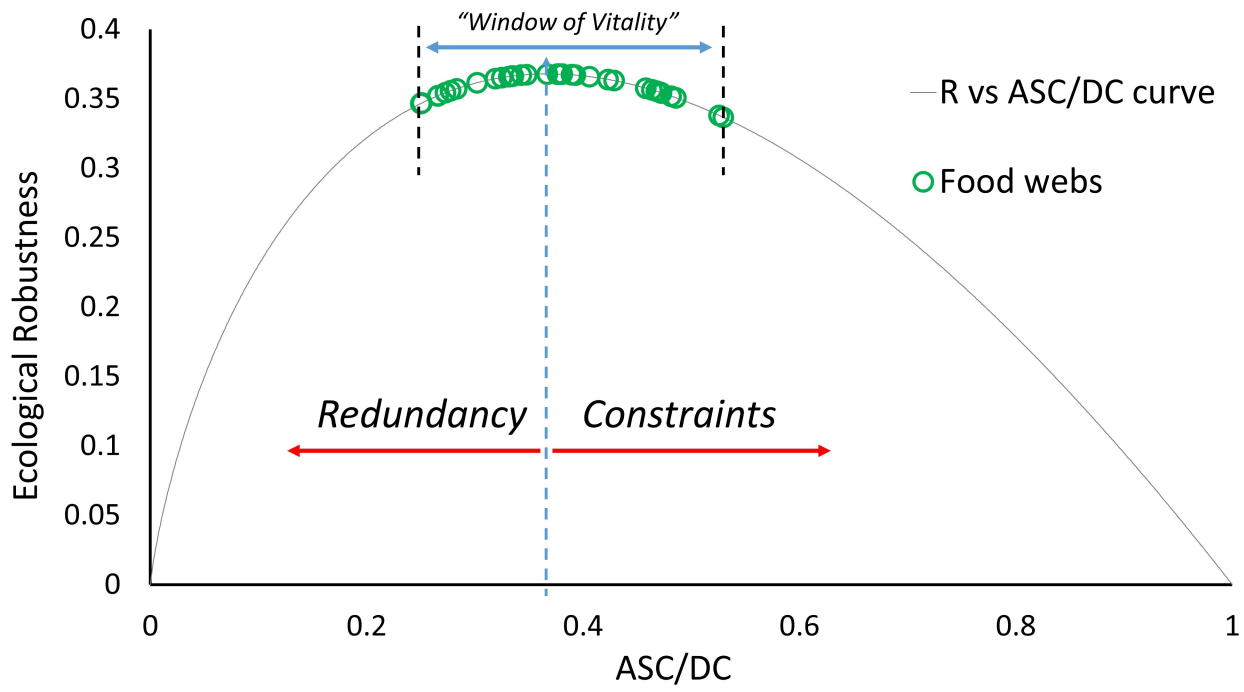

Figure 4.3: Ecological robustness plotted against the ratio *ASC/DC*. Thirty eight food webs taken from the datasets of [5] are plotted on the curve fit, illustrating the "window of vitality" that most ecosystems reside in. The peak of the curve corresponds to a *R* value of 0.368 and an *ASC/DC* value of 0.368. Figure used with permission from [6].

Natural systems have been found by ecologists as having up to 25% redundancy [121]. This redundancy is believed to equip the system with additional flow paths and allows for effective reorganization of the network in the face of disturbances. Redundancy in human networks and systems, however, is usually seen as an inefficiency that increases costs. Redundancy in these systems/networks is usually traded for efficiency and profit maximization by optimizing the network configuration.

Ecological robustness (Eq. 3.15), as described in chapter 3, is the product of the degree of system order (*ASC/DC*) and the negative of its natural logarithm ($ln(ASC/DC)$). Ecologists hypothesize that the network configuration corresponding to the peak of the curve is indicative of Nature having achieved a successful balance between pathway efficiency and redundancy, that

results in a robust and sustainable state [37, 31]. Human networks often experience disturbances analogous to ecosystems: for example, weather changes and variations in supply and demand. The ecological robustness metric is thus potentially very useful to quantify the capacity of human networks - in terms of their organization - to sustain functioning during disruptions.

4.3 Results: Ecological flow based analysis of thermodynamic power cycles

Thermal efficiencies and four flow-based ecosystem metrics: Shannon index (*H*), average mutual information (*AMI*), *ASC/DC*, and ecological robustness (*R*) were evaluated for 23 Brayton and Rankine power cycles. The results are listed in Table 4.3. The modifications on the basic Brayton cycle include the addition of regeneration, intercooling and reheat, creating a total of 8 different Brayton cycles with increasing efficiencies. B represents the basic Brayton cycle and B1 has added regeneration B2 has added intercooling and reheat (resulting in 2 turbines), and B3 is the same as B2 but with 3 turbines. Modifications to the Rankine cycle were similar but were carried out as two sets of variations, creating a total of 15 Rankine cycles: 1) adding an increasing number of open feedwater heaters to the simple Rankine cycle (RO1 adds one open feedwater heater and RO2 adds two) and 2) adding reheat and open feedwater heaters to the simple Rankine cycle (RRO1 adds reheat and one open feedwater heater, RRO2 adds reheat and two open feedwater heaters, etc.). Average values of ecological robustness and *ASC/DC* for 38 food webs from [5] are also listed for comparison in Table 4.3.

Figure 4.4 shows how the ratio ascendency to development capacity (*ASC/DC*) for the thermodynamic cycles varies with increasing thermal efficiency. Figure 4.5 shows ecological robustness (Fig. 4.5) for the thermodynamic power cycles with respect to increasing thermal efficiency. Both Fig. 4.4 and 4.5 show the corresponding linear trend lines. Generally increasing and decreasing trends are seen for *ASC/DC* and *R*, respectively, with increasing efficiencies, with some exceptions. Figure 4.6 shows the relationship between thermal efficiency and AMI. Figure 4.7 depicts the relationship between thermal efficiency and Shannon Index (H). Strictly increasing trends are observed between the ENA metrics and thermal efficiency for these two figures.

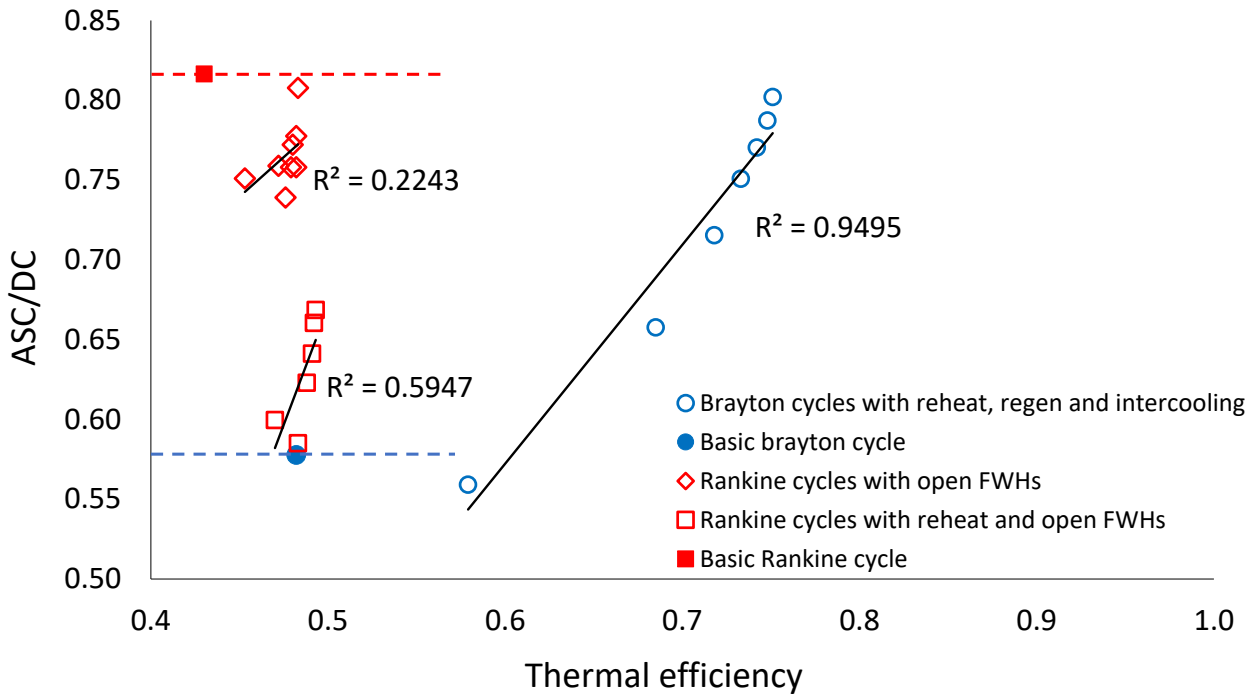

Figure 4.4: Thermal efficiency plotted against the ratio *ASC/DC* for the three sets of thermodynamic cycle improvements. The *ASC/DC* values of the basic Brayton and Rankine cycles are highlighted by the red and blue dotted lines.

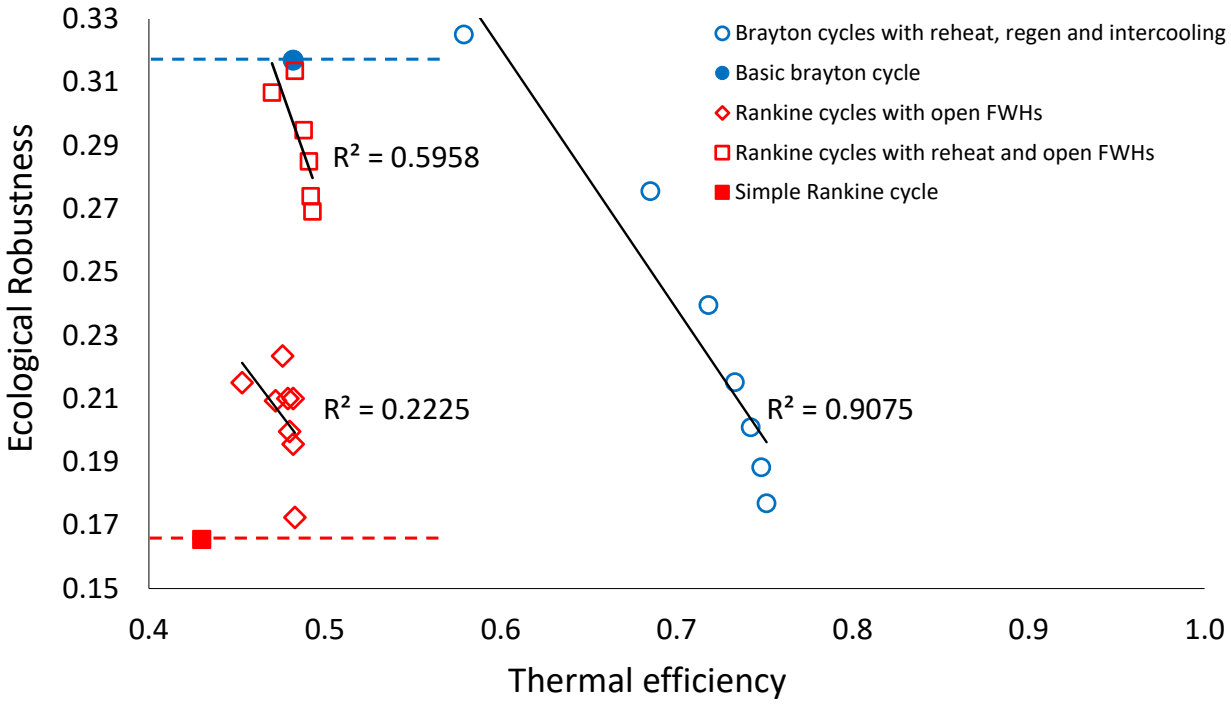

Figure 4.5: Thermal efficiency plotted against ecological robustness for the three sets of thermodynamic cycle improvements. The R values of the basic Brayton and Rankine cycles are highlighted by the red and blue dotted lines.

Cycle	η_I	AMI	H	ASC/DC	R
FWs average	-	1.610	3.880	0.414	0.365
B	0.482	1.495	2.588	0.578	0.317
B1	0.579	1.676	2.999	0.559	0.325
B2	0.685	2.441	3.711	0.658	0.276
B3	0.718	2.957	4.133	0.715	0.240
B4	0.733	3.342	4.450	0.751	0.215
B5	0.742	3.635	4.718	0.770	0.201
B6	0.748	3.886	4.936	0.787	0.188
B7	0.751	4.106	5.120	0.802	0.177
R	0.430	1.968	2.410	0.817	0.166
RO1	0.453	2.164	2.880	0.751	0.251
RO2	0.472	2.367	3.202	0.739	0.223
RO3	0.476	2.574	3.392	0.759	0.209
RO4	0.479	2.742	3.617	0.758	0.210
RO5	0.480	2.929	3.792	0.772	0.200
RO6	0.482	3.032	3.898	0.778	0.196
RO7	0.482	3.195	4.215	0.758	0.210
RO8	0.483	3.414	4.226	0.802	0.172
RRO1	0.470	2.007	3.347	0.600	0.301
RRO2	0.483	2.082	3.558	0.585	0.314
RRO3	0.488	2.288	3.673	0.623	0.295
RRO4	0.491	2.444	3.811	0.641	0.285
RRO5	0.492	2.608	3.949	0.661	0.274
RRO6	0.493	2.691	4.024	0.669	0.269

Table 4.3: The sets of modifications made to each cycle and the corresponding changes in thermal efficiency η_I, average mutual information (*AMI*), the Shannon Index (*H*), the degree of system order (*ASC/DC*), and ecosystem robustness (*R*). B1-7: Gradual addition of regeneration, intercooling and reheat. RO1-8: Gradual addition of open feed-water heaters. RRO1-6: Gradual addition of reheat and open feed-water heaters.

4.4 Discussion

Intended and unintended modifications can both cause system development and evolution. The ability to design human systems results in most connections being very intentional. Unintended linkages can emerge in some systems however, like trade and economic networks, due to extrinsic constraints imposed on the system (e.g. profit maximization and regulations). Most ecosystems evolve due to such externally imposed requirements. The different variations of Rankine and

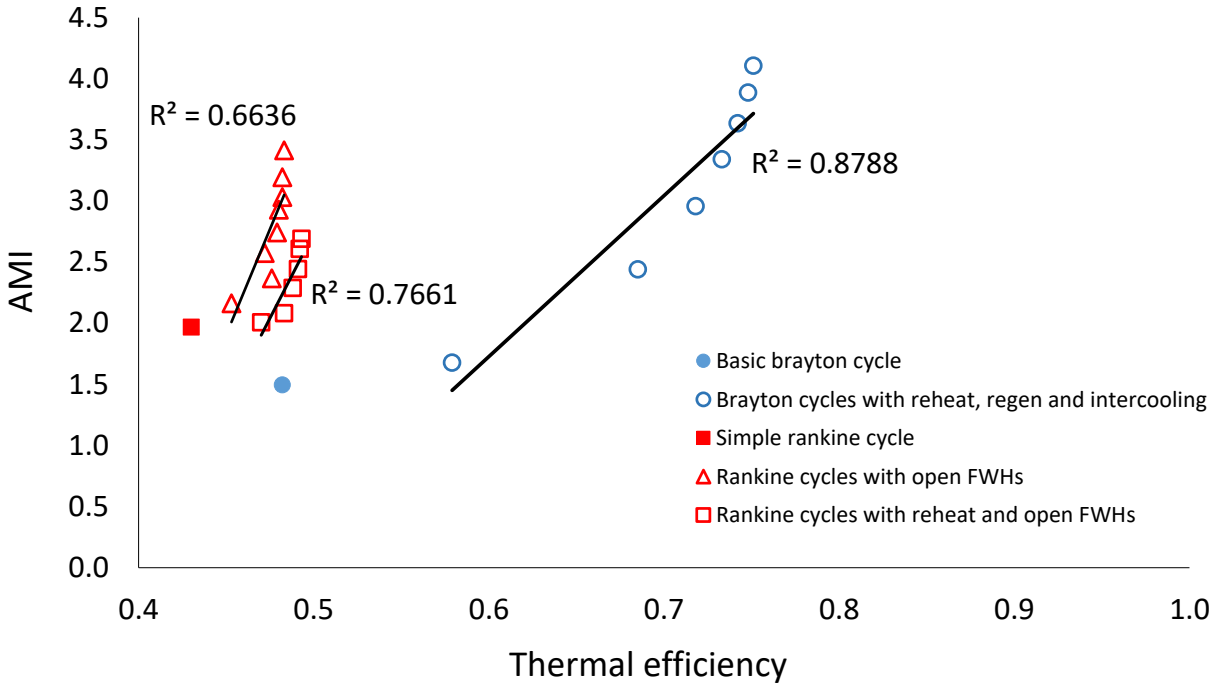

Figure 4.6: Thermal efficiency plotted against average mutual information (*AMI*) for the three sets of thermodynamic cycle improvements.

Brayton cycles analyzed here consist of intended modifications to increase the thermal efficiency. A benefit to the analysis presented here is that these purposeful design changes have clear effects. Although network robustness is not usually considered in the design of these cycles, they provide an opportunity to compare network modifications made to increase work output with the evolution seen in naturally sustainable ecosystems. This would lead to an understanding as to whether maximizing output aids or impedes the development of sustainable human systems through biomimicry.

The discussion focuses on two interesting findings: 1) the relationship of thermal efficiency with ecological pathway efficiency (*ASC/DC*) and robustness and 2) the correlations of thermal efficiency with *AMI* and *H*.

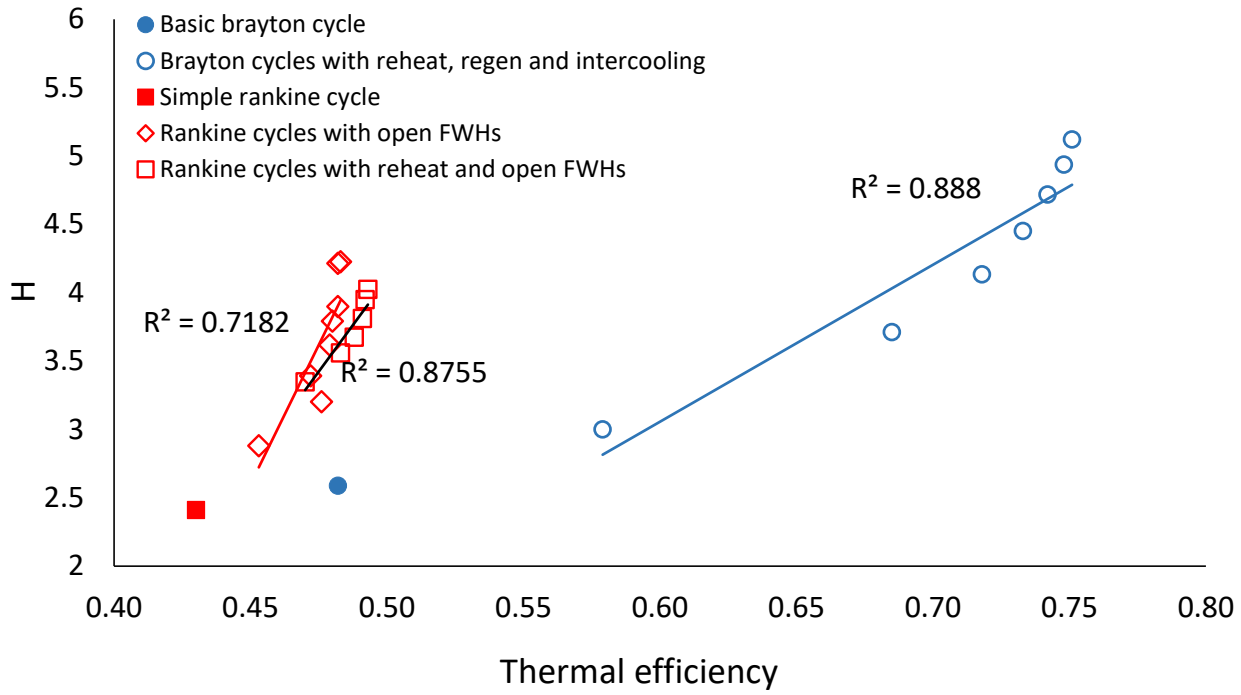

Figure 4.7: Thermal efficiency plotted against Shannon Index (H) for the three sets of thermodynamic cycle improvements.

4.4.1 *ASC/DC* and 1st law efficiency

Efficiency from an engineering perspective measures the useful output generated from a specified input. Ecological efficiency however, measures the efficiency of the network structure in terms of the number of pathways available for any given unit of flow. The design goals of engineered systems are often seen as striving towards a highly organized structure, and as a result one would expect higher *ASC/DC* values. This is not necessarily the case though and is most likely the result of some human systems containing critical components requiring redundant supply pathways that function as backup in cases of system malfunctions. An *ASC/DC* value closer to one indicates a more streamlined network structure with less pathway diversity. Values of *ASC/DC* closer to zero indicate more pathway diversity, or a higher number of pathways available for any given unit of flow. *ASC/DC* values for some human water networks [44] were found to have values further

from one, ranging from 0.48–0.61, which are closer to those found in Nature. A Chesapeake Bay ecosystem was found to have an *ASC/DC* of 0.60 [122] and a South Florida Everglades ecosystem had an *ASC/DC* of 0.55 [123].

The set of 38 food webs used here have an average *ASC/DC* value of 0.414 (first row of Table 4.3). All of the thermodynamic cycles investigated here in contrast have higher values of *ASC/DC*, ranging from 0.57 to 0.81. Despite the conceptual difference between engineering efficiency and ecosystem efficiency, the results comparing *ASC/DC* to η_I in Fig. 4.4 show that for many of the cycles with a high thermal efficiency this also equates to a high pathway efficiency. This comparison suggests that design decisions made to increase η_I in thermodynamic power systems mimic a minimization of pathway diversity, resulting in a system that is significantly more streamlined in structure than what is found on average in ecosystems. This relationship, between engineering efficiency increases and ecological efficiency increases, however is not found to be strictly positive within each set of modifications. The relationship also differs between the two different types of power cycles.

The B1 to B7 Brayton cycles show an increasing trend between ASC/DC and thermal efficiency, as seen in Fig. 4.4. The Brayton cycle B1 has the lowest ASC/DC and B7 has the highest, 0.56 and 0.80 respectively, resulting in a high R^2 value of 0.95 that suggests a strong connection between increases in thermal efficiency and increases in ecological pathway efficiency. The two sets of Rankine cycle variations, with open feedwater heaters and with reheat *and* open feedwater heaters, both show an initial negative relation between ASC/DC and thermal efficiency from the first modification to the second resulting in much lower R^2 values of 0.22 and 0.59 respectively. This corresponds conceptually to the new added components requiring multiple additional pathways as a pattern is set up that increase the ratio between pathways and components. After this first modification though the relationship is positive. This inconsistent trend in the Rankine cycle modifications, one that is not seen for the Brayton cycles, could be due to the relatively small increases in thermal efficiency between the different Rankine cycles. The η_I increases are small when compared to the increases made between the different Brayton cycles. Fig. 4.4 highlights

the small changes in η_I for the Rankine cycles corresponding to larger changes in ASC/DC values. Amongst the two type of modifications made to the Rankine cycles Fig. 4.4 also shows that while both modifications increase the pathway redundancy (which results in changes to ecological robustness as discussed in the next subsection), adding reheat *and* open feed water heaters introduces more redundancy in flow paths than adding only open feed water heaters. The correlations in Fig. 4.4 indicate that improving the energy efficiency of human systems does *not always* result in more streamlined flow paths, but can sometimes lead to redundant flow paths. The responses of the two sets of power cycles show that while that ecological pathway efficiency does not perfectly correlate with engineering/thermal efficiency the two generally increase with each other amongst specific cycle modification sets.

4.4.2 Ecological robustness and 1st law efficiency

Systems with high *ASC/DC* values efficiently use a minimal number of pathways to deliver all the energy/materials needed to their species. These ecosystems however are also vulnerable to disturbances, every pathway is crucial and if lost will result in some consumer need not being met. Systems with low *ASC/DC* values tend to be more resilient to disturbances, with redundant pathways to deliver energy and materials where they are needed. Extreme redundancy however can result in waste and increases in dissipation (longer pathways traveled), and higher costs in human engineered systems. Sustainable ecosystems have been found to cluster around what is known as the "window of vitality" (highlighted in Fig. 4.3), that encompasses the maximum ecological robustness value of $R = 0.367$ or $1/e$) [37, 124, 125]. That ecosystems tend to reside in this window is believed by ecologists to represent a unique balance achieved by Nature between pathway efficiency and redundancy. All the thermodynamic cycles investigated here lie to the right of the window, suggesting that they have a lower robustness compared to ecosystems resulting from relatively high pathway efficiency (higher *ASC/DC* values). Figure 4.5 illustrates the generally negative correlation between *R* and η_I in each of the 3 sets of power cycle modifications (B2–7, RO1–8 and RRO1–6). Once again though this trend is not the rule, at least one variation in both the Rankine and Brayton cycles have higher ecological robustness *as well as* higher thermal

efficiencies than their basic configurations. Figure 4.5 also highlights a significant difference in the ecological robustness values of the basic versions of the Rankine ($R = 0.166$) and the Brayton ($R = 0.317$) power cycles (red and blue dotted lines cutting the vertical axis).

Robustness increases immediately with the first modification for the Brayton cycles. This increase can be attributed to the structural changes that are meant to increase the thermal efficiency adding redundancy that increases the robustness. Adding regeneration to the basic Brayton cycle, (B) to (B1), both the thermal efficiency and ecological robustness increase ($\eta_I = 0.48$ to 0.58 and $R = 0.32$ to 0.33, see Table 4.3). This initial modification increasing both η_I and R is not seen for either of the two Rankine cycle modification sets and can be conceptually explained by looking at how the modification changes the structure of the cycle. The extra component added to the basic Brayton cycle, as seen in Fig. 4.8, does not require *any* additional energy input (the new actor ii - heat exchanger, going from Fig 5.1(b) to 4.8(b)). All the other modifications of the Brayton cycles as well as all of the Rankine cycle variations (B2–7, RO1–8, and RRO1–6) conversely require *additional* energy to run the new components (pumps, compressors, and combustors). These subsequent modifications in both the Rankine and Brayton cycles increase the thermal efficiency but decrease both the pathway redundancy and the ecological robustness.

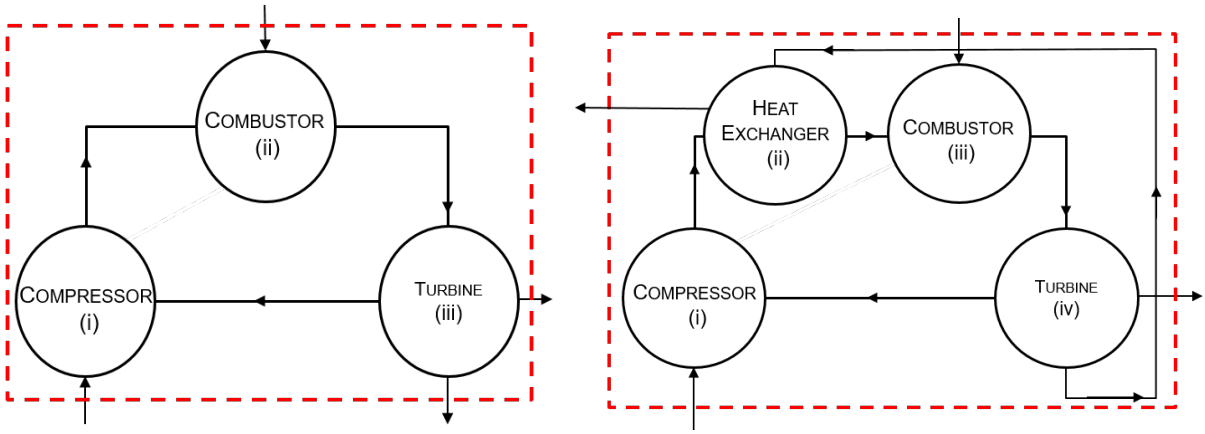

(a) (b)

Figure 4.8: (a) Energy flow diagram for the basic Brayton cycle (B in Table 4.3) and (b) Energy flow diagram for the Brayton cycle with regeneration (B1 in Table 4.3). Energy flows are shown between components and across the system boundaries (denoted by dashed box).

The result shown in Fig. 4.5, while generally negative do show that *it is possible* to make design decisions that *both* increase engineering efficiency *and* robustness. This discovery is especially important for systems that might be vulnerable to disturbances. Rather than achieving energy efficiency through highly streamlined and pathway efficient organization, these systems may be able to achieve their energy efficiency goals without having to loose important redundancy – possibly by mimicking ecosystem structures. The generally negative correlation between thermal efficiency and ecological robustness, which is considered a measure of sustainability for ecosystems, points out the incompatibility between the energy conservation perspective [59, 33, 60] and the network perspective of sustainability. A more holistic and possibly bio-inspired approach that considers both connectivity and energy related aspects may lead to system designs that are able to improve their overall sustainability without sacrificing engineering efficiency.

4.4.3 AMI & Shannon index and 1st law efficiency

Correlating ecological metrics (*AMI* and Shannon Index) that go into defining ecosystem robustness with thermal efficiency revealed more consistent and stronger trends across variations for both Rankine and Brayton cycles.

Shannon Index (*H*) quantifies the total capacity for organization in an ecosystem. Average mutual information (*AMI*) quantifies the realized portion of that organizational capacity [37]. Ecosystems are hypothesized to increase both *AMI* and *H* as they evolve [126]. Thermodynamic power cycles also see an increase in *AMI* and *H* with modifications made to increase thermal efficiency. *AMI* and *H*, the basis for formulating both *R* and *ASC/DC*, were found here to have strong positive correlations with thermal efficiency (Fig. 4.6 and 4.7). Unlike ecosystem robustness (*R*) and its dependent variable *ASC/DC*, the *AMI* and *H* for power cycles were found to strictly increase with increasing thermal efficiency (Fig. 4.6 and 4.7).

The relationship between *AMI* and *H* resembles the relationship between thermal efficiency and Carnot efficiency. Carnot efficiency gives the maximum thermal efficiency that can be achieved by a power cycle operating between a given source and sink temperature. Thermodynamic first law efficiency is the *actual* realized efficiency. Irreversibility, the difference between maximum possible output and the actual output, arises due to entropy generation and prevents the thermal efficiency of these power cycles from ever reaching their Carnot efficiency. Similarly in ecosystems, pathway redundancy prevents *AMI* from ever reaching *H*. One difference however is that, for all the modified power cycles considered here, *H* changes but the Carnot efficiency remains the same as the basic version. This is because *H* depends on the structural potential of the system, which the Carnot efficiency is predetermined by the source and sink temperatures, which are kept constant across the power cycle variations.

The R^2 values for the linear correlations between *AMI* and η_I (Fig. 4.6) are 0.88, 0.66 and 0.76 for the modified B, RO and RRO series, respectively. The R^2 values for the correlation between *H* and η_I (Fig. 4.7) are 0.88, 0.72 and 0.87 for the modified B, RO and RRO series, respectively. Such a strong positive connection between quantitative measurements of ecosystem development and thermodynamic performance improvements suggests that the same fundamental principles may govern the development of both ecosystems and human systems. If further analyses prove this true, it would result in two developments: 1) the study of ecosystems would become normative as opposed to the current descriptive efforts and 2) mimicking the development observed in naturally

sustainable ecosystems in human systems also becomes normative as a result. The first addresses an issue that some ecologists have brought up regarding the existing discordant theories for the study of ecosystems [26, 60]. The second benefits the current efforts in the field of industrial ecology by providing norms for strengthening the analogy between ecological and human systems.

4.5 Conclusions

The ecological flow metrics investigated here (*AMI*, *H*, *ASC/DC* and *R*) quantify pathway efficiency and robustness, describing the network characteristics and evolution of biological ecosystems. The strong correlations between thermal efficiency and the ecological measures *AMI* and *H* suggest that similar fundamental principles may govern the development of ecosystems and human systems. This has the potential to develop the study of natural ecosystems and industrial ecosystems into normative science. The flow metrics studied also suggest potential to provide inherently-sustainable tools for the design of human engineered systems. The application of these ecological metrics to thermodynamic power cycles provided a quantitative engineering-based understanding. Ecological pathway efficiency and thermal efficiency positively correlate among a single set of power cycle modifications, and although increases in thermal efficiency tend to reduce system robustness, the relationship is not a general one. The three types of power cycle modifications have suggested that the possibility of designing systems that have redundancy in their structure without sacrificing engineering efficiency may be realized via bio-inspired system design, resulting in systems that improve both their robustness *and* their energy efficiency. Human systems, such as critical infrastructure networks can experience economic instability, component failures, and climate disturbances and therefore can benefit from mimicking ecosystem robustness levels, preventing efficiency focused design decisions that result in highly streamlined pathways causing the system to be vulnerable to disturbances. The continued application of ecosystem robustness to human systems will provide more insights into developing a holistic approach to assess sustainability of human systems that accounts for both the system form and function, energy conservation and system organization.

5. BIO-INSPIRED DESIGN FOR ROBUST POWER GRID TRANSMISSION NETWORKS[1]

5.1 Introduction

This chapter deals with the application of ENA to power grid transmission networks to improve their robustness and resilience. As outlined in the literature review, establishing a link between ecosystem robustness and redundancy in power grids may offer unique insights into improving both the robustness and resilience of power systems. The primary goal of this application is to present a new perspective for achieving the long term robust design of the grid by *imitating the balance between pathway efficiency and redundancy* observed in naturally sustainable biological ecosystems, contributing toward the goal of making a more robust and resilient grid. A set of five power grids, available in PowerWorld Simulator software [7] are analyzed for a comprehensive understanding of the organizational analogy between power grids and food webs. An optimization model is created which maximizes $ecosystem\ robustness$ (equivalent to imitating food web balance between pathway efficiency and redundancy) while still meeting all power balance constraints for the five power grids.

5.2 Modeling power systems as ecological networks

The flows between various components in a power system can be modeled as prey-predator interactions in a food web. The process documents the flows between components and across the system boundaries as a directional graph or $digraph$, where actors become $nodes$ and connections between them become $directed\ edges$ from producer to consumer. Interactions that cross boundaries are broken down into system inputs, useful system exports, and dissipation or non-useful system exports [26]. A flow matrix is then created and ENA metrics are calculated from this matrix [36].

Assumptions made in this application of ENA to power systems include:

[1]Material presented in this chapter is reprinted with permission from "Bio-inspired design for robust power grid networks" by Panyam et al., 2019. Applied Energy, 251, 113349, Copyright [2019] by Elsevier

1. Energy flows are modeled as flows of real power (MW). The integration of real power over time is the energy flow in the system, which provides a direct analogy between power systems and food webs. Real power (as opposed to complex power [127]) flow analysis, is deemed acceptable for medium-to-long term transmission planning [128].

2. Steady-state real power flows are utilized for long-term planning objective. The power flows vary with time due to the change of online loads. However, fundamental frequency based steady-state analysis is essential for the day-to-day operation as well as future planning of the grid [129]. Thus, it is reasonable to use steady-state power flow for network optimization here.

3. Transmission lines are considered as lossless. Considering the real power losses are small compared to the power flow magnitudes in transmission lines, at this stage, the negligible impact of real power losses is ignored.

ENA is potentially very useful for larger and more realistic grids with thousands of components, in which many components have similar functions. Functionally similar species in highly complex and large ecosystems are often aggregated as a single actor in their food web representations [45]. Each individual organism in a large real ecosystem cannot realistically be accounted for; thus, ENA simplifies the analysis of complex ecosystem models by enabling aggregation of species into functional groups, highlighting functionally important relationships.

Since long term planning of grid connections is the focus here, only buses and generators are considered as actors in this analysis. Transformers and transmission lines are modeled as connections between these actors, representing the directed edges between the nodes. The power consumers[2] or loads (homes, industries, stores, etc.), are placed outside the system boundaries as the users of the exported power, mimicking the useful system exports of a food web. This is consistent with the food web modelling done by ecologists where the receivers of final useful exports from an ecological network are placed outside the system boundary. Moreover, the exclusion

[2]The word "consumers" is used in this paper to refer to final users of the electric power whereas the word "load" is commonly used in power systems terminology to refer to the same.

of consumers from the system boundary has no impact on the analysis as the focus here is on transmission networks.

5.2.1 Power flows in a power system

The ecosystem flows T_{ij} are equivalent to the amount of real power (MW) flow from generator or buses i to j, given by P_{ij} in a power system. Real and reactive power flows, P_{ij} and Q_{ij} respectively, are calculated by solving a set of nonlinear equations formed using network line parameters:

$$P_{ij} = V_i^2[-G_{ij}] + V_i V_j[G_{ij}cos(\theta_{ij}) + B_{ij}sin(\theta_{ij})] \tag{5.1}$$

$$Q_{ij} = V_i^2[B_{ij}] + V_i V_j[G_{ij}sin(\theta_{ij}) - B_{ij}cos(\theta_{ij})] \tag{5.2}$$

where V_i is the voltage magnitude of bus i, θ_{ij} is the phase angle difference between bus i and j, and G_{ij} and B_{ij} denote the elements in the i,j position of the real and imaginary components of the system admittance matrix $\mathbf{Y_{bus}} = \mathbf{G} + j\mathbf{B}$ [127].

The power systems in this paper are treated as lossless ($\mathbf{G = 0}$) and voltage magnitudes of each bus are assumed constant at 1.0 per unit such that the power flow equations (5.1) and (5.2) can be simplified as:

$$P_{ij} = B_{ij}(\theta_i - \theta_j) \tag{5.3}$$

which is a set of linear equations [127]. This model is known as âĂIJdcâĂİ $power\ flow$, a method extensively used in contingency screening, transmission loading relief, transfer analysis, and medium-to-long term transmission planning [128]. The energy produced from generators and consumed by loads is then measured as real power over time.

5.2.2 PowerWorld simulator and test cases

PowerWorld Simulator [7], a software program that allows users to simulate and analyze electric power systems, is used to solve the optimized network. The power flow solutions given by PowerWorld fully define the power flow magnitudes between any two components in the grid. A small number of test cases (with up to 14 buses) are used in this analysis; four of these come from the training cases available in PowerWorld simulator, and one is an IEEE test case. These systems represent realistic grid interactions at a significantly smaller scale than real world power grids and are useful for analysis purposes as data of real power grids is difficult to obtain. Five of these power systems, with 5,6,7,9 and 14 buses, are used in this analysis. The one line diagrams of all five grids can be seen in the Figure 5.1. The number of buses and the total load on each system are given in Table 5.1.

Network	**# Buses**	**Total load (in MW)**	**# Actors**	**# Links**
B5	5	500	7	5
B6	6	600	10	7
B7	7	800	12	11
B9	9	315	12	9
B14	14	259	19	20

Table 5.1: Loads, number of buses, and total number of actors and links for the five test case grids used. Original table published in Panyam et al. [2].

A flow matrix **[T]** for the 5-bus system (Figure 5.1A) has 2 generators, 5 buses, 1 transformer, 4 loads and a total load of 500 MW, is illustrated in Figure 5.2, with all values in units of megawatts (MW). The inter-compartmental exchanges (light grey shaded center entries in Figure 5.2) are defined by the selection of the system boundary, which places the consumers outside the system. The first row (cross-hatched) contains inputs to the system from outside; for the 5-bus power grid these are inputs to the two generators. The last two columns correspond to the energy that leaves the system that is useful (traveling to consumers) and lost (as dissipation to the environment) respectively. Flow matrices for the other systems were similarly created.

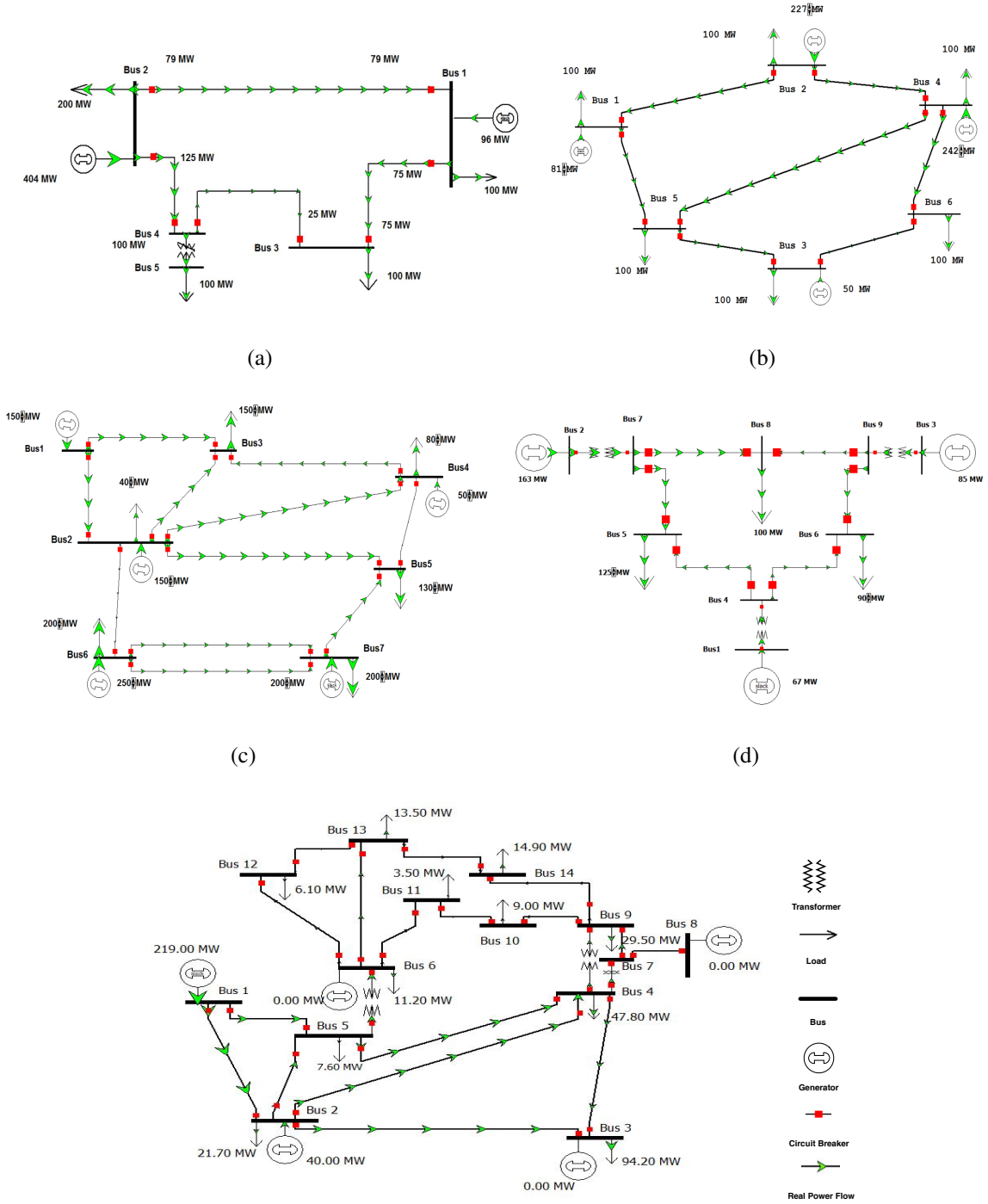

Figure 5.1: One line diagrams of the: (a) 5-Bus Power Grid [7], (b) 6-Bus Power Grid [7], (c) 7-Bus Power Grid [7], (d) WSCC 9-Bus Power Grid [8] and (e) IEEE 14-Bus Power Grid [9] in their traditionally optimized forms. The relative size of the green arrows represents the magnitude of real power flowing across that line. The generation capacities and loads provided are in megawatts (MW). Original figure published in Panyam et al. [2].

			Generator	Bus 1	Bus 2	Bus 3	Bus 4	Bus 5	Slack Generator	Output	Dissipation
		1	2	3	4	5	6	7	8	9	10
Input	1	0	404	0	0	0	0	0	96	0	0
Generator	2	0	0	0	404	0	0	0	0	0	0
Bus 1	3	0	0	0	0	74	0	0	0	100	0
Bus 2	4	0	0	78	0	0	126	0	0	200	0
Bus 3	5	0	0	0	0	0	0	0	0	100	0
Bus 4	6	0	0	0	0	26	0	100	0	0	0
Bus 5	7	0	0	0	0	0	0	0	0	100	0
Slack Generator	8	0	0	96	0	0	0	0	0	0	0
	9	0	0	0	0	0	0	0	0	0	0
	10	0	0	0	0	0	0	0	0	0	0

Figure 5.2: The 5-bus power grid represented as an ecological flow matrix [**T**]. Flow is entered from rows to columns. The first row represents inputs to the grid from outside the system and the last two columns are outputs from inside the system. Original figure published in Panyam et al. [2].

5.3 Bio-inspired optimization process

The formulation of ecosystem robustness using pathway efficiency and redundancy is valuable for the design of power systems in that it guides the incorporation of redundancy to achieve structures characteristic of sustainable biological ecosystems [25]. An optimization model was built to maximize ecological robustness for each of the five test grids. Ecosystems cluster around the peak of the R vs ASC/DC curve shown in figure 5.4, where there is a unique balance between pathway efficiency and redundancy. Thus, optimizing power grid networks to attain maximum ecological robustness mimics the balance found in food webs. Ecological robustness is nonlinear with respect to the ratio (ASC/DC) as can be seen graphically in figure 5.4. ASC and DC are dependent on the elements in the flow matrix **[T]**, which becomes the design variable [36]. Imposed line flow limits and power balance constraints for the network and each component do not affect the continuity of the problem. Thus, the proposed bio-inspired optimization is a non-linear continuous

problem. A gradient based method, using *fmincon* in MATLAB 2017a [130] was implemented for the optimization search. Further information about gradient based methods for nonlinear programming can be found in [131]. The optimization results in a new flow matrix with the maximum possible ecological robustness R. However, only power balances and line limits are satisfied in this configuration and so it is then fed into PowerWorld, which adjusts the flow magnitudes by small amounts to ensure that the dc power flow equations are satisfied for the given loads and generation. The flow matrix for this slightly modified configuration is generated and the final robustness value is computed. The optimization problem is formulated as follows (5.4a)-(5.4h):

$$\max_{\mathbf{T}} \quad R(\mathbf{T}) \tag{5.4a}$$

$$s.t: \quad T_{ij} \leq P_{ij}^{max}; \;\; (i,j) \in I \tag{5.4b}$$

$$\sum_{(i,j)\in I} T_{ij} = \sum_{i \in I} P_{Di} \tag{5.4c}$$

$$\sum_{j \in I} T_{ij} = \sum_{j \in I} T_{ji} \tag{5.4d}$$

$$T_{i,i} = 0; \;\; i \in I \tag{5.4e}$$

$$If \;\; T_{ij} \neq 0 \;\; then \;\; T_{ji} = 0; \;\; (i,j) \in I \tag{5.4f}$$

$$T_{i,g} = P_{Gi}; \;\; i \in I; \; g \in G \tag{5.4g}$$

$$T_{i,N+2} = P_{Di}; \;\; i \in I \tag{5.4h}$$

where set I represents all buses, sets G and D denote the original system's generators and loads, N is the total number of actors in the system, and T_{ij} represents the power flow from actor i to j in the flow matrix.

The constraints in the optimization problem ensure that the power flow is within the limits and there is a power balance between generation and loads:

- Eq.(5.4b) indicates that, during the optimization process, the elements in the flow matrix

[**T**] are within corresponding power system transmission lines' maximum capabilities. The capacities for new lines are set to the capacity of the lowest existing lines' capacity.

- Eq.(5.4c) ensures the total flow within the flow matrix [**T**] equals the net load in power grids.
- Eq.(5.4d) ensures the total incoming flow to bus i equals the outgoing flow from bus i.
- Eq.(5.4e) requires there is no flow within bus i itself.
- Eq.(5.4f) defines the flow direction as only from one bus to another.
- Eq.(5.4g) - (5.4h) keep the input flow and output flow equal to corresponding generator outputs and loads respectively.

Traditionally, optimal power grid design with the constraints of power flow, generation cost and transmission line capacity is done using mixed-integer programming [132], linear programming [133] and heuristic techniques [134]. These models assign a binary variable to each possible transmission line and evaluate all possible combinations of connections to optimize the objective function which usually is cost [134]. Recently, with computational advances and increase in distributed generation, other planning methods have also been proposed, including solving the optimization problem with an AC model [135], planning the transmission network under security and environmental constraints [136] and considering the uncertain renewable generation and load for transmission network expansion design [137]. The two-step process used here is different from these traditional optimizations in that ecological robustness is used as the objective value and the flow matrix is used as the design variable (hence the implementation of gradient based method). This allows the optimizer to search in a wider continuous domain than if power flow equations were also included in the search constraints.

A bio-inspired power network design algorithm was written to implement the whole process in MATLAB using PowerWorld's automation server SimAuto [7]. The algorithm converts a power system model in PowerWorld Simulator into the ENA representation, calculates the ecological flow metrics, optimizes the matrix if robustness is less than maximum, outputs a modified flow

matrix with the best robustness value possible under the imposed constraints, and creates a feasible network model in PowerWorld based on the optimization solution's matrix. The optimization runtime for all the grid networks ranged from 15-30 minutes on a computer with 16 GB RAM and a quad-core 3.60 GHz processor. Methods to increase the computational efficiency for large-scale realistic power systems are being investigated by the authors as an important next step that will be reported in future work.

5.4 Validation

A robust network is able to function and deliver power to its consumers despite disturbances. Determining the relative robustness of the traditional vs. the bio-inspired networks here requires the testing of these different network designs when they are under stress. The ability of grid designs to handle contingencies is validated here using $N - X$ contingency analyses in PowerWorld Simulator, for 'X' values ranging from one to three. The N-1 contingency analysis is considered the primary reliability standard by the North American Electric Reliability Corporation (NERC) [21]. Contingency analyses for power systems are steady state analyses that assesses grid performance under contingencies, or scenarios where one or more components become "affected" and stop functioning [138]. This method presents a conventional approach to test traditional grid improvements against improvements made to enhance ecological robustness. The grid performance in $N - X$ is measured in terms of the number of violations in network functioning, where a violation is when consumer needs are not met without increasing line capacities. The fewer the violations the better the network ranks. The violations observed, due to the 'dc' power flow model, are actually capacity overloads in unaffected transmission lines when the network tries to meet consumer needs. These overloads in real life can lead to wide area outages and blackouts.

The total possible contingency scenarios in a $N - X$ contingency analysis equals $\binom{N}{X}$, where N is the number of major components in the system and X is the number of removed elements. $N-1$, $N-2$, and $N-3$ contingency analyses were used to validate the improvement in optimized networks. $N - 1$ contingency analysis checks if a system can function with $N - 1$ components in service [139], $N - 2$ and $N - 3$ contingency analyses are similar, but simultaneously impose

double and triple contingencies. $N-1$, $N-2$, and $N-3$ contingency analyses were done for the traditional and bio-inspired systems using PowerWorld. The number of violations in $N-1$, $N-2$, and $N-3$ analyses are grid dependent, and thus can be normalized using the maximum possible number of violations for each case, providing a measure of improvement that is independent of system size. $N-4$ and higher contingency analyses are computationally expensive due to the high number of contingency scenarios and there are certain techniques to deal with this problem. Davis et al. [140] presented two methods based on the sensitivity information and branch flow information respectively to select severe contingencies for solving and checking the systemâĂŹs reliability, thus avoiding the evaluation of all the possible contingency scenarios. Such information is also related to network topology and it will be interesting to perform contingency screening on bio-inspired grids in future work.

5.5 Results

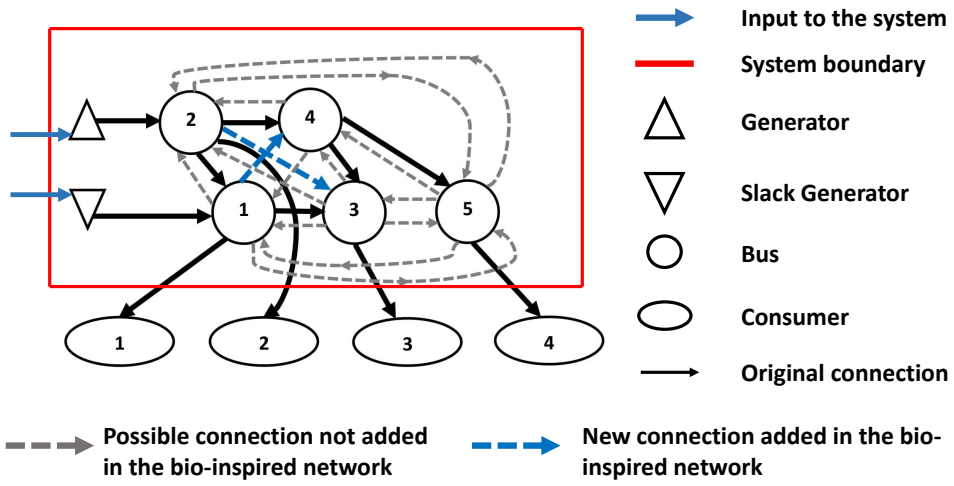

Figure 5.3: The connections in the traditional 5-bus system contrasted with the possible and added connections in the bio-inspired network. Original figure published in Panyam et al. [2].

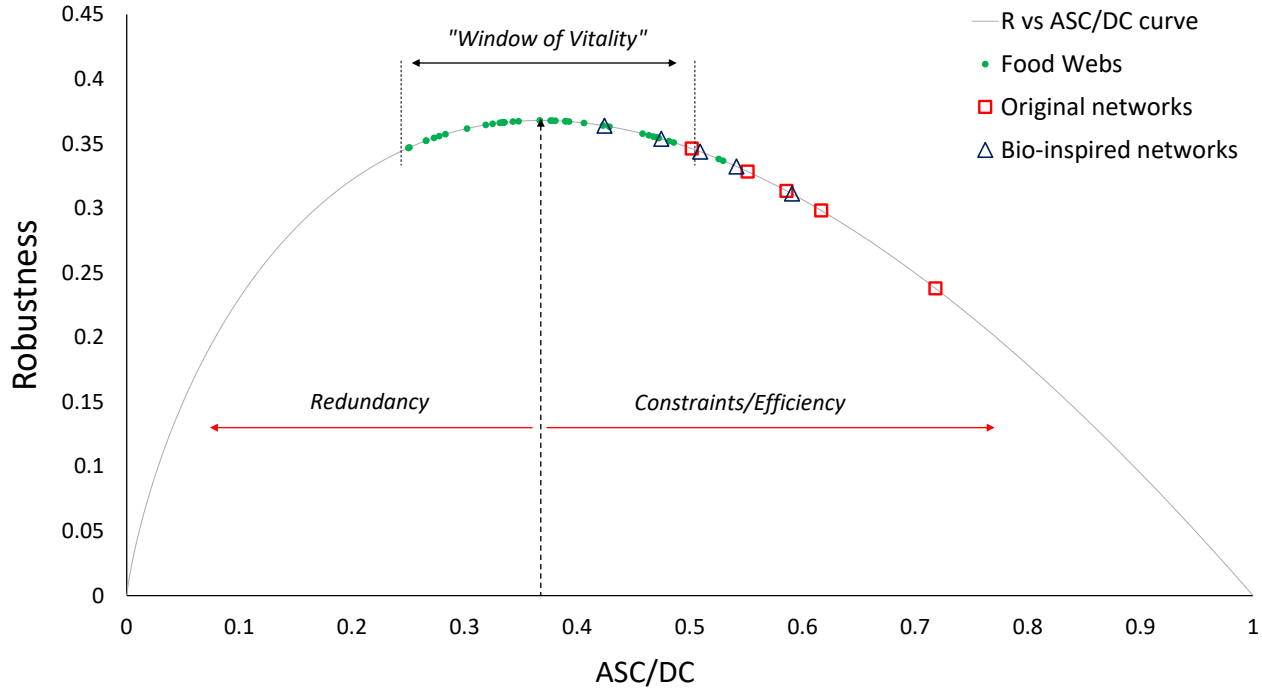

Figure 5.4: The ecological robustness curve depicting the five traditional (original) grids and their bio-inspired optimized versions, as well as a set of 38 food webs. An increase towards a more biological state is seen in all 5 grids. Original figure published in Panyam et al. [2].

Network	# Lines	ASC/DC	R	# N-1 violations	# N-2 violations	# N-3 violations
Average Food webs	-	0.38	0.36	-	-	-
Traditional B5	5	0.61	0.29	7	59	120
Bio-inspired B5	7 (Δ=2)	0.59	0.31	3	29	120
Traditional B6	7	0.50	0.34	9	122	460
Bio-inspired B6	12 (Δ=5)	0.47	0.35	0	18	210
Traditional B7	11	0.55	0.32	7	159	1243
Bio-inspired B7	18 (Δ=7)	0.51	0.34	1	36	485
Traditional B9	9	0.71	0.23	8	276	1029
Bio-inspired B9	31 (Δ=22)	0.54	0.33	0	0	0
Traditional B14	20	0.58	0.31	8	314	4450
Bio-inspired B14	80 (Δ=60)	0.424	0.363	0	1	94

Table 5.2: The ecological metrics ASC/DC and R for the food webs (averages for a set of 38 food webs) and traditional and bio-inspired versions of each grid. Original table published in Panyam et al. [2].

The ASC/DC and R values of all the five analyzed systems are given in the table 5.2. Traditional configurations of all the five systems are plotted on the robustness vs. ASC/DC curve in figure 5.4 alongside a set 48 of food webs. Ecologists refer to the region at the top of the curve as the *window of vitality*, the area where biological food webs cluster that indicates a slight biological preference for redundancy over efficiency [11]. Traditional configurations of all the grids can be seen to have higher organizational efficiency (as measured by an ASC/DC closer to one) resulting in a lower robustness. The 9-bus grid falls farthest to the right on this curve, with a robustness value of 0.237 and an ASC/DC value of 0.718, indicating it has the least redundancy in its connections among the all power systems investigated. The 6-bus grid has the highest redundancy

and correspondingly a higher robustness of 0.346 and an ASC/DC of 0.501, just putting it in the window of vitality. The other grids have robustness values in between these two systems.

The bio-inspired optimization was successful in moving all the networks closer to the maximum, as shown in figure 5.4. The optimization suggested the addition of connections in each system to achieve this improvement. The modifications all resulted in an increase in redundancy and a decrease in organizational efficiency since all the grids were originally overly efficient according to this measure. The added redundant connections are chosen by the optimization from a large number of available connections with the goal of maximizing ecological robustness under the imposed limits and constraints. The optimization of the 5-bus system (seen in the figure 5.3) added 2 connections, resulting in a 4.36 % increase in ecological robustness. The increases in robustness become smaller as the peak of the curve is approached. The total number of transmission lines in the traditional and bio-inspired configurations for each grid can be seen in table 5.2. The difference in the number of transmission lines in both types of networks for each grid is also shown in table 5.2.

The number of violations for all ten grid cases are listed in table 5.2. Normalized $N - X$ measures for the traditional and bio-inspired networks are shown in figures 5.8, 5.9 and 5.10. The number of total possible contingency scenarios increases from $N - 1$ to $N - 3$ analysis. The total number of violations observed also go up with the number of possible contingencies. The bio-inspired networks all show fewer violations than their traditional counterparts in the $N - 1$, $N - 2$, and $N - 3$ scenarios, clearly indicating that bio-inspired networks are able to better redistribute flows during contingencies without violating undamaged transmission line capacities. The bio-inspired networks perform consistently well, even as the number of possible contingencies increases from the $N - 1$ to $N - 3$ analysis. Figures 5.5, 5.6 and 5.7 depict the drop in $N - 1$, $N - 2$, and $N - 3$ violations due to the corresponding increase in ecological robustness. The plots of ecological robustness versus normalized measures of N-1, N-2, and N-3 violations and the corresponding coefficients of determination are shown in Figures 5.11–5.13.

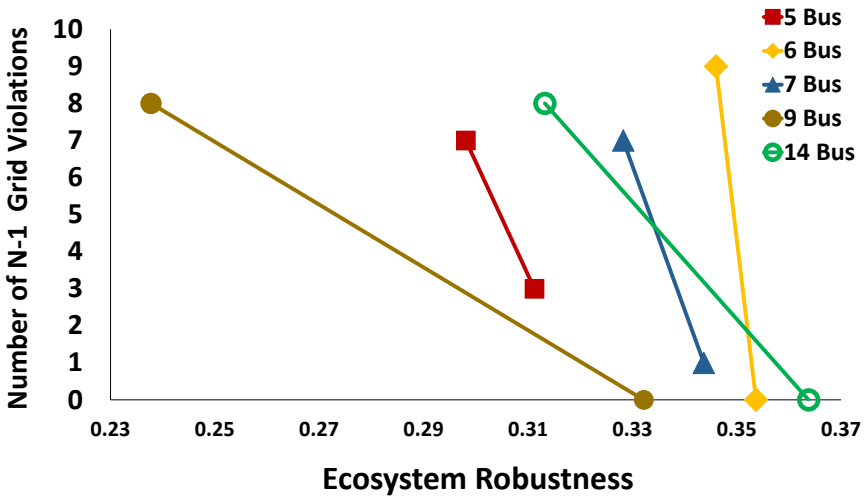

Figure 5.5: The drop in N-1 violations from the five traditional grids to their bio-inspired versions as ecosystem robustness increased. Original figure published in Panyam et al. [2].

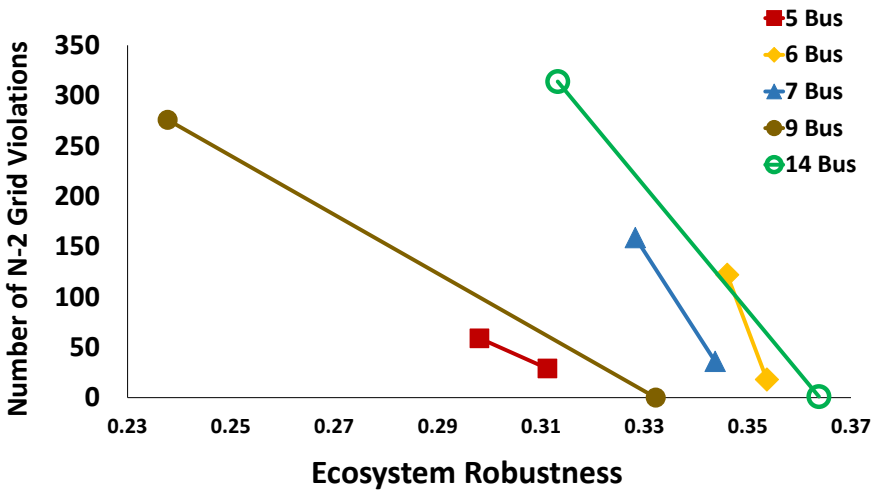

Figure 5.6: The drop in N-2 violations from the five traditional grids to their bio-inspired versions as ecosystem robustness increased. Original figure published in Panyam et al. [2].

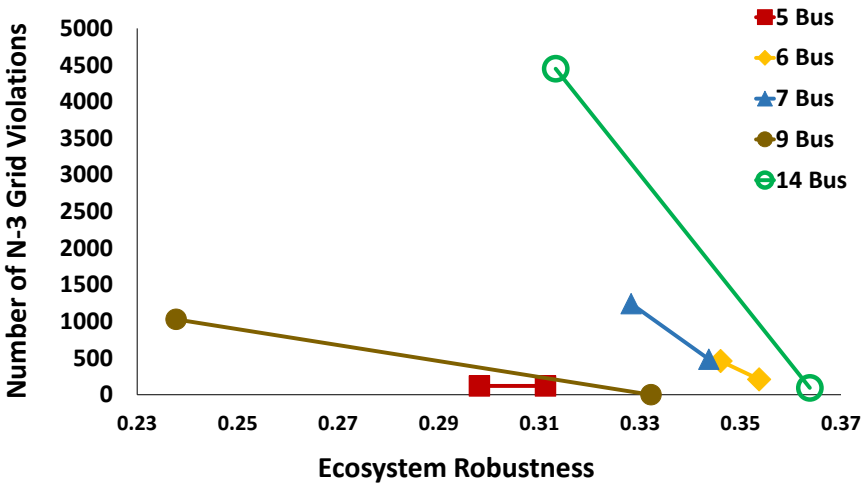

Figure 5.7: The drop in N-3 violations from the five traditional grids to their bio-inspired versions as ecosystem robustness increased. Original figure published in Panyam et al. [2].

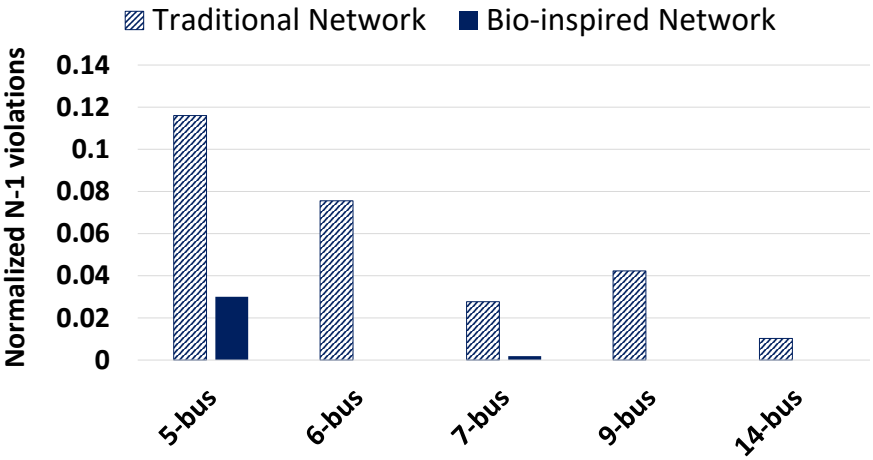

Figure 5.8: The number of actual N-1 violations normalized by the maximum possible number of N-1 violations, for the traditional and bio-inspired networks. Original figure published in Panyam et al. [2].

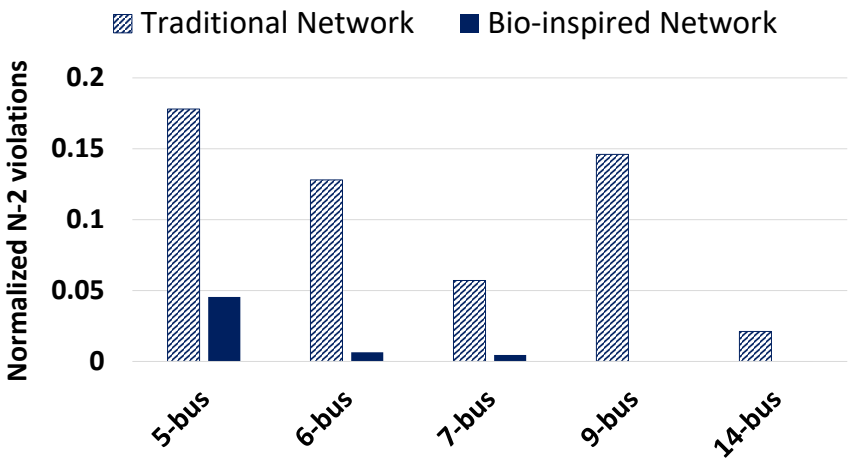

Figure 5.9: The number of actual N-2 violations normalized by the maximum possible number of N-2 violations, for the traditional and bio-inspired networks. Original figure published in Panyam et al. [2].

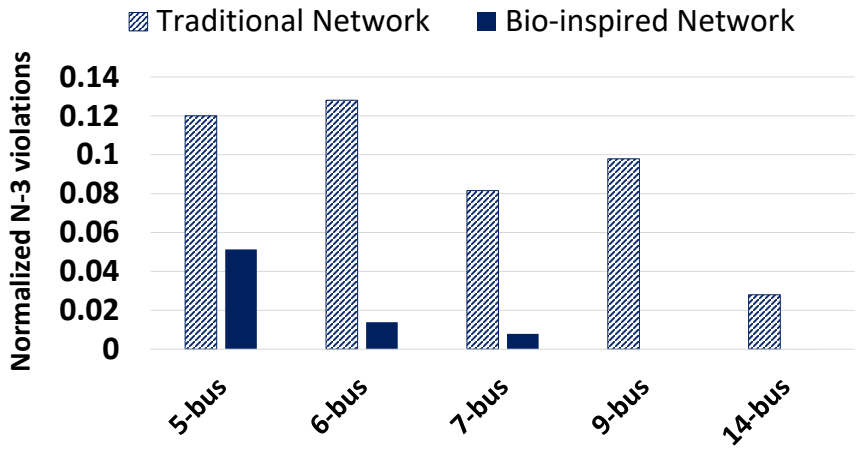

Figure 5.10: The number of actual N-3 violations normalized by the maximum possible number of N-3 violations, for the traditional and bio-inspired networks. Original figure published in Panyam et al. [2].

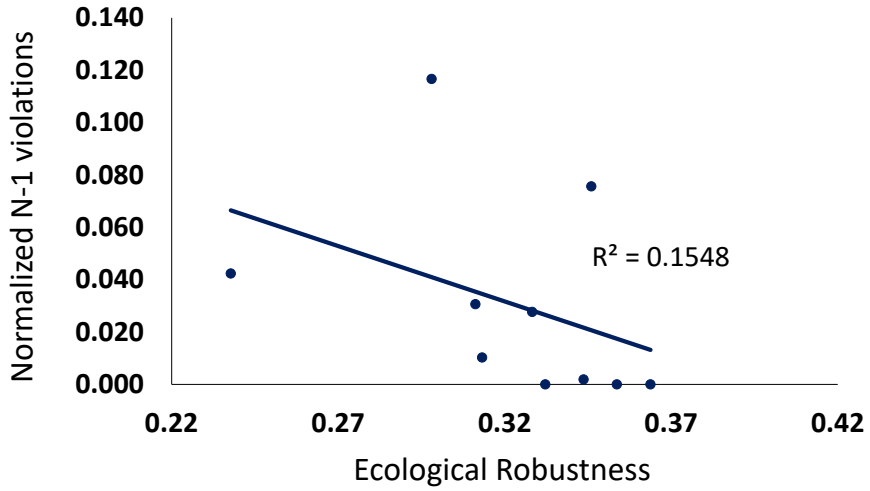

Figure 5.11: Normalized N-1 violations (actual/maximum possible) vs. ecological robustness. Original figure published in Panyam et al. [2].

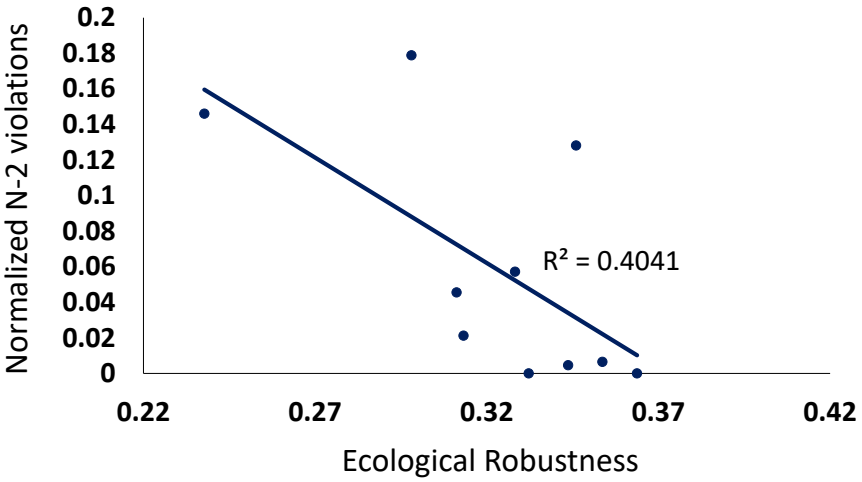

Figure 5.12: Normalized N-2 violations (actual/maximum possible) vs. ecological robustness. Original figure published in Panyam et al. [2].

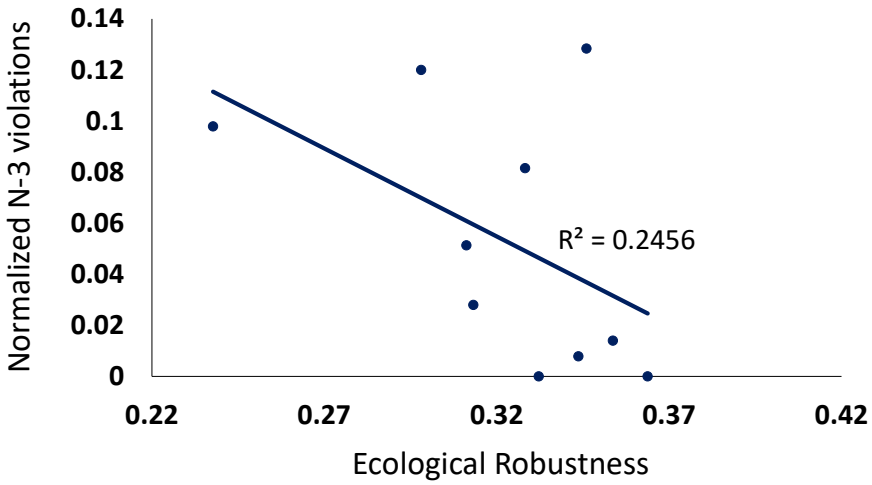

Figure 5.13: Normalized N-3 violations (actual/maximum possible) vs. ecological robustness. Original figure published in Panyam et al. [2].

5.6 Discussion

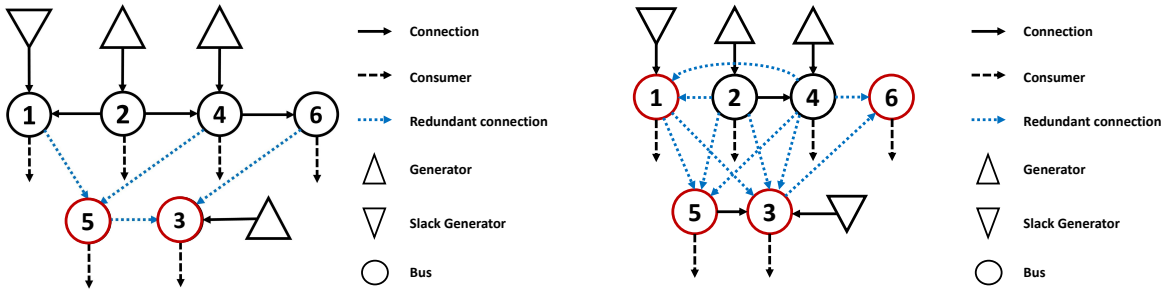

(a) (b)

Figure 5.14: The redundancy in the traditional 6-bus system (a) and bio-inspired 6-bus system (b) in dotted blue arrows contrasted with other connections. The buses in red are connected to loads and are centers of receiving end of redundant connections. A connection is labelled redundant if there is at least one other connection going into the same node. Original figure published in Panyam et al. [2].

Application of ENA to the five power grids revealed that their ecological robustness is less than optimal. This approach presents a potential innovative method for power providers to estimate the biological similarity of the organizational state of grid infrastructure. The food webs' "window of vitality" robustness was achieved for four out of the five grid systems following the optimization. The robustness of the 5-bus grid improved but did not reach the window of vitality. The higher robustness values observed in the bio-inspired networks were achieved through selectively added redundant connections since the traditional grids all had higher organizational efficiency than what is found in most food webs. The new connections added are primarily between buses. These added connections, while unnecessary for normal operation, add a redundancy that is uniquely balanced similarly to food webs. The number of additional lines required to mimic ecosystems' robustness increases rapidly with an increase in number of buses, as seen in table 5.2. Thus, the bio-inspired design of very large power grids (thousands of buses) may require the construction of thousands of new lines, which warrants significant investments. A case in point is the bio-inspired 14-bus case. Sixty new transmission lines are added, as compared to 20 in the original case, to achieve the maximum possible ecological robustness. The capacity usage remains low in most of the newly added lines, even during contingencies, questioning the need from an economic standpoint as to the value of adding all the recommended new lines. An understanding of the economic value of higher ecological robustness would enable an economical trade-off to be determined between adding lines to achieve improved robustness.

The $N - X$ contingency analyses are used to provide a traditional measure of grid performance under duress. When compared against the grids ecosystem robustness rating, a connection between food web organization and improved grid design may be established. The number of violations is the total number of line overloads in the system for all possible contingency scenarios.A comparison of the traditional and bio-inspired grids, in terms of number of violations, may point to specific regions where overloads can occur. An important assumption here is that the new lines in the bio-inspired system have the same capacity as the originally existing lines. The number of contingency scenarios in the $N - 2$ and $N - 3$ contingency analyses increases compared to $N - 1$

contingencies due to an increase in possible permutations of single element contingencies. The traditional configurations, which all result in $N-1$, $N-2$, and $N-3$ violations, had a mean of 0.082 normalized violations (normalized by the maximum possible violations in each case) and a maximum and minimum of 0.178 and 0.010 respectively. The bio-inspired networks all significantly reduced the number of violations presenting a new mean for normalized violations of only 0.002 and a maximum and minimum of 0.051 and 0 respectively (there were 5 cases the bio-inspired networks had zero violations as seen in table 5.2).

The traditional design of power networks seem to be well equipped to handle single element contingencies but experiences large numbers of violations for $N-2$ and $N-3$ contingencies. An average 10.6 % increase in ecological robustness across the five grids resulted in an average decrease of *7* $N-1$ violations, *169* $N-2$ violations, and *1279* $N-3$ violations. This suggests that for individual grid performance, redesigns that improve ecological robustness results in improvements in the network capability to handle single, double and triple element contingencies. The 5-bus grid presents an outlier in its $N-3$ contingency analysis, showing no improvements between the two designs. The violations in this case remain the same at 120 for both the traditional and bio-inspired grids. This behavior could largely be attributed to the small size of the system. Since there are only five buses, any permutation of three single element contingencies is devastating to the system. However when the number of violations are compared to the total possible violations the 5-bus grid still sees an improvement, with normalized violations falling from 0.12 to only 0.051. Ecological robustness thus holds significant potential to redesign for power grid improvements, better redistributing flows among the undamaged lines during contingencies. The consistent improvements seen in all the $N-X$ analyses suggest that similar improvements: a reduction in both total violations and normalized violations could reasonably be expected for higher number of contingencies in larger grids. Analysis of bigger power systems is needed to validate this hypothesis.

Ecological robustness weighs pathway redundancy towards all nodes equally, thus valuing the whole system's ability to survive and manage disturbances in terms of redundancy and effi-

ciency. There is no distinction between uniformly distributed robustness and robustness concentrated around certain nodes. This presents a disadvantage for power systems with very high or low numbers of consumers. Since the goal of a power system is to ensure power supply to consumers, redundancy in and around each consumer may be more beneficial, as evident by the behavior of the traditional and bio-inspired 6-bus and 9-bus grids. The structural configurations of the traditional and bio-inspired 6-bus grids are shown in the figure 5.14(a) and 5.14(b). The traditional design in the 6-bus grid has a robustness value of 0.346 and 6 consumers. The redundant pathways in the grid resulting in this relatively high ecosystem robustness value are concentrated towards buses 5 and 3, the two highlighted nodes in red in figure 5.14(a). This concentration causes the system to falter during the contingency analysis, showing 9 violations out of a possible 119 in the $N-1$ contingency analysis. The bio-inspired 6-bus system increases the robustness by only 2.02% but the number of violations are reduced to zero (out of a possible 264). This is because the redesign increases the redundancy in a distributed manner as seen in figure 5.14(b). Four out of the six buses supplying consumers are now supported by redundant connections. The traditional 9-bus grid has a relatively low ecological robustness value of 0.233 and 3 consumers and has 8 violations out of a possible 189 in the $N-1$ contingency analysis. However, once again it can be shown that this redundancy is concentrated around only one third of the buses (3 out of 9). The bio-inspired design introduces network-wide distributed redundancy, resulting in zero violations similar to the bio-inspired 6-bus grid. The importance of certain consumers (for example hospitals might be more important than residential households) may require that redundant connections not be distributed evenly across the grid, however for the purposes of the investigation here overall grid improvements are sought. Future work may address changes to individual component importance. Ecosystems with keystone species may present a good paradigm to model power systems with critical consumers.

The bio-inspired design of power systems is shown here to be an innovative approach that produces a generally more robust power grid, as measured by basic $N-X$ analyses. The hypothesized correlation between ecological robustness and the normalized measure of number of $N-X$

violations was that an increase in the robustness of the grid would lead to a lower number of violations. However, the concentrated robustness of the traditional 6-bus and 9-bus grids in addition to the small data set size (only 10 total) prevent a meaningful correlation from being established at this stage. $N-X$ contingency analyses also do not necessarily capture all aspects of the possible improvements achieved using the bio-inspired approach. The added structural redundancy advised by the bio-inspired optimization here does require significant financial investments in some cases. Models that consider transmission line construction costs against the costs of outages would better validate the bio-inspired design proposals. Finally it is important to note that neither this approach nor any other can remedy scenarios that cause total destruction of grid infrastructure. Success in the analyses here was with only 10-30 % of the grid affected. Future work will use a larger data set that includes larger grids, as well as simulate more detailed and realistic outage events on the two grid designs to provide further insight into the potential benefits of the bio-inspired modifications. This in turn may lead to better designs of power system networks, in terms of infrastructure that can enhance grid robustness and resilience.

5.7 Conclusions

The biological food web-inspired approach presented here defines and assesses the ecological similarity of power system robustness. The optimization method developed has been shown to improve the ecological robustness of power systems and in turn their resultant $N-X$ ratings. The application of the ecological metric $robustness$ to power systems has shown two significant advantages: 1) Robustness is quantified on a simple scale and 2) Power systems reconfigured to mimic the balance of natural ecosystems between pathway redundancy and efficiency improves overall grid $N-X$ ratings. Although installing redundant lines is a known way to enhance resilience of power systems, the effective use of redundancy was heretofore not well investigated. The presented approach has the potential to leverage the success of ecosystems to achieve robust and resilient power systems.

6. DEALING WITH DISSIPATION IN HUMAN NETWORKS[1]

6.1 Introduction

The exchanges in food webs are prey-predator interactions, where one species (predator or consumer) *directly* consumes another species (prey or producer). This is an important factor that has previously been overlooked in modeling human networks as ecosystems. Unlike a prey-predator interaction, a physical entity is required to facilitate exchanges in most human network interactions. Trucks, trains, or airplanes transport materials/products between companies in industrial systems; pipelines distribute liquids and gases; and transmission lines distribute electricity. The extent of dissipation, additional energy requirements, and emissions during transport depends on the transportation type. Prior work has always represented the industries/components as nodes and the energy/material exchanges between the industries/components as edges [43, 115, 44, 121, 36, 4]. The amount of dissipation in some networks might be small enough to be neglected: leakages in newer pipelines for example may be negligible. However water infrastructure, especially in densely populated urban areas, is old [141] and leakages can be significant. Water loss average in US water distribution networks has been estimated to be 3-4 % [141], whereas for global networks it is about 35% [142, 143]. Industrial networks transport material through pipes and also trucks and trains, which consume energy and release emissions. Power systems in the US experienced line losses that amounted to 6% of the total electricity generated in 2014 [144]. The consideration of these significant losses and dissipation in power grids and water networks is crucial to ensure accurate analyses and conclusions.

No impact quantification has yet been done to determine the consequences of lost information when exchange mechanisms in human networks are treated as equivalent to links in a food web. The rise of the use of ecosystem modeling techniques for human network analysis and design makes it important to understand and quantify the impact of omitting link dissipation and transport

[1]Material presented in this chapter is reprinted with permission from"Bio-inspired modeling approaches for human networks with link dissipation" by Panyam and Layton, 2019. ASME International Design Engineering Technical Conferences Proceedings, Copyright [2019] by ASME

efforts.

Consideration of links in human networks as actors when translated to an ecosystem model is investigated in this chapter to quantify the effects of this historical oversight. Three hypothetical power grids and three Italian water networks are modeled as ecosystems to test two modeling approaches: one modeling configuration is done with the links as actors and one configuration is done in the more traditional approach, with links left as edges, disregarding link dissipation. The primary objective is to understand how the values of standard ENA metrics differ in the two modeling approaches and the potential significance of those differences.

6.2 Case studies

Information about high-level material/water flows of industrial and water distribution networks is often available, but quantitative information about material dissipation in links can be very difficult to obtain. Industrial networks are complex networks comprising layers of sub-networks of material, energy and water [145, 112]. Addressing the needs of energy and water networks can thus directly benefit industrial networks as well. Hence power grids and water networks are used in this analysis for comparing the two modeling approaches. Water loss averages in different water distribution networks around the world are used here to approximate water losses in pipelines. Electrical energy losses in power transmission lines are calculated from power flow data.

6.2.1 Power grids

Power grids are networks of generators and consumers connected through buses (representing substations). The size of a power grid is specified by the number of buses. Security concerns limit the use of real power grid data [146] and so PowerWorld Simulator, a commercial power grid modeling software [**?**] is used for its realistic synthetic power grid cases. Three grids containing 7, 9, and 10 buses are used, providing a range of sizes (12, 15, and 17 actors respectively) and complexity (800, 315, and 880 MW loads respectively). Real power flows (MW) between the components are considered the flow elements of a power grid network [36].

Power grid network models fall into two types: non-linear *ac* models and linear *dc* models.

The solved linear or non-linear equations provide the power flow magnitudes between any two components. The dc models are a simplification of the ac models as they assign zero resistance to transmission lines, resulting in no dissipation. As a result dc models are used for long term design planning of power systems [36]. Although difficult to solve, ac models offer a more accurate representation of real grids. All three grids here were solved using ac models in PowerWorld, unlike the power grid models used in chapter 5.

6.2.2 Water networks

Three urban Italian water distribution networks originally investigated by Bodini *et al.* [121] are used here with slight modifications, introducing an average 10 % dissipation in selected links. This approximation, based on water loss averages reported in [141, 142, 143] is used as the original dissipation/loss information was not provided. The links with high amount of water flows were chosen for introducing dissipation because they are critical in network functionality. Common classes of users and entities were grouped as one actor by Bodini et al. [121] in the original analysis and are maintained here. All the residential and commercial consumers, for example, are grouped as one actor named "families and commerce" (node 2). Figure 6.1 shows an illustration of water network in the city of Albareto. The original network only contained dissipation from nodes 2 and 4. The dissipation seen in the links in Fig. 6.1 have been introduced.

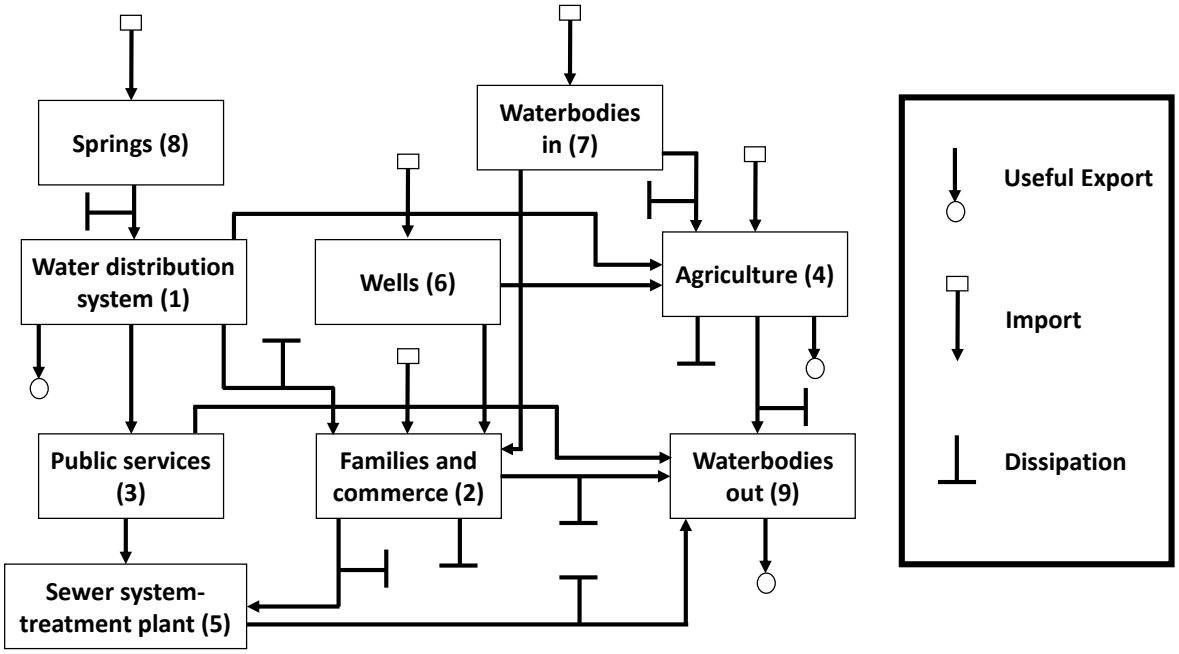

Figure 6.1: The food web network diagram of the Albareto water network with link dissipation. Original figure published in Panyam and Layton [10].

Component	Dissipation (m^3/year)
Actor 2 (Families and commerce)	1117E+03
Actor 4 (Agriculture)	1425E+07
Link 1 to 2	**1464E+04**
Link 2 to 5	**8564E+03**
Link 2 to 9	**3992E+04**
Link 4 to 9	**2126E+05**
Link 5 to 9	**9302E+04**
Link 7 to 4	**3154E+05**
Link 8 to 1	**5587E+04**

Table 6.1: Dissipation from the nodes and links of Albareto water network shown in Fig. 6.1. The bold values are from links and therefore are not documented when links are modeled as edges. Original table published in Panyam and Layton [10].

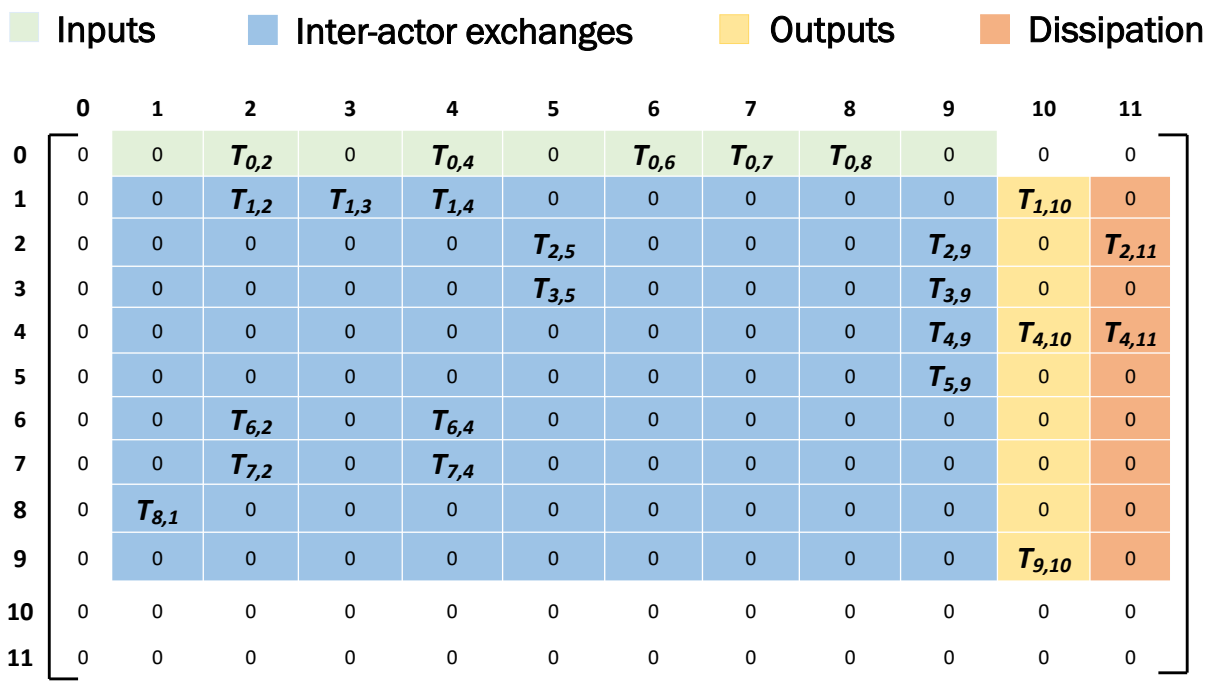

	0	1	2	3	4	5	6	7	8	9	10	11
0	0	0	$T_{0,2}$	0	$T_{0,4}$	0	$T_{0,6}$	$T_{0,7}$	$T_{0,8}$	0	0	0
1	0	0	$T_{1,2}$	$T_{1,3}$	$T_{1,4}$	0	0	0	0	0	$T_{1,10}$	0
2	0	0	0	0	0	$T_{2,5}$	0	0	0	$T_{2,9}$	0	$T_{2,11}$
3	0	0	0	0	0	$T_{3,5}$	0	0	0	$T_{3,9}$	0	0
4	0	0	0	0	0	0	0	0	0	$T_{4,9}$	$T_{4,10}$	$T_{4,11}$
5	0	0	0	0	0	0	0	0	0	$T_{5,9}$	0	0
6	0	0	$T_{6,2}$	0	$T_{6,4}$	0	0	0	0	0	0	0
7	0	0	$T_{7,2}$	0	$T_{7,4}$	0	0	0	0	0	0	0
8	0	$T_{8,1}$	0	0	0	0	0	0	0	0	0	0
9	0	0	0	0	0	0	0	0	0	0	$T_{9,10}$	0
10	0	0	0	0	0	0	0	0	0	0	0	0
11	0	0	0	0	0	0	0	0	0	0	0	0

Figure 6.2: The flow matrix for the Albareto water network shown in Fig. 6.1, constructed using the traditional food web modeling approach LE where the links are edges. Matrix row and column numbers correspond to the actors numbered in Fig. 6.1. Original figure published in Panyam and Layton [10].

6.3 Methods

Both structural and flow ENA metrics are used here to assess the impact of considering links as actors. The elements of the flow matrix are power flows in MW for power grid networks and volume of water in m^3/year for water networks. The makeup of the flow matrix for Albareto water network of Fig. 6.1 is shown in Fig. 6.2.

6.3.1 Modeling links as edges (LE)

The traditional modeling approach used in prior works [42, 115, 147, 44, 121, 112] models all exchanges linking actors as edges in the digraph. This modeling approach is labeled LE (referring to links as edges). Dissipation in the links *is **not** accounted* in this approach.

6.3.2 Modeling links as actors (LA)

The alternate modeling scenario also considers the transfer mechanism an actor. This modeling approach is labeled LA (referring to links as actors). Dissipation in the links *is accounted* in this approach. The basic structure of the network remains the same, but transfer actors are documented in the digraph between the original actors, increasing the number of actors and links. All the links in water networks are considered as actors because all of them are a part of the distribution network. All the links except those connecting generators and buses in power grid networks are considered as actors because those connections are not a part of the transmission system and do not have any dissipation. Fig. 6.3 illustrates digraphs in the LE and LA models for a simple two node network with one link.

6.4 Results

Three structural metrics: linkage density (L_d, Eq. 3.1), connectance (C, Eq. 3.2) and prey to predator ratio (P_R, Eq. 3.3) and three flow metrics: Shannon Index (H, Eq. 3.6), average mutual information (AMI, Eq. 3.13) and ecological robustness (R, Eq. 3.15) were used to evaluate the three power grids and three water networks under both the LE and LA modeling approaches. The results of the six ENA metrics and the number of actors and links are shown in Table 6.2. Average

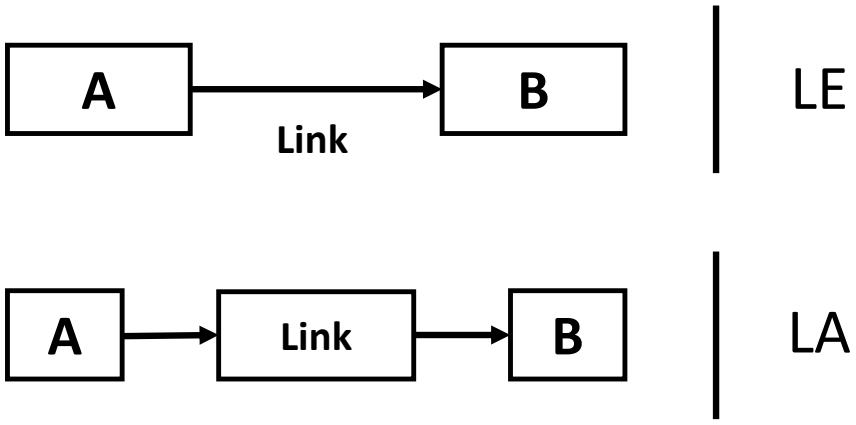

Figure 6.3: A two node (**A** & **B**) network with one exchange linking them. LE models this link as an edge (arrow) while LA models this link as an actor (boxed). Original figure published in Panyam and Layton [10].

food web values for the six metrics are also listed for comparison, with averages derived from a set of 38 food webs [11]. The results show that for the LE modeling technique, all the metric values except P_R are closer to FW averages than when LA modeling is used (comparing the 2nd row of Table 6.2 to all the following rows).

The plot of R vs ASC/DC is used by ecologists to visualize the unique ecological balance between efficiency and redundancy that food webs characterize [25]. Food webs have been found to primarily reside on top of the curve, where pathway redundancy is slightly higher than pathway efficiency [25]. Most human networks on the other-hand have been found to be more efficient, falling to the right side of the peak indicating a higher prevalence of efficient pathways [11] cf. [51]. Going from LE to LA for the power grids and water networks here results in a drop in R and an increase in ASC/DC as seen in Fig. 6.4 and 6.5, respectively. Although the value of R reduces following the consideration of links as actors for all the networks, the magnitude of the decrease changes. The Saramato water network has the highest decrease in R. The magnitude of the decrease is so large that it changes the relative positions of the Saramato and Ravenna water

networks on the robustness curve: when modeled using LE the Saramato network shows a more robust configuration than the Ravenna network, however the Ravenna network shows a more robust network configuration using the LA modeling technique (Fig. 6.5 solid vs. hollow points). The power grids all retain their relative positions on the ecological robustness curve (Fig. 6.4) between the two modeling approaches.

All three structural metrics (linkage density Fig. 6.6, connectance Fig. 6.7, and prey to predator ratio Fig. 6.8) see a decrease when links are considered as actors. Outlier of this observation is found again for the Saramato water distribution network: the prey-predator ratio increases going from LE to LA. Outliers are also found for the 9-bus power grid, for which linkage density and prey to predator ratio remains unchanged between LE and LA.

Network	N	L	L_d	C	P_R	AMI	H	R
FWs (Average)	48	479	7.64	0.17	1.11	1.69	4.57	0.368
B7-LE	12	15	1.25	0.1	1.428	2.35	4.35	0.33
B7-LA	23	26	1.13	0.05	1.11	2.88	4.72	0.3
B9-LE	15	15	1	0.07	1	3.41	4.24	0.17
B9-LA	27	27	1	0.04	1	4.3	4.92	0.12
B10-LE	17	23	1.35	0.08	1.6	2.7	4.85	0.32
B10-LA	33	39	1.18	0.036	1.23	3.47	5.42	0.285
Albareto-LE	9	14	1.55	0.17	1.33	1.17	2.41	0.35
Albareto-LA	23	28	1.22	0.052	1.1	1.62	2.83	0.32
Saramato-LE	10	16	1.6	0.16	0.87	1.52	2.84	0.33
Saramato-LA	26	32	1.23	0.04	0.96	2.7	3.99	0.26
Ravenna-LE	11	19	1.72	0.15	1.25	1.9	3.29	0.32
Ravenna-LA	30	38	1.26	0.04	1.07	2.38	3.65	0.28

Table 6.2: ENA metrics for food webs (averages for a set of 38 FWs [11]), three power grids and water networks using the LE and LA approaches. Original table published in Panyam and Layton [10].

6.5 Discussion

A major difference between ecological food webs and human networks is that the transfers between actors happen directly, actor to actor, in food webs and indirectly, through a transport method, in human networks. Often dissipation occurs during the transport: leaks in pipelines and losses across transmission lines for example. Since food webs don't experience dissipation during exchanges, a potential breakdown in the analogy between the two network types can occur. The water networks and power networks here are good case studies for quantifying the potential impact of including transport methods as actors in and of themselves (LA) in a food web model of human

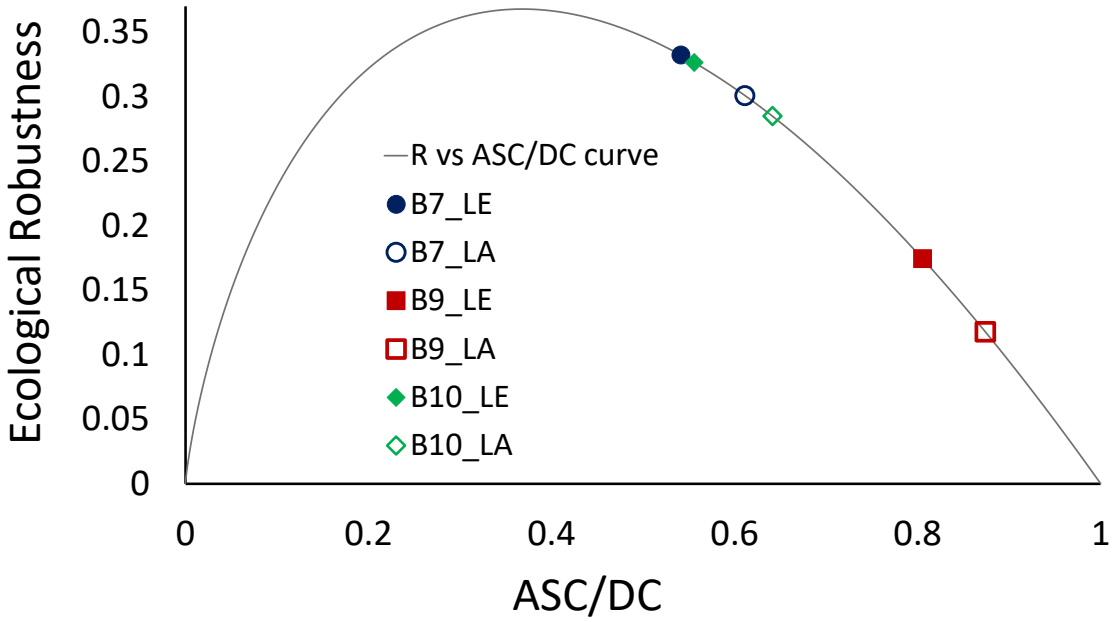

Figure 6.4: Ecological robustness vs. ASC/DC for three power grids, 7-bus (B7), 9-bus (B9), and 10-bus (B10). Links modeled as edges (LE) are signified with solid points and links modeled as actors (LA) with hollow points. Original figure published in Panyam and Layton [10].

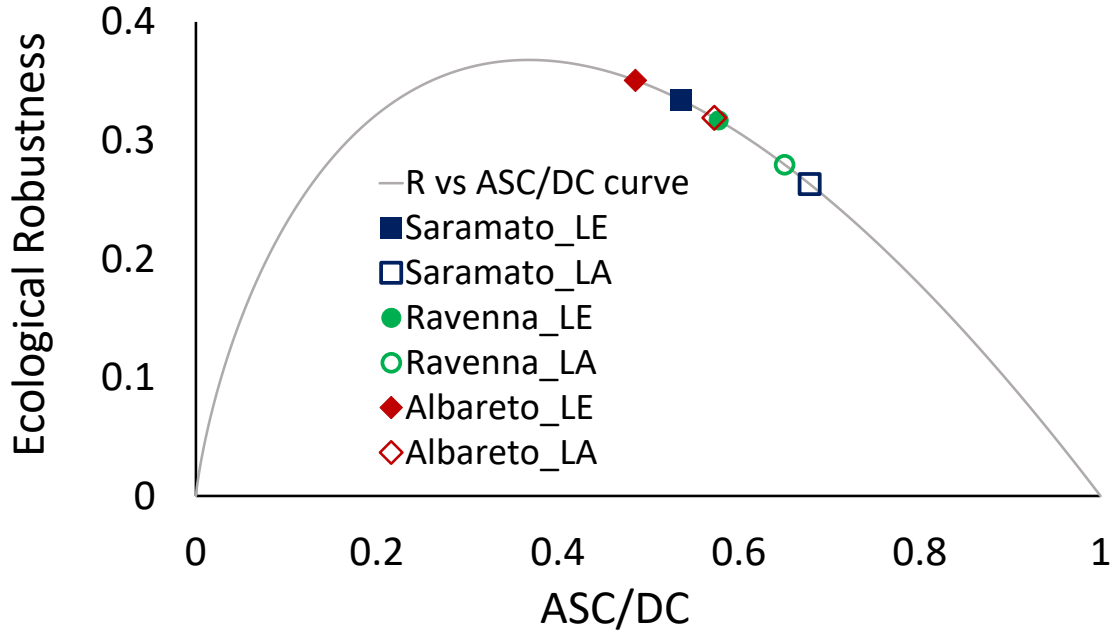

Figure 6.5: Ecological robustness vs. ASC/DC for the three Italian water networks: Saramato, Ravenna, and Albareto. Links modeled as edges (LE) are signified with solid points and links modeled as actors (LA) with hollow points. Original figure published in Panyam and Layton [10].

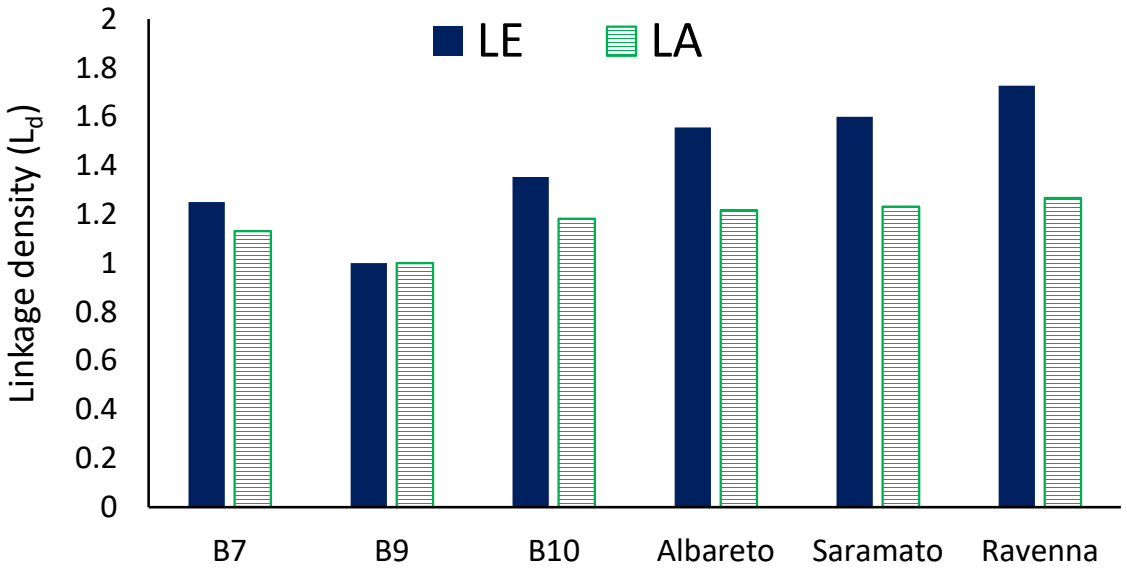

Figure 6.6: Variations in the linkage density between the LE (solid) and LA (lines) modeling approaches for the power grids (B7, B9, B10) and water networks. Original figure published in Panyam and Layton [10].

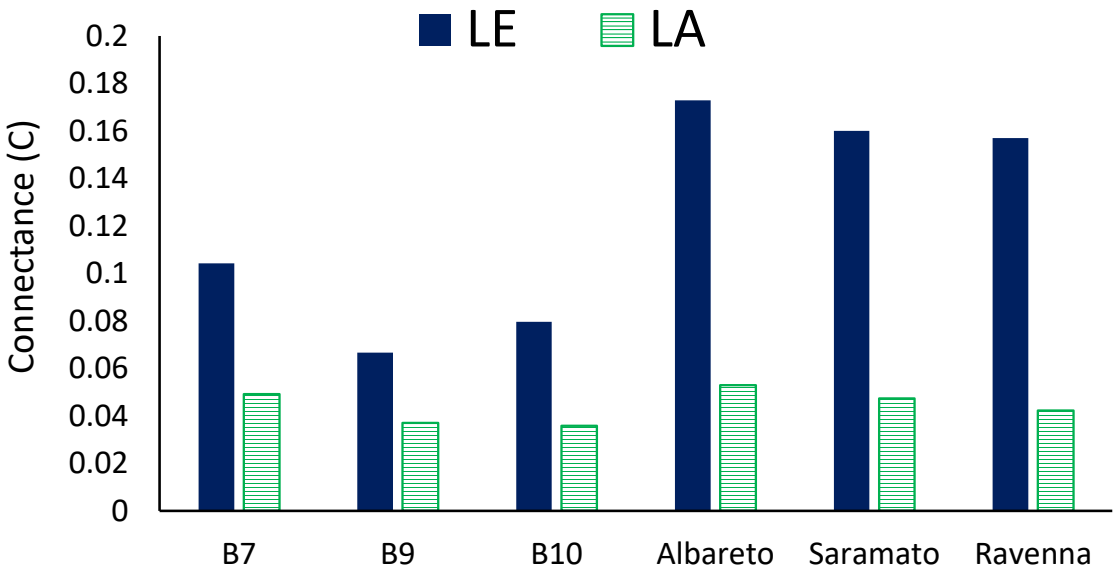

Figure 6.7: Variations in connectance between LE (solid) and LA (lines) modeling approaches for the power grids (B7, B9, B10) and water networks. Original figure published in Panyam and Layton [10].

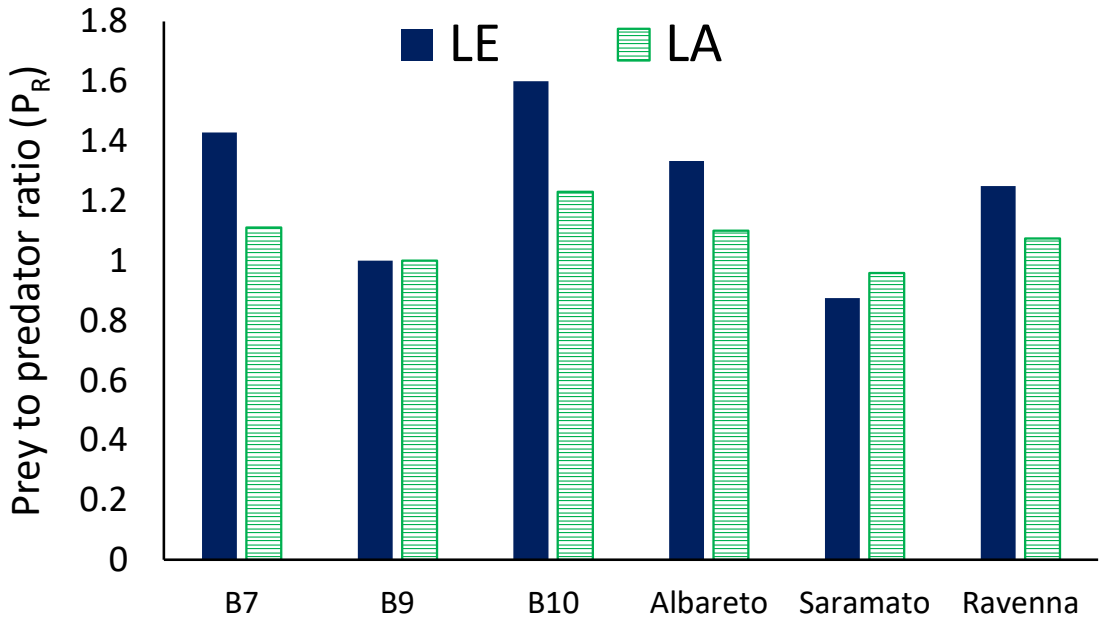

Figure 6.8: Variations in the values of prey to predator ratio between the LE (solid) and LA (lines) modeling approaches for the power grids (B7, B9, B10) and water networks. Original figure published in Panyam and Layton [10].

networks.

6.5.1 LE vs. LA - structural metrics

Modeling the links as actors versus edges changes the size of the network, the metric values, and in some cases the relative values between different networks. Modeling the networks following the LA method, links as actors, does not change the actual network structure. However new actors do appear, one for every link being considered, in the digraph. These new actors in most cases have very limited connectivity, each has only one input and one output. These ”new" actors cause a change in all the structural metrics, primarily due to the simple change that one link has become one actor and two links (increasing the number of links and actors each by 1 for every link that become an actor). Decreases in both connectance and linkage density, which both depend on the relative number of actors and links, are summarized in Table 6.2. These decreases are due to larger percentage changes in the number of actors than in the number of links. The linkage density of the 9-bus power grid network is the outlier, it remains the same due to the low (equal to one, compared

to values greater than one for others) linkage density of the original LE network.

All six networks experience larger decreases in connectance than linkage density when going from an LE to an LA model. Connectance squares the number of actors in the denominator and so a larger decrease in C vs. L_D is expected. This amplification results in even the 9-bus power grid network experiencing a drop in connectance. The prey to predator ratio also generally decreases when modeled using the LA approach, except for the 9-bus grid and the Saramato water network. Prey to predator ratio for the 9-bus grid doesn't change, which could be due to its low initial linkage density (one or less). The ratio increases for the Saramato water network, possibly due to the high number of predators or consumers in the real network (P_R less than one): those networks that saw a decrease in P_R all had initial LE P_R values greater than one. Overall, the changes in structural metrics are in line with the analytical expectations.

6.5.2 LE vs. LA - flow metrics

Ecological robustness R has been an ENA metric of interest for designing bio-inspired human networks. ENA flow metrics, of which robustness is one, are calculated using the flow matrix [**T**] that includes dissipation information from each actor (Fig. 6.2). As such, it is important to investigate how R might be affected using LE vs. LA (adding in the dissipation information listed in Table 6.1). Table 6.2 lists the values of robustness using the two modeling approaches. Robustness is directly affected by AMI and H (Eq. 3.15). These both are seen to increase when dissipation is considered (LA). AMI (information or pathway efficiency) increases more than H (pathway redundancy) in all six networks. Pathway efficiency and redundancy in ecological food webs are measured in terms of the number of options for the next step that a unit of flow has when it is at any one node, and therefore this increase in AMI signifies a higher level of constraint on the flows or overall lower number of options in the network when each link is modeled as an actor. The LA modeling approach therefore suggests that the network robustness is also a function of the transportation method used to have the material/energy travel from one actor to another. Transmission lines and pipelines can be damaged by hazards and disturbances and the LA modeling technique accounts for these vulnerabilities making it a potentially helpful approach for

these types of human networks. This vulnerability accounting is seen here for the power grids and water networks, the increase in the ratio AMI/H (i.e. ASC/DC) results in a decrease in R (the decrease caused by AMI/H increasing in Fig. 6.4 and 6.5).

There is an interesting reversal in the relative positioning of the networks, seen in Fig.6.5. The Ravenna water network becomes more robust than the Saramato network when it is modeled using LA, while it was less robust when modeled using LE. This reversal of relative positions strongly suggests that the neglect of dissipation may have significant consequences in using ENA and food web inspiration in the design of human networks, reiterating the dangers of ecological metaphors pointed out by Wells [109], that different interpretations can result in different conclusions.

6.5.3 Comparison to food webs

A significant advantage of using ENA for bio-inspired human network design is that the ENA metrics allow for an almost direct comparison with food webs, enabling designers to work towards configurations characteristic of food webs [36]. Average values of the structural metrics for food webs are, in general (P_R is the outlier), higher than for the power grids and water networks (Table 6.2). When links are considered actors (LA) the values of all the metrics move further away from the food web averages, suggesting a network configuration that is less bio-mimetic. Food webs generally have more connections between species (L) and these diverse pathways partially contribute to their high robustness. The shift away from food webs when using LA may be explained by the increase in actors with low connectance (only one input and output), something that is uncommon in food webs. Additional information about the transport methods in the network being modeled may change some of these results further. Figure 6.9 illustrates how additional knowledge about connections may impact how an LA approach may differ. Two hypothetical exchange scenarios for a distribution network are shown: scenario (i) sends material from A to B and C using two separate links and scenario (ii) has a single pipeline that connects A to both B and C. Scenario (i) modeled using LA would document each connection as a separate actor with one input and output. Scenario (ii) modeled using LA would document the connection as *one* actor with one input and *two* outputs. Knowing whether the connections in a network look more like (i) or (ii)

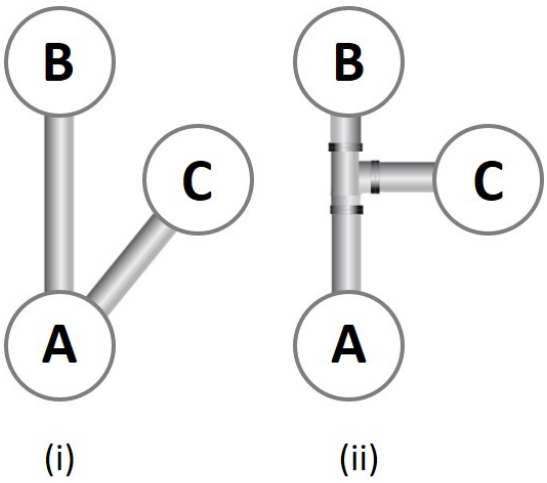

Figure 6.9: Two hypothetical exchange scenarios for a distribution network: scenario (i) sends material from A to B and C using two separate links while scenario (ii) has only one link that connects A to both B and C. Original figure published in Panyam and Layton [10].

requires a higher level of detailed information about the network but better represents the impact of the transportation in a ecological robustness analysis of a human network.

The intended use of ENA for power grids and other human networks based on structural similarities is two fold: quantifying network behaviour and mimicking food web characteristics. Often the significance of dissimilarities tends to get lost in analogical analyses as focus is mostly on similarities. Dissipation in links is one such important dissimilarity between natural ecosystems and human networks, which was heretofore neglected. The comparison of metric averages for food webs with those obtained using modeling approaches LE and LA quantitatively underlines this fundamental dissimilarity and its effect on the intended usage, suggesting that other dissimilarities between food webs and human networks may also need to be given careful consideration.

6.6 Conclusions

Considering links as actors is shown in this chapter to be one potential modeling method that can account for link dissipation and better map biological ecosystem definitions to human networks. The results presented in this chapter show that both structure and flow-based ecological metrics vary significantly for a given network, often shifting further away from food web averages

when links are considered actors in an ecosystem-based analysis. Although most networks investigated here followed a certain increasing or decreasing trend between modeling links as edges vs actors, the variations were not general. This work concludes that the choice of how to model an interaction between two entities in a human network is not inconsequential. Careful thought must therefore be given before analyzing human networks using ENA. Further research is required to determine the best way to account for dissipation and the functional role of transport in ecosystem-based analyses of human networks.

7. AN ECOSYSTEM PERSPECTIVE FOR THE DESIGN OF SUSTAINABLE POWER SYSTEMS[1]

7.1 Introduction

As outlined in chapter 2, grids are evolving to be more bi-directional with increasing distributed generation at consumers. The literature review also highlighted the lack of a concrete definition of sustainability for power systems. This chapter thus deals with building a theoretical framework for defining a two-fold approach to improve the sustainability of power systems, addressing grid reliability and renewable energy integration into the grid using ecological cycling metrics. First, ecological cycling is investigated as a measure to quantify cyclic pathways in grids with and without generation at consumers and second, this cycling is related to the N-1 reliability of the grid.

7.2 Methods and model

7.2.1 Power grid test cases

Eight hypothetical grids and two realistic grids are used as test cases. The grids are again simulated using PowerWorld Simulator [7]. Nine out of these ten grids are free models included in PowerWorld. The tenth grid is a 37-bus real power grid from [148].

7.2.2 Modelling power grids as food webs

The ecological flow matrix [**T**] and the food web matrix used for power grids in this chapter is slightly different from the ones used in chapter 5, because consumers are modeled as actors here whereas they were modeled as outputs there. Modeling consumers as actors is critical to the analysis here as cycling originates due to consumer power generation.

[1]Material presented in this chapter is reprinted with permission from "An ecosystem perspective for the design of sustainable power systems" by Panyam et al., 2019. Procedia CIRP, 80, 269-274, Copyright [2019] by Elsevier

		1	2	3	4	5	6	7	8	9	10	11	12	13	14
			Generator 1	Bus 1	Bus 2	Bus 3	Bus 4	Bus 5	Slack Generator	Transformer 1	Transformer 2	Consumer 1	Consumer 2	Output	Dissipation
Input	1	0	420	0	0	0	0	0	489	0	0	0	0	0	0
Generator 1	2	0	0	0	0	420	0	0	0	0	0	0	0	0	0
Bus 1	3	0	0	0	0	0	0	0	0	489	0	0	0	0	0
Bus 2	4	0	0	0	0	0	0	0	0	0	0	250	0	0	2.1
Bus 3	5	0	0	0	0	0	0	0	0	0	0	0	650	0	0.9
Bus 4	6	0	0	0	91	0	0	0	0	0	231	0	0	0	2.4
Bus 5	7	0	0	0	161	0	325	0	0	0	0	0	0	0	3.7
Slack Generator	8	0	0	489	0	0	0	0	0	0	0	0	0	0	0
Transformer 1	9	0	0	0	0	0	0	489	0	0	0	0	0	0	0
Transformer 2	10	0	0	0	0	231	0	0	0	0	0	0	0	0	0
Consumer 1	11	0	0	0	0	0	0	0	0	0	0	0	0	250	0
Consumer 2	12	0	0	0	0	0	0	0	0	0	0	0	0	650	0
	13	0	0	0	0	0	0	0	0	0	0	0	0	0	0
	14	0	0	0	0	0	0	0	0	0	0	0	0	0	0

Figure 7.1: Flow matrix [**T**] for the 5-bus power grid (B5_2).The inner light grey section documents the inter-compartmental flows. The inputs, useful outputs, and dissipation that crosses the system boundaries are documented in the cross hatched top row, the medium grey second to last column, and the dark grey last column respectively. Original figure published in Panyam et al. [4].

7.2.3 Ecological cycling metrics

The metrics *cyclicity* (λ_{max}) and *cycling index* (*CI*) are used by ecologists to measure the presence and strength of cyclic pathways and cycling in an ecosystem. Cyclicity is calculated from the food web matrix and *CI* from the flow matrix.

Cyclicity quantifies the presence and strength of structural cycles in a network and is calculated as the magnitude of the largest real eigenvalue of the structural adjacency matrix [**A**], Eq. 7.1 [98]. The structural adjacency matrix [**A**] is the transpose of the food web matrix. The Perron-Frobenius theorem guarantees the existence of an eigenvalue with a modulus greater than all others for non-negative matrices [149]. A simple proof of how maximum eigenvalue captures cyclic pathways in graphs described using spectral properties of digraphs can be found in [149]. Cyclicity can be a value of zero (no cyclic pathways present), one (at least a single cycle with a path length greater than 1), or any value greater than one. Cyclicity also measures the rate at which the number of

cycles in a network proliferate with increasing path length. Food webs are made up of many highly complex cyclic pathways and therefore are characteristic of higher cyclicity values [150].

$$|\mathbf{A} - \lambda\mathbf{I}| = 0 \tag{7.1}$$

Cycling index (*CI*, also known as Finn Cycling Index *FCI*) is the ratio of the cycled throughflow (TSTc) to the total internal throughflow (TSTf) in the network (Eq. 7.2) [151, 97]. Cyclicity and *CI* quantify the extent of cycling from different perspectives. *TSTf*, following Eq. 7.3, is the sum of inputs and all the inter-compartmental exchanges in [**T**] [151]. *TSTc* is computed following Eq. 7.4, where [**L**] is the Leontief's inverse matrix whose diagonal elements (L_{jj}) indicate the average number of times a quantum of flow passes through the same actor [94].

$$CI = \frac{TSTc}{TSTf} \tag{7.2}$$

$$TSTf = \sum_{i=0}^{N}\sum_{j=0}^{N} T_{ij} \tag{7.3}$$

$$TSTc = \sum_{j=1}^{N} T_j \left(\frac{L_{jj} - 1}{L_{jj}}\right) \tag{7.4}$$

7.2.4 Grid modifications

Two 5-bus power grids, $B5\_1$ and $B5\_2$ (which have different loads and components), were selected for modification from the set of sample cases available. The three modifications made to each mimic distributed generation that occurs in real power grids. $B5\_1$ and $B5\_2$ are moderately complex with realistic loads and connections, making them ideal for demonstrating the newly transpiring cyclic pathways caused by distributed generation. The distributed generation is created by adding a generator with varying capacities in the place of the load, representing a consumer becoming a small source of power generation, as seen in Fig. 7.2(b), where a 200 MW generator replaces consumer-1 changes, thereby changing the connections from the original B5_1 grid Fig.

7.2(a). The addition of a generator changes the phase angles at different buses in the grid leading to change in power flow magnitudes and directions in some of the transmission lines.

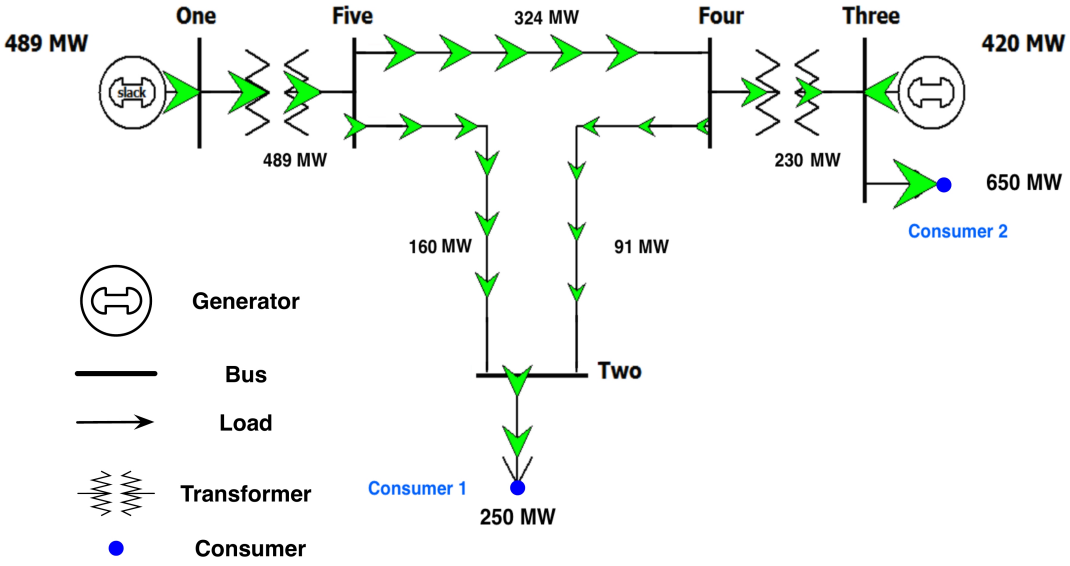

(a)

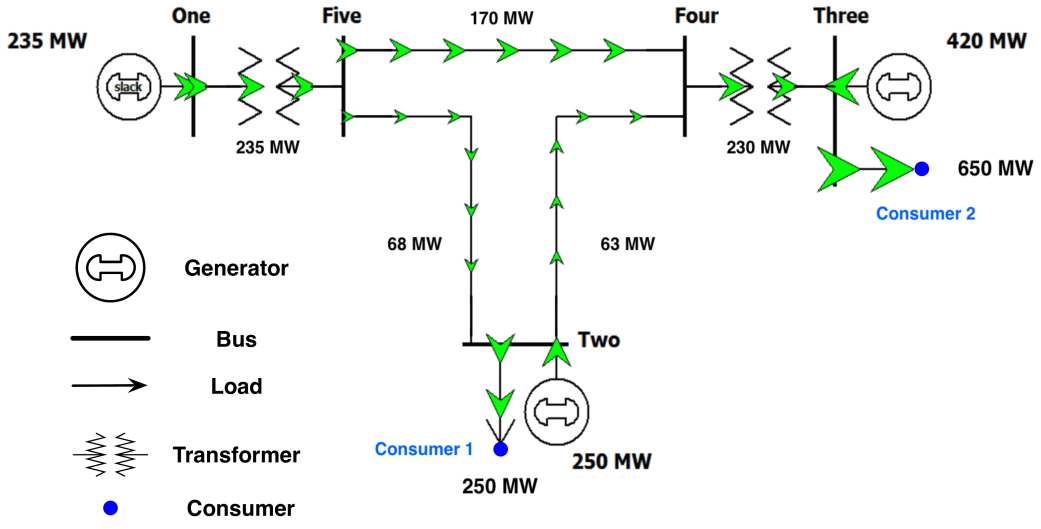

(b)

Figure 7.2: (a) The original grid $B5\_2$ as represented in PowerWorld and (b) the modification of customer-1 generating 200 MW. Original figure published in Panyam et al. [4].

Three consumer-1 modifications of increasing generation capacity (50, 150, 250 MW) are made to the $B5\_2$ grid. An assumption is made that the excess generation at consumer-1 is supplied to the grid only during half of its active time period, since renewable energy can be unpredictable. During the non-generation period consumer-1 is assumed to receive power from the grid, and the original grid configuration is active. The sum of the corresponding power flows (T_{ij}) in each period are considered as the entries in the flow matrix, representing the average network structure and function. The 4 consumer $B5\_1$ grid is modified with 40MW generating capacities at one, two, and three consumers.

7.2.5 Validation

N-1 contingency analysis is used for validation of all the grid scenarios to examine whether the added cycling due to distributed generator corresponds to a more or less reliable grid.

7.3 Results

The λ_{max} and CI for the eight original grids and one of the two realistic grids are all zero. The 37-bus realistic grid however has a λ_{max} value of 1.0 and a *CI* of 0.00089. The cyclic pathways in the modified B5_2 grid are highlighted in Fig. 7.3, showing that a total of three cycles exist in the system when consumer-1 is producing an excess generation of 200 MW.

Analysis of 104 food web models [152], available in the package $enaR$ for use in the free programming language R, reveals that food webs have a mean λ_{max} value of 4.35 and a mean CI of 0.39. The grid modifications are summarized in Table 7.1 and show that the cycling that is introduced through the consumer generation brings the grid closer to the average cyclic structure and function of food webs. The reliability of the modified networks, as measured by the N-1 contingency analysis, is also shown to increase with these modifications. The number of violations in the N-1 contingency analysis of the original and modified power grids are shown in Table 7.1. An exponential decrease in the number of violations is observed in the N-1 contingency analysis as the modifications increase the number of cycles in the grid. Increasing cyclicity and *CI* both show a smooth exponential correlation with decreases in the number of N-1 violations, as seen in

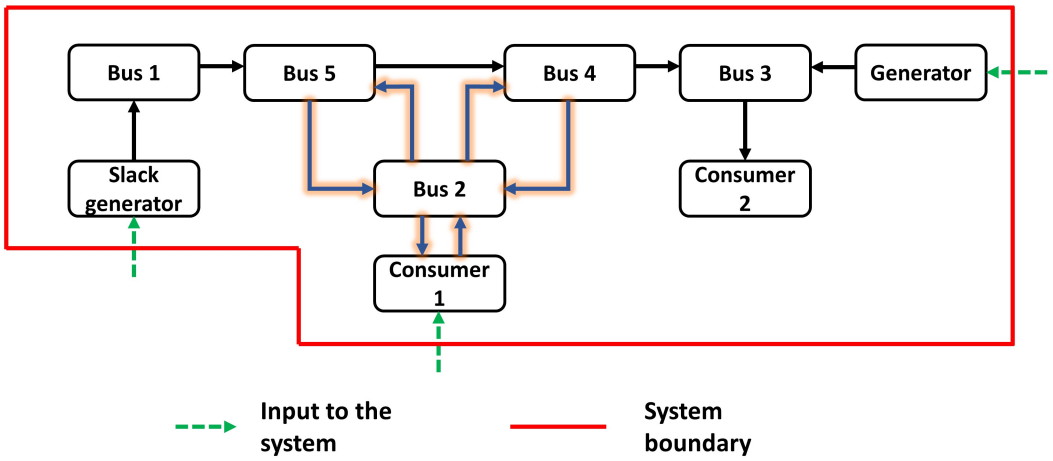

Figure 7.3: The modified B5_2 pathways and connections averaged over an entire day when consumer-1 has an excess generation of 200 MW. This representation is the combination of the two network scenarios shown in Fig. 7.2. Original figure published in Panyam et al. [4].

Fig. 7.4 and 7.5.

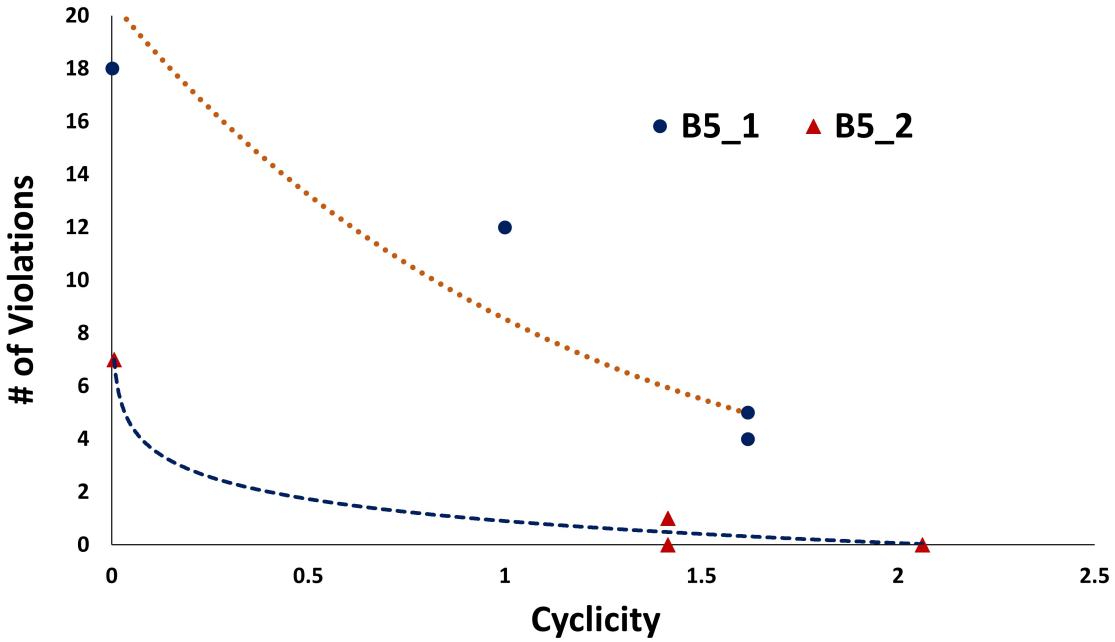

Figure 7.4: Modifications to both the B5_1 and B5_2 grids show an exponential decay in the number of N-1 violations (y-axis) as cyclicity increases (x-axis). Original figure published in Panyam et al. [4].

Grid ID	Grid modifications	λ_{max}	CI	# N-1 violations
B5_1	Sample case - original	0	0	18
B5_1a	40 MW at consumer-2	1	0.0135	12
B5_1b	40 MW at consumer-2 and 4	1.618	0.0878	5
B5_1c	40 MW at consumer-2, 3, 4	1.618	0.136	4
B5_2	Sample case - original	0	0	7
B5_2d	50 MW at consumer-1	1.414	0.0158	1
B5_2e	150 MW at consumer-1	1.414	0.0347	0
B5_2f	250 MW at consumer-1	2.06	0.0637	0

Table 7.1: The cycling index (CI), cyclicity (λ_{max}), and N-1 contingency analysis violations of the original grids (B5_1 and B5_2), grids modified with excess generation at consumer 2 (B5_1a), consumers 2 and 4 (B5_1b), and consumers 2, 3, and 4 (B5_1c), and consumer 1 (B5_2d, B5_2e, B5_2f). The grid IDs are used for identifying modifications to the original B5_1 and B5_2 grids. Original table published in Panyam et al. [4].

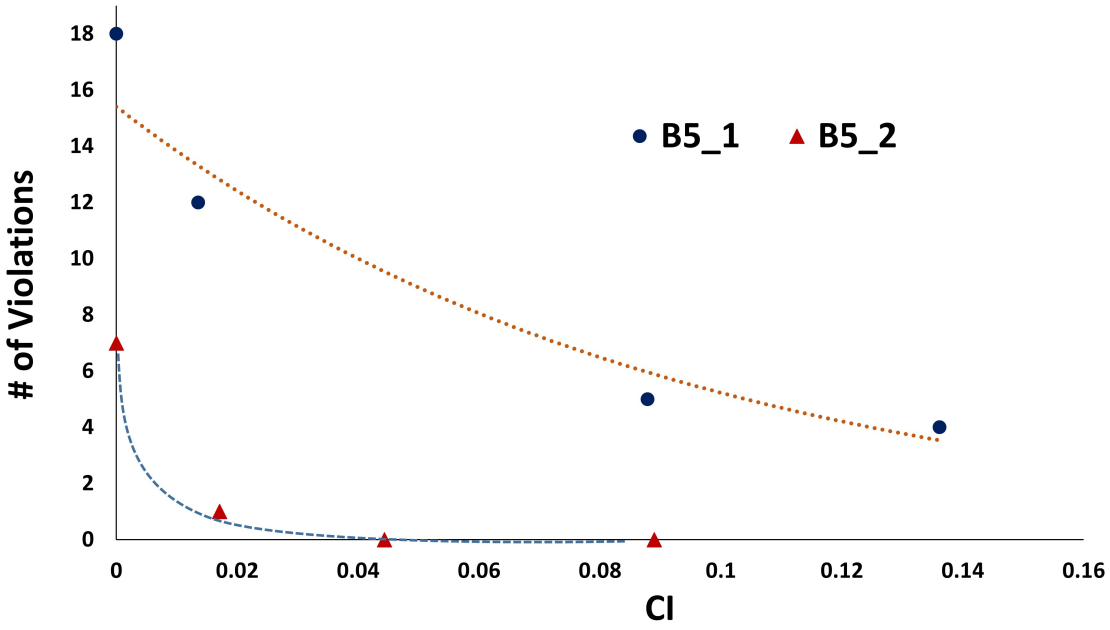

Figure 7.5: Modifications to both the B5_1 and B5_2 grids show an exponential decay in the number of N-1 violations (y-axis) as cycling index (CI) increases (x-axis). Original figure published in Panyam et al. [4].

7.4 Discussion

The results suggest that cycles are not present in traditional power grids, all the unmodified grids except for the 37-bus system had λ_{max} and CI values of zero. The 37-bus system did demonstrate extremely weak and simple cycling with a CI of 0.00089 and a λ_{max} of one. Based on the behavior of the other nine grids this appears to be an exception rather than the rule, however more large grids need to be investigated to further support that traditional power grids have a one-way chain-like structure. The two cycling metrics are used in ecology to identify cyclic energy pathways that influence food web network characteristics such as robustness, organizational efficiency etc. The results suggest that they may be useful in the design of robust power systems as well, as the two metrics effectively quantify power cycles and correlate strongly with improved N-1 reliability ratings.

Cycles in power systems at an instant cannot exist because it requires real power to traverse over a loop and come back to its origin that is against Kirchhoff's laws and dissipates excess power.

Considering power flows over longer time periods may vary the magnitudes but will not change the flow directions in the traditional grids. Directional changes do however occur in the consumer sell-back grid scenarios, as seen in Figure 7.3. It is important to note however that, from a resilience perspective, in the modified configurations not all links are simultaneously active and the intermittent and somewhat unpredictable nature of renewables due to their dependence on weather conditions, unlike traditional fossil-fuel based electricity generation, makes these connections difficult to depend on in critical situations.

Modifications made to the 5-bus grids show increasing improvements to the N-1 reliability measure, with the number of violations in the network exponentially decreasing as the amount of cycling increased. The largest amount of total excess generation that was sold back to the grid saw the highest CI, 120MW total in B5_1c had a CI of 0.136. The highest amount of generation at a single consumer resulted in the highest λ_{max} and the best N-1 rating, 250MW in B5_2f had a λ_{max} of 2.06 and zero N-1 violations. The violations counted by the N-1 analysis can be either overflow in transmission line, voltage exceeding its limit in a bus, or both. A lower number of N-1 violations means more consumers receive the required power without disruptions. Future work will focus on analyzing power grids with more consumers, enabling a higher number of distributed generation systems to be placed in the grid.

7.4.1 Renewable energy storage

The integration of renewables locally requires a reliable and affordable energy storage system for such distributed generators, especially in scenarios with higher generation values and thus higher cycling. Electricity storage devices can store electricity when production exceeds demand and use the storage during peak-demand periods to ensure a balance for demand and supply [153]. The grid with the highest λ_{max}, B5_2f, also has the highest generation of 250MW. The higher cyclicity value in B5_2f is due to the slack generator receiving power, which does not occur for B5_2d and B5_2e where the lower generations of 50 and 150 MW are not enough power to require storage. The unexpected intervals that occur with renewable source require energy storage, a field that is still relatively new. These electricity storage technologies must be robust, reliable

and economically competitive [154]. Commercial electricity storage technologies, for example pumped hydro, flywheels, electrical batteries, and compressed air energy storage, are available for large scale renewable energy generation. The problem of optimal placement of storage devices with the objective of maximizing reliability is an area of further work.

7.4.2 Cyclicity vs cycling index for power systems

Differences in meaning between cyclicity and cycling index gives value to using both metrics, and can be explained using the grids B5_2d and B5_2e. Figure 7.4 shows that cyclicity for these two grids is the same, whereas the number of violations observed are different (the same is true for B5_1b and B5_1c). *CI* however varies for all the modified grids. The physical connections in B5_2d are the same as those in B5_2e resulting in λ_{max} remaining the same, however the 150MW excess generation in B5_2e leads to a higher magnitude of power being cycled (higher CI). A larger data set of power grids needs to be investigated to further reveal the relationship between N-1 reliability and cycling.

7.5 Conclusion

Distributed generation resulting from consumer installed renewable energy generators has seen a steady increase over the years, resulting in a rise in consumer sell-back to the grid. The circular power flow pathways that result from this sell back resemble the cyclic structure and organization characteristic of ecological food webs. Traditional power grids have revealed that no cyclic structure exists, however when modified to mimic basic consumer sell back the grids showed both cyclic structure and an increasing magnitude of cycled power. The ecological metrics cyclicity and cycling index are able to quantitatively measure the presence and complexity of cyclic pathways in the grid as well as the magnitude of power that is cycled. The results suggest that increasing the prevalence and magnitude of consumer power generation increases the ecosystem-type cycling as well as corresponds to improved N-1 reliability rating of the grid. The characteristically cyclic organization of ecosystems may thus provide a new approach to analyze these emerging sustainable two-way grids.

8. SUMMARY AND FUTURE WORK

8.1 Summary

This thesis presents an innovative biologically inspired approach to improve the robustness and resilience of power grid networks. The structural similarity between these two system-types is exploited through the application of ecological properties and analysis techniques to power grid design.

First, twenty-three variations on the Brayton and Rankine cycles are used to understand the relationship between design decisions that maximize a system's efficient use of energy (measured by thermodynamic first law efficiency) and ecological measures of robustness and structural efficiency. The results reveal that thermodynamic efficiency and ecological pathway efficiency do not always correlate and that while on average modifications to increase energy efficiency reduce the robustness of the system, the engineering understanding of ecological network design presented here can enable decisions that are able to increase both energy efficiency *and* robustness.

Second, a framework is established to create food web models of power grid networks. The level of biological similarity between these two system-types is quantitatively investigated and compared by computing ecological network metrics for a set of synthetic power systems and food webs. The comparison substantiates the use of the ecological robustness metric for optimizing the design of power grid networks. A bio-inspired optimization model is implemented, which restructures the synthetic power systems to mimic ecosystem robustness. The bio-inspired optimal networks are evaluated using N-1, N-2, and N-3 contingency analyses to assess system performance under the loss of 1, 2, and 3 components respectively. The bio-inspired grids all experienced significantly fewer violations in each loss scenario compared to traditional configurations, further supporting the application of the ecological robustness metric for power system robustness. The results provided insights into how ecological robustness can guide the design of power systems for improved infrastructural resilience to better survive disturbances.

Third, the cyclic organization of food webs is proposed as a design principle to quantify the effectiveness of two-way connections between the grid and consumers. Two hypothetical 5-bus grids are modified to replicate the two-way exchanges of real power systems with consumer renewable energy generation. The results show a positive correlation between increased structural cycling in grids and reliability improvements measured using N-1 contingency analysis. These results suggest that the metrics cyclicity and cycling index can play a role in quantifying and improving the sustainability of power grids.

8.2 Future work

The work done in this thesis provides strong evidence to support the hypothesis that power grid networks can benefit by mimicking the naturally sustainable structures of food webs. Numerous research questions arise from the results, presenting interesting avenues for the following future work in this field:

8.2.1 Cost-benefit analysis of the bio-inspired power grid networks

A previous analysis of ecosystems and industrial networks hypothesized that the high connectivity in ecosystem networks could be the predominant reason for their high ecological robustness value [25]. This hypothesis was observed to be true for power systems as well: all the power grids needed additional transmission lines to increase the ecological robustness value. However, it may not be economically feasible for power grids to replicate the high connectivity seen in food webs. Each additional transmission line requires significant investment. Thus unanswered questions remain regarding the financial feasibility of the bio-inspired design approach which depend on the quantitative relationship between ecological robustness and the number of links. A preliminary investigation aimed at answering these questions (shown in figures 8.1, 8.2 and 8.3) revealed that robustness of the networks only improves marginally as more and more links are added prompting a careful selection of the links to be added when using ecological robustness as a design objective. Future research can investigate if these results hold true for larger power systems as well. Future research can also look at how other important ecological metrics vary in these different

configurations of the same grid systems.

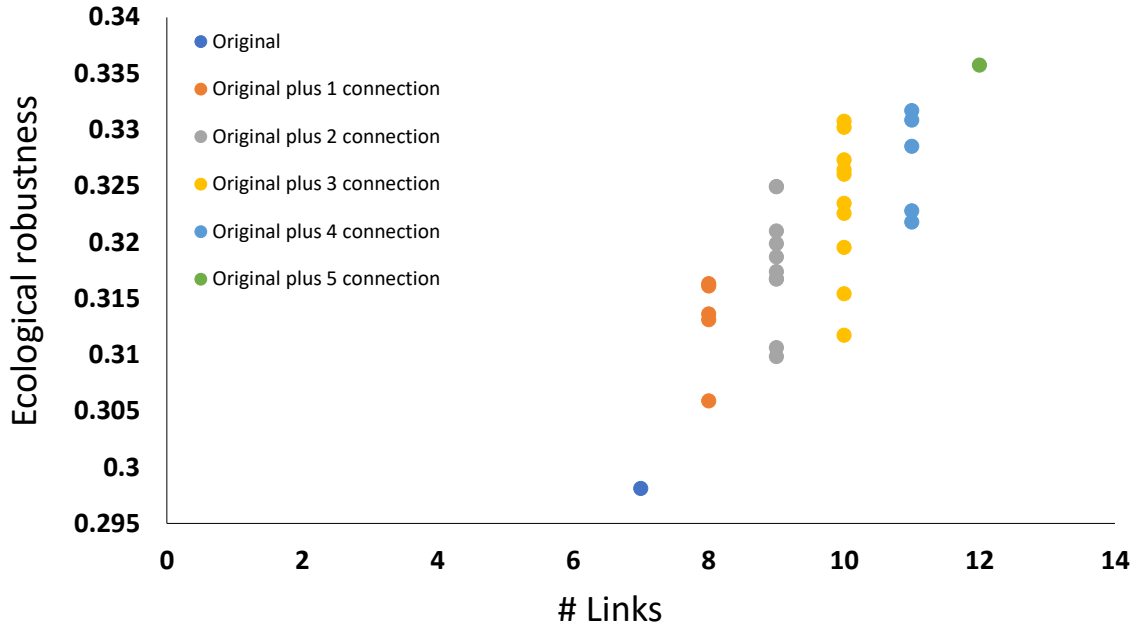

Figure 8.1: The plot of ecological robustness vs. the number of links for a 5-bus test system. Different points on the plot indicate different configurations of the same system with same load

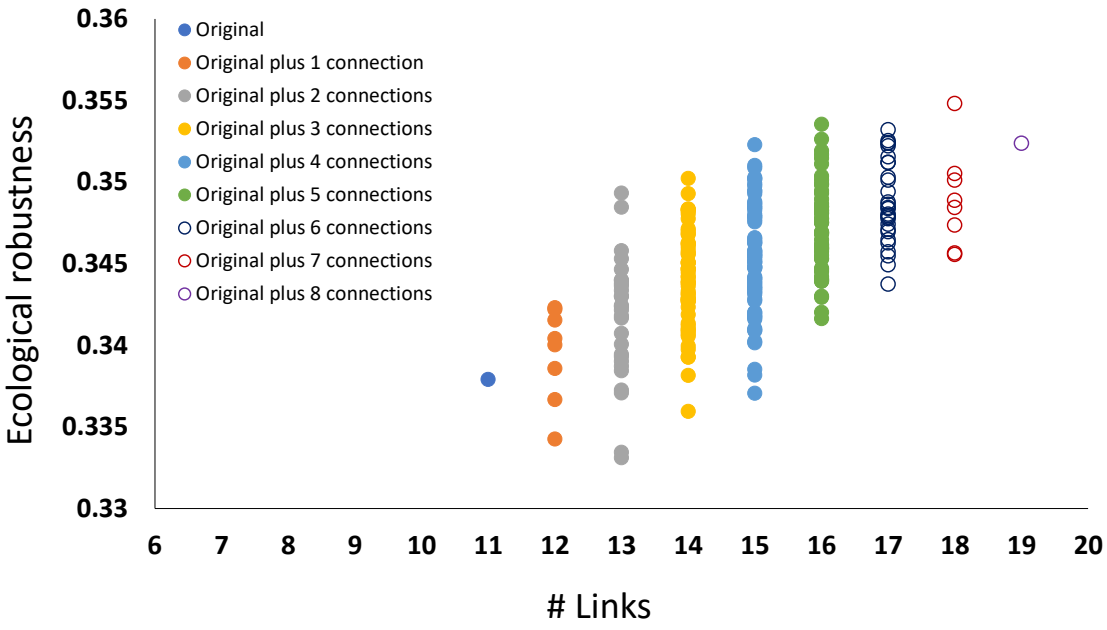

Figure 8.2: The plot of ecological robustness vs. the number of links for a 6-bus test system. Different points on the plot indicate different configurations of the same system with same load

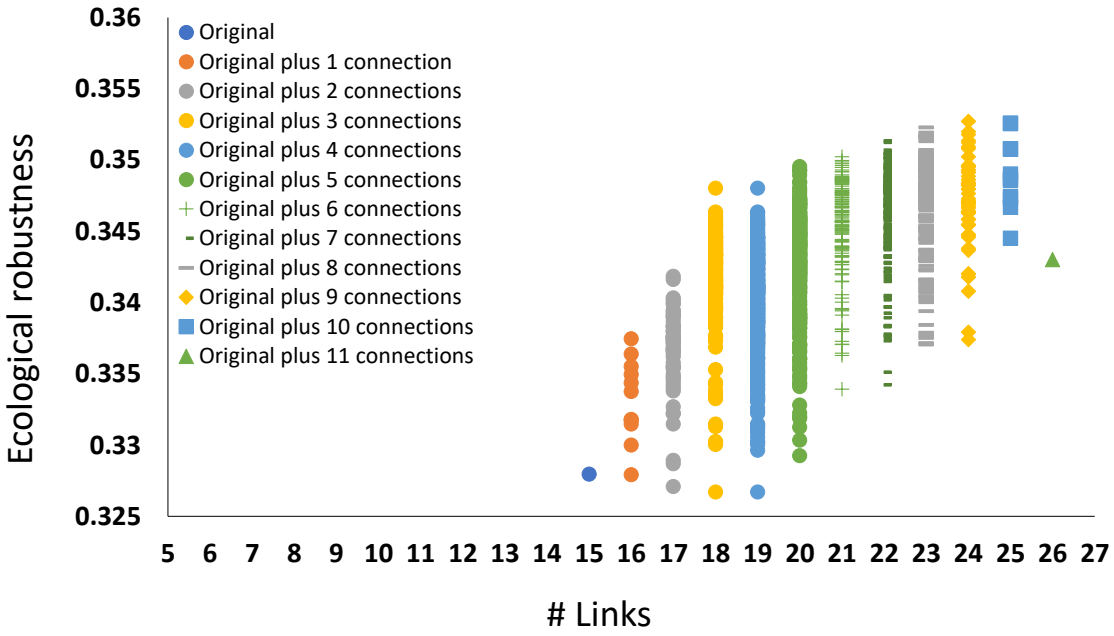

Figure 8.3: The plot of ecological robustness vs. the number of links for a 7-bus test system. Different points on the plot indicate different configurations of the same system with same load

8.2.2 Dynamic ENA analysis for power grids

A major limitation of comprehensively applying ENA to power grids is the steady state assumption. Power grids in reality are highly dynamic with power flow values changing rapidly. Thus, one important area of future work should be in addressing this limitation of ENA. This will also help shift the focus of bio-inspired design from fundamental architecture of power systems to their operational characteristics enabling more innovative applications of ENA to power systems.

8.2.3 Dealing with dissipation in the bio-inspired design of power grids

A major difference between ecological food webs and human networks is that the transfers between actors happen directly, actor to actor, in food webs and indirectly, through a transport method, in human networks. Often dissipation occurs during the transport: leaks in pipelines and losses across transmission lines for example. The consideration of links as actors to account for dissipation can have significant effect on the ecological metrics that are commonly used to evaluate human networks. New questions that arise based on the observations in chapter 6 ask - what is the right way to account for link dissipation and the functional role of transport in an ecosystem-based analysis of human networks. Only the approach considering links as actors is investigated here, however there are other potential methods to account for link dissipation. A correction factor derived from common trends, such as the decrease in connectance, could be multiplied by the equations. However more network types need to be investigated before this can be considered. Not all physical links experience dissipation and therefore considering only those links that experience dissipation as actors may also be a plausible approach. This could however introduce inconsistencies if the modeler were not careful.

8.2.4 Defining sustainability for power systems

Defining sustainability for power systems holds significant value for future research efforts to improve long term robustness and resilience of power grids. Different aspects of long term survivability that include robustness and resilience against disturbances can all be taken into consideration in an all encompassing definition of sustainability for power systems. Future work can

focus on integrating social and environmental aspects into the proposed bio-inspired method to assess how they impact sustainability of power systems.

REFERENCES

[1] U.S. Department of Energy, "Quadrennial energy review: Energy transmission, storage, and distribution infrastructure," tech. rep., 2015.

[2] V. Panyam, H. Huang, K. Davis, and A. Layton, "Bio-inspired design for robust power grid networks," *Appl. Energy*, vol. 251, p. 113349, Oct 2019.

[3] US Energy Information Administration (EIA), "Participation in electric net-metering programs increased sharply in recent years - Today in Energy," 2018.

[4] V. Panyam, H. Huang, K. Davis, and A. Layton, "An ecosystem perspective for the design of sustainable power systems," *Procedia CIRP*, vol. 80, pp. 269–274, Jan 2019.

[5] S. R. Borrett and A. K. Salas, "Evidence for resource homogenization in 50 trophic ecosystem networks," *Ecol. Modell.*, vol. 221, pp. 1710–1716, 2010.

[6] V. Panyam, T. Dave, and A. Layton, "Understanding ecological efficiency and robustness for network design using thermodynamic power cycles," in *Proc. ASME 2018 Int. Des. Eng. Tech. Conf. Comput. Inf. Eng. Conf.*, pp. 1–9, 2018.

[7] Power World Corporation, "PowerWorld Simulator," 2019.

[8] A. AL-Hinai, "Voltage collapse prediction for interconnected power systems," Master's thesis, West Virginia University, 2000.

[9] N. Mithulananthan, C. A. Cañizares, and J. Reeve, "Indices to detect hopf bifurcations in power systems," in *Proc. of NAPS*, vol. 2, pp. 15–23, Citeseer, 2000.

[10] V. Panyam and A. Layton, "Bio-inspired modelling approaches for human networks with link dissipation," in *Proc. ASME 2019 Int. Des. Eng. Tech. Conf. Comput. Inf. Eng. Conf.*, pp. 1–9, 2019.

[11] A. Layton, B. Bras, and M. Weissburg, "Ecological robustness as a design principle for sustainable industrial systems," in *Proc. ASME 2015 Int. Des. Eng. Tech. Conf. Comput. Inf. Eng. Conf. IDETC/CIE 2015 August 2-5, 2015, Boston, Massachusetts, USA*, pp. 1–8, 2015.

[12] X. Wang, Y. Koc, R. E. Kooij, and P. Van Mieghem, "A network approach for power grid robustness against cascading failures," in *2015 7th International Workshop on Reliable Networks Design and Modeling (RNDM)*, pp. 208–214, Oct 2015.

[13] Executive Office of the President of the United States, "Economic Benefits of Increasing Electric Grid Resilience To Weather Outages," tech. rep., 2013.

[14] National Academy of Engineering, "Enhancing the Resilience of the Nation's Electricity System," tech. rep., 2017.

[15] N. Nezamoddini, S. Mousavian, and M. Erol-Kantarci, "A risk optimization model for enhanced power grid resilience against physical attacks," *Electr. Power Syst. Res.*, pp. 329–338.

[16] Z. Bie, Y. Lin, G. Li, and F. Li, "Battling the Extreme: A Study on the Power System Resilience," *Proc. IEEE*, vol. 105, no. 7, pp. 1253–1266, 2017.

[17] A. Castillo, "Risk analysis and management in power outage and restoration: A literature survey," *Electr. Power Syst. Res.*, vol. 107, pp. 9–15, 2014.

[18] D. H. Kim, D. A. Eisenberg, Y. H. Chun, and J. Park, "Network topology and resilience analysis of South Korean power grid," *Phys. A Stat. Mech. its Appl.*, pp. 13–24.

[19] R. Kinney, P. Crucitti, R. Albert, and V. Latora, "Modeling cascading failures in the North American power grid," *Eur. Phys. J. B*, vol. 46, no. 1, pp. 101–107, 2005.

[20] G. Andersson, P. Donalek, R. Farmer, N. Hatziargyriou, I. Kamwa, P. Kundur, N. Martins, J. Paserba, P. Pourbeik, J. Sanchez-Gasca, *et al.*, "Causes of the 2003 major grid blackouts in north america and europe, and recommended means to improve system dynamic performance," *IEEE transactions on Power Systems*, vol. 20, no. 4, pp. 1922–1928, 2005.

[21] L. Chuck, E. Luke, D. Michael, K. David, T. Mark, and G. Wayne, "Transmission system planning performance requirements," application guide, North American Electric Reliability Corporation (NERC), 2015.

[22] G. Strbac, D. Kirschen, R. Moreno, *et al.*, "Reliability standards for the operation and planning of future electricity networks," *Foundations and Trends® in Electric Energy Systems*, vol. 1, no. 3, pp. 143–219, 2016.

[23] K. A. Akkemik, "Potential impacts of electricity price changes on price formation in the economy: a social accounting matrix price modeling analysis for turkey," *Energy Policy*, vol. 39, no. 2, pp. 854–864, 2011.

[24] M. J. Burke and J. C. Stephens, "Political power and renewable energy futures: A critical review," *Energy Research & Social Science*, vol. 35, pp. 78–93, 2018.

[25] R. E. Ulanowicz, S. J. Goerner, B. Lietaer, and R. Gomez, "Quantifying sustainability: Resilience, efficiency and the return of information theory," *Ecol. Complex.*, vol. 6, no. 1, pp. 27–36, 2009.

[26] R. E. Ulanowicz, *Growth and Development: Ecological Phenomenology*. New York: Springer-Verlag, 1 ed., 1986.

[27] L. Cuadra, S. Salcedo-Sanz, J. Del Ser, S. Jiménez-Fernández, and Z. W. Geem, "A critical review of robustness in power grids using complex networks concepts," *Energies*, vol. 8, no. 9, pp. 9211–9265, 2015.

[28] M. Panteli and P. Mancarella, "The Grid: Stronger, Bigger, Smarter?," *IEEE Power Energy Mag.*, no. May/June, pp. 58–66, 2015.

[29] G. Gallopin, "A systems approach to sustainability and sustainable development," tech. rep., Santiago, 2003.

[30] M. A. Rosen, "Engineering sustainability: A technical approach to sustainability," *Sustainability*, vol. 4, no. 9, pp. 2270–2292, 2012.

[31] B. D. Fath, "Quantifying economic and ecological sustainability," *Ocean Coast. Manag.*, vol. 108, pp. 13–19, 2015.

[32] T. Kuhlman and J. Farrington, "What is sustainability?," *Sustainability*, vol. 2, no. 11, pp. 3436–3448, 2010.

[33] S. Parkin, F. Sommer, and S. Uren, "Sustainable development: understanding the concept and practical challenge," *Eng. Sustain.*, vol. 156, no. 1, pp. 19–26, 2003.

[34] W. Chen, J. K. Allen, K.-L. Tsui, and F. Mistree, "A Procedure for Robust Design: Minimizing Variations Caused by Noise Factors and Control Factors," *J. Mech. Des.*, vol. 118, no. 4, pp. 478–485, 1996.

[35] G. Box, "Signal-to-Noise Ratios, Performance Criteria, and Transformations," *Technometrics*, vol. 30, no. 1, pp. 1–17, 1988.

[36] V. Panyam, H. Huang, B. Pinte, K. Davis, and A. Layton, "Bio-Inspired Design for Robust Power Networks," *2019 IEEE Texas Power and Energy Conference*, no. 1, pp. 1–6, 2019.

[37] R. E. Ulanowicz, "The dual nature of ecosystem dynamics," *Ecol. Modell.*, vol. 220, pp. 1886–1892, 2009.

[38] S. J. Goerner, B. Lietaer, and R. E. Ulanowicz, "Quantifying economic sustainability: Implications for free-enterprise theory, policy and practice," *Ecol. Econ.*, 2009.

[39] J. Huang and R. E. Ulanowicz, "Ecological Network Analysis for Economic Systems: Growth and Development and Implications for Sustainable Development," *PLoS One*, vol. 9, no. 6, p. 100923, 2014.

[40] A. Kharrazi, E. Rovenskaya, and B. D. Fath, "Network structure impacts global commodity trade growth and resilience," *PLoS One*, vol. 12, no. 2, pp. 1–13, 2017.

[41] A. Layton, B. Bras, and M. Weissburg, "Designing Industrial Networks Using Ecological Food Web Metrics," *Environ. Sci. Technol.*, no. 20, pp. 11243–11252.

[42] A. Layton, B. Bras, and M. Weissburg, "Improving performance of eco-industrial parks," *Int. J. Sustain. Eng.*, no. 4-5, pp. 250–259.

[43] A. Layton, B. Bras, and M. Weissburg, "Industrial Ecosystems and Food Webs: An Expansion and Update of Existing Data for Eco-Industrial Parks and Understanding the Ecological Food Webs They Wish to Mimic," *J. Ind. Ecol.*, vol. 20, no. 1, pp. 85–98, 2016.

[44] A. Bodini and B. Cristina, "Bodini 2002 sustainanble-water resource-wholesystem.pdf," *Int. J. Environ. Pollut.*, vol. 18, no. 5, pp. 463–485, 2002.

[45] B. D. Fath, U. M. Scharler, R. E. Ulanowicz, and B. Hannon, "Ecological network analysis: network construction," *Ecol. Modell.*, vol. 208, no. 1, pp. 49–55, 2007.

[46] M. K. Lau, S. R. Borrett, B. Baiser, N. J. Gotelli, and A. M. Ellison, "Ecological network metrics: Opportunities for synthesis," *Ecosphere*, vol. 8, no. 8, 2017.

[47] S. R. Borrett and M. K. Lau, "enaR: An R package for Ecosystem Network Analysis," *Methods Ecol. Evol.*, vol. 5, no. 11, pp. 1206–1213, 2014.

[48] R. E. Ulanowicz, "Information theory in ecology.," *Comput. Chem.*, no. 4, pp. 393–399.

[49] R. E. Ulanowicz, "Quantitative methods for ecological network analysis," *Comput. Biol. Chem.*, vol. 28, no. 5-6, pp. 321–339, 2004.

[50] R. Bailey, B. Bras, and J. K. Allen, "Applying Ecological Input-Output Flow Analysis to Material Flows in Industrial Systems: Part II: Flow Metrics," *J. Ind. Ecol.*, no. 1-2, pp. 69–91.

[51] A. Kharrazi, E. Rovenskaya, B. D. Fath, M. Yarime, and S. Kraines, "Quantifying the sustainability of economic resource networks: An ecological information-based approach," *Ecol. Econ.*, vol. 90, pp. 177–186, 2013.

[52] S. M. Malone, M. J. Weissburg, and B. Bras, "Industrial Ecosystems and Food Webs: An Ecological-Based Mass Flow Analysis to Model the Progress of Steel Manufacturing in China," *Engineering*, no. 2, pp. 209–217.

[53] S. Chen and B. Chen, "Urban energy consumption: Different insights from energy flow analysis, input-output analysis and ecological network analysis," *Appl. Energy*, pp. 99–107.

[54] Y. Zhang, S. Li, B. D. Fath, Z. Yang, and N. Yang, "Analysis of an urban energy metabolic system: Comparison of simple and complex model results," *Ecol. Modell.*, no. 1, pp. 14–19.

[55] R. Guo, X. Zhu, B. Chen, and Y. Yue, "Ecological network analysis of the virtual water network within China's electric power system during 2007-2012," *Appl. Energy*, pp. 110–121.

[56] S. Wang, B. Fath, and B. Chen, "EnergyâĂŞwater nexus under energy mix scenarios using inputâĂŞoutput and ecological network analyses," *Appl. Energy*, no. 19, pp. 827–839.

[57] S. Chen and B. Chen, "Urban energyâĂŞwater nexus: A network perspective," *Appl. Energy*, pp. 905–914.

[58] S. Chen, B. Xu, and B. Chen, "Unfolding the interplay between carbon flows and socioeconomic development in a city: What can network analysis offer?," *Appl. Energy*, vol. 211, pp. 403–412, 2018.

[59] G. P. Hammond, "Engineering sustainability: Thermodynamics, energy systems, and the environment," *Int. J. Energy Res.*, vol. 28, no. 7, pp. 613–639, 2004.

[60] E. Schneider and J. Kay, "Life as a manifestation of the second law of thermodynamics," *Math. Comput. Model.*, vol. 19, pp. 25–48, Mar 1994.

[61] A. Layton, J. Reap, B. Bras, and M. Weissburg, "Correlation between Thermodynamic Efficiency and Ecological Cyclicity for Thermodynamic Power Cycles," *PLoS One*, vol. 7, no. 12, pp. 1–7, 2012.

[62] J. H. Eto and K. H. Lacommare, "Tracking the Reliability of the U.S. Electric Power System: An Assessment of Publicly Available Information Reported to State Public Utility Commissions," Tech. Rep. October.

[63] Å. J. Holmgren, "Using graph models to analyze the vulnerability of electric power networks," *Risk Analysis*, vol. 26, no. 4, pp. 955–969, 2006.

[64] A. Gholami, T. Shekari, M. Hassan, F. Aminifar, H. Amini, and A. Sargolzaei, "Toward a Consensus on the Definition and Taxonomy of Power System Resilience," *IEEE Access*, vol. 6, pp. 1–15, 2018.

[65] P. Dehghanian, S. Aslan, and P. Dehghanian, "Maintaining Electric System Safety Through An Enhanced Network Resilience," *IEEE Trans. Ind. Appl.*, vol. 54, no. 5, pp. 4927–4937, 2018.

[66] M. Panteli, D. N. Trakas, P. Mancarella, and N. D. Hatziargyriou, "Power Systems Resilience Assessment: Hardening and Smart Operational Enhancement Strategies," *Proc. IEEE*, vol. 105, no. 7, pp. 1202–1213, 2017.

[67] M. Panteli, D. N. Trakas, P. Mancarella, and N. D. Hatziargyriou, "Boosting the power grid resilience to extreme weather events using defensive islanding," *IEEE Transactions on Smart Grid*, vol. 7, no. 6, pp. 2913–2922, 2016.

[68] Z. Li, M. Shahidehpour, F. Aminifar, A. Alabdulwahab, and Y. Al-Turki, "Networked microgrids for enhancing the power system resilience," *Proceedings of the IEEE*, vol. 105, no. 7, pp. 1289–1310, 2017.

[69] H. Farzin, M. Fotuhi-Firuzabad, and M. Moeini-Aghtaie, "Enhancing power system resilience through hierarchical outage management in multi-microgrids," *IEEE Transactions on Smart Grid*, vol. 7, no. 6, pp. 2869–2879, 2016.

[70] A. Gholami, T. Shekari, F. Aminifar, and M. Shahidehpour, "Microgrid scheduling with uncertainty: The quest for resilience," *IEEE Transactions on Smart Grid*, vol. 7, no. 6, pp. 2849–2858, 2016.

[71] H. Davarikia and M. Barati, "A tri-level programming model for attack-resilient control of power grids," *Journal of Modern Power Systems and Clean Energy*, vol. 6, no. 5, pp. 918–929, 2018.

[72] S. A. Zonouz, K. M. Rogers, R. Berthier, R. Bobba, W. H. Sanders, and T. J. Overbye, "Scpse: Security-oriented cyber-physical state estimation for power grid critical infrastructures.," *IEEE Trans. Smart Grid*, vol. 3, no. 4, pp. 1790–1799, 2012.

[73] G. A. Weaver, K. Davis, C. M. Davis, E. J. Rogers, R. B. Bobba, S. Zonouz, R. Berthier, P. W. Sauer, and D. M. Nicol, "Cyber-physical models for power grid security analysis: 8-substation case," in *Smart Grid Communications (SmartGridComm), 2016 IEEE International Conference on*, pp. 140–146, IEEE, 2016.

[74] H. Huang and K. Davis, "Extracting substation cyber-physical architecture through intelligent electronic devices' data," in *Texas Power and Energy Conference (TPEC), 2018 IEEE*, pp. 1–6, IEEE, 2018.

[75] K. R. Davis, C. M. Davis, S. A. Zonouz, R. B. Bobba, R. Berthier, L. Garcia, and P. W. Sauer, "A cyber-physical modeling and assessment framework for power grid infrastructures," *IEEE Transactions on Smart Grid*, vol. 6, no. 5, pp. 2464–2475, 2015.

[76] K. Davis, R. Berthier, S. Zonouz, G. Weaver, R. Bobba, E. Rogers, P. Sauer, and D. Nicol, "Cyber-physical security assessment (cypsa) for electric power systems," *IEEE-HKN: The Bridge*, vol. 112, no. 2, pp. 8–19, 2016.

[77] M. Panteli, P. Mancarella, D. N. Trakas, E. Kyriakides, and N. D. Hatziargyriou, "Metrics and quantification of operational and infrastructure resilience in power systems," *IEEE Transactions on Power Systems*, vol. 32, no. 6, pp. 4732–4742, 2017.

[78] M. Panteli and P. Mancarella, "Influence of extreme weather and climate change on the resilience of power systems: Impacts and possible mitigation strategies," *Electric Power Systems Research*, vol. 127, pp. 259–270, 2015.

[79] W. Ellens, F. M. Spieksma, P. Van Mieghem, A. Jamakovic, and R. E. Kooij, "Effective graph resistance," *Linear Algebra Appl.*, vol. 435, no. 10, pp. 2491–2506, 2011.

[80] Y. Koç, M. Warnier, R. E. Kooij, and F. M. Brazier, "An entropy-based metric to quantify the robustness of power grids against cascading failures," *Safety science*, vol. 59, pp. 126–134, 2013.

[81] X. Zhang and K. T. Chi, "Assessment of robustness of power systems from a network perspective," *IEEE Journal on Emerging and Selected Topics in Circuits and Systems*, vol. 5, no. 3, pp. 456–464, 2015.

[82] H. Tu, Y. Xia, H. H.-C. Iu, and X. Chen, "Optimal robustness in power grids from a network science perspective," *IEEE Transactions on Circuits and Systems II: Express Briefs*, vol. 66, no. 1, pp. 126–130, 2019.

[83] A. Azzolin, L. Dueñas-Osorio, F. Cadini, and E. Zio, "Electrical and topological drivers of the cascading failure dynamics in power transmission networks," *Reliability Engineering & System Safety*, vol. 175, pp. 196–206, 2018.

[84] L. Mili, "Taxonomy of the characteristics of power system operating states," in *2nd NSF-VT Resilient and Sustainable Critical Infrastructures (RESIN) Workshop*, pp. 13–15, Jan 2011.

[85] M. Child, O. Koskinen, L. Linnanen, and C. Breyer, "Sustainability guardrails for energy scenarios of the global energy transition," *Renewable and Sustainable Energy Reviews*, vol. 91, no. April 2017, pp. 321–334, 2018.

[86] E. Santoyo-Castelazo and A. Azapagic, "Sustainability assessment of energy systems: integrating environmental, economic and social aspects," *Journal of Cleaner Production*, vol. 80, pp. 119–138, 2014.

[87] U.S. Department of Energy, "Transforming the nation's electricity system: The second installment of the quadrennial energy review," tech. rep., January 2017.

[88] J. Minkel, "The 2003 Northeast Blackout–Five Years Later," *Scientific American*, 2008.

[89] D. Henry and J. E. Ramirez-Marquez, "On the impacts of power outages during hurricane sandy: A resilience-based analysis," *Systems Engineering*, vol. 19, no. 1, pp. 59–75, 2016.

[90] P. Beiter, M. Elchinger, and T. Tian, "2016 renewable energy data book," tech. rep., National Renewable Energy Laboratory, 2017.

[91] B.-W. Yi, J.-H. Xu, and Y. Fan, "Inter-regional power grid planning up to 2030 in china considering renewable energy development and regional pollutant control: A multi-region bottom-up optimization model," *Applied Energy*, vol. 184, pp. 641–658, 2016.

[92] C. Schelly, E. P. Louie, and J. M. Pearce, "Examining interconnection and net metering policy for distributed generation in the united states," *Renewable Energy Focus*, vol. 22, pp. 10–19, 2017.

[93] J. Marsden, "Distributed generation systems: A new paradigm for sustainable energy," in *Green Technologies Conference (IEEE-Green), 2011 IEEE*, pp. 1–4, IEEE, 2011.

[94] S. Allesina and R. E. Ulanowicz, "Cycling in ecological networks: Finn's index revisited," *Computational Biology and Chemistry*, vol. 28, no. 3, pp. 227–233, 2004.

[95] S. R. Borrett and B. C. Patten, "Structure of pathways in ecological networks: Relationships between length and number," *Ecological Modelling*, vol. 170, no. 2-3, pp. 173–184, 2003.

[96] B. C. Patten, "On the quantitative dominance of indirect effects in ecosystems," in *Developments in Environmental Modelling*, vol. 5, pp. 27–37, Elsevier, 1983.

[97] B. C. Patten, "Energy cycling in the ecosystem," *Ecological Modelling*, vol. 28, no. 1-2, pp. 1–71, 1985.

[98] B. D. Fath and G. Halnes, "Cyclic energy pathways in ecological food webs," *Ecological Modelling*, vol. 208, no. 1, pp. 17–24, 2007.

[99] A. Layton, B. Bras, J. Reap, and M. Weissburg, "Biologically inspired closed loop manufacturing networks," in *Proceedings of the ASME 2013 International Mechanical Engineering Congress and Exposition*, pp. 1–10, 2013.

[100] E. P. Odum, "The strategy of Ecosystem development," *Science (80-.).*, vol. 164, pp. 262–270, 1969.

[101] R. E. Ulanowicz, "Identifying the structure of cycling in ecosystems," *Math. Biosci.*, vol. 65, no. 2, pp. 219–237, 1983.

[102] D. DeAngelis, P. Mulholland, A. Palumbo, A. Steinman, M. Huston, and J. Elwood, "Nutrient dynamics and food-web stability," *Annual Review of Ecology and Systematics*, vol. 20, no. 1, pp. 71–95, 1989.

[103] R. Herendeen, "Energy intensity, residence time, exergy, and ascendency in dynamic ecosystems," *Ecological Modelling*, vol. 48, no. 1-2, pp. 19–44, 1989.

[104] M. Loreau, "Material cycling and the stability of ecosystems," *The American Naturalist*, vol. 143, no. 3, pp. 508–513, 1994.

[105] R. Bailey, B. Bras, and J. K. Allen, "Applying ecological input-output flow analysis to material flows in industrial systems: Part ii: Flow metrics," *Journal of Industrial Ecology*, vol. 8, no. 1-2, pp. 69–91, 2004.

[106] G. Liu, Z. Yang, M. Su, and B. Chen, "The structure, evolution and sustainability of urban socio-economic system," *Ecological Informatics*, vol. 10, pp. 2–9, 2012.

[107] D. Baird, B. D. Fath, R. E. Ulanowicz, H. Asmus, and R. Asmus, "On the consequences of aggregation and balancing of networks on system properties derived from ecological network analysis," *Ecol. Modell.*, vol. 220, no. 23, pp. 3465–3471, 2009.

[108] M. B. Hesse, *Models and Analogies in Science*. University of Notredame Press, 2nd ed., 1970.

[109] P. E. Wells, "Re-writing the ecological metaphor: Part 1," *Prog. Ind. Ecol. An Int. J.*, vol. 3, no. 1/2, p. 114, 2006.

[110] J. Ehrenfeld, "Putting a Spotlight on Metaphors and Analogies in Industrial Ecology," *J. Ind. Ecol.*, vol. 7, no. 1, pp. 1–4, 2003.

[111] R. Husar, "Ecosystem and the biosphere: metaphors for human-induced material flows," in *Ind. Metab. Restruct. Sustain. Dev.* (R. U. Ayres and U. E. Simonis, eds.), pp. 21–29, United Nations Unviersity Press, 1994.

[112] M. R. Chertow, "Industrial Symbiosis : Literature and taxonomy," *Annu. Rev. Energy Environ.*, vol. 25, pp. 313–337, 2000.

[113] A. Layton, *Food webs: realizing biological inspirations for sustainable industrial resource networks*. PhD thesis, Georgia Institute of Technology, 2014.

[114] J. A. Dunne, R. J. Williams, and N. D. Martinez, "Food-web structure and network theory: The role of connectance and size," *PNAS*, vol. 99, no. 20, pp. 12917–12922, 2002.

[115] A. Layton, B. Bras, and M. Weissburg, "Designing Industrial Networks Using Ecological Food Web Metrics," *Environ. Sci. Technol.*, vol. 50, no. 20, pp. 11243–11252, 2016.

[116] C. Shannon, "A Mathematical Theory of Communication," *Bell Syst. Tech. J.*, vol. 27, no. April 1928, pp. 379–423, 1948.

[117] R. E. Ulanowicz and J. S. Norden, "Symmetrical overhead in flow networks," *International Journal of Systems Science*, vol. 21, no. 2, pp. 429–437, 1990.

[118] R. W. Rutledge, B. L. Basore, and R. J. Mulholland, "Ecological stability: An information theory viewpoint," *J. Theor. Biol.*, vol. 57, pp. 355–371, 1976.

[119] R. E. Ulanowicz, "An Hypothesis on the Development of Natural Communities," *J. theor. Biol*, vol. 85, pp. 223–245, 1980.

[120] R. E. Sonntag, C. C. Borgnakke, G. J. G. J. Van Wylen, and G. J. G. J. Van Wylen, *Fundamentals of Thermodynamics*. Wiley, 1998.

[121] A. Bodini, C. Bondavalli, and S. Allesina, "Cities as ecosystems: Growth, development and implications for sustainability," *Ecol. Modell.*, vol. 245, pp. 185–198, 2012.

[122] D. Baird and R. E. Ulanowicz, "The Seasonal Dynamics of The Chesapeake Bay Ecosystem," *Ecol. Monogr.*, vol. 59, no. 4, pp. 329–364, 1989.

[123] J. J. Heymans, R. E. Ulanowicz, and C. Bondavalli, "Network analysis of the South Florida Everglades graminoid marshes and comparison with nearby cypress ecosystems," tech. rep., 2002.

[124] R. E. Ulanowicz and L. G. Abarca-Arenas, "An informational synthesis of ecosystem structure and function," *Ecol. Modell.*, vol. 95, pp. 1–10, 1997.

[125] R. E. Ulanowicz, S. J. Goerner, B. Lietaer, and R. Gomez, "Quantifying sustainability: Resilience, efficiency and the return of information theory," *Ecol. Complex.*, vol. 6, no. 1, pp. 27–36, 2009.

[126] L. G. Latham and E. P. Scully, "Quantifying constraint to assess development in ecological networks," *Ecological Modelling*, vol. 154, no. 1-2, pp. 25–44, 2002.

[127] J. Duncan Glover, M. Sarma, and T. Overbye, *Power System Analysis and Design*. Cengage Learning, 5th ed., 2012.

[128] B. Stott, J. Jardim, and O. Alsaç, "Dc power flow revisited," *IEEE Transactions on Power Systems*, vol. 24, no. 3, pp. 1290–1300, 2009.

[129] A. Pandey, M. Jereminov, M. R. Wagner, D. M. Bromberg, G. Hug, and L. Pileggi, "Robust power flow and three-phase power flow analyses," *IEEE Transactions on Power Systems*, vol. 34, no. 1, pp. 616–626, 2019.

[130] MathWorks, "MATLAB 2017a," 2017.

[131] R. H. Byrd, M. E. Hribar, and J. Nocedal, "An Interior Point Algorithm for Large-Scale Nonlinear Programming," *SIAM J. Optim.*, vol. 9, no. 4, pp. 877–900, 2003.

[132] R. Adams and M. Laughton, "Optimal planning of power networks using mixed-integer programming. part 1: Static and time-phased network synthesis," in *Proceedings of the Institution of Electrical Engineers*, vol. 121, pp. 139–147, IET, 1974.

[133] R. Villasana, L. Garver, and S. Salon, "Transmission network planning using linear programming," *IEEE Transactions on Power Apparatus and Systems*, no. 2, pp. 349–356, 1985.

[134] G. Oliveira, A. Costa, and S. Binato, "Large scale transmission network planning using optimization and heuristic techniques," *IEEE Transactions on Power Systems*, vol. 10, no. 4, pp. 1828–1834, 1995.

[135] M. Rider, A. Garcia, and R. Romero, "Power system transmission network expansion planning using ac model," *IET Generation, Transmission & Distribution*, vol. 1, no. 5, pp. 731–742, 2007.

[136] A. K. Kazerooni and J. Mutale, "Transmission network planning under security and environmental constraints," *IEEE Transactions on Power Systems*, vol. 25, no. 2, pp. 1169–1178, 2010.

[137] R. Jabr, "Robust transmission network expansion planning with uncertain renewable generation and loads," *IEEE Transactions on Power Systems*, vol. 28, no. 4, pp. 4558–4567, 2013.

[138] A. J. Wood and B. F. Wollenberg, *Power generation, operation, and control*. John Wiley & Sons, 2012.

[139] NERC, *Transmission transfer capability: a reference document for calculating and reporting the electric power transfer capability of interconnected electric systems*. NERC, 1995.

[140] C. M. Davis and T. J. Overbye, "Multiple element contingency screening," *IEEE Transactions on Power Systems*, vol. 26, no. 3, pp. 1294–1301, 2011.

[141] K. S. Naik and M. Glickfeld, "Water Distribution System Efficiency: An Essential or Neglected Part of the Water Conservation Strategy for Los Angeles County Water Retailers?," Tech. Rep. November, 2015.

[142] T. AL-Washali, S. Sharma, and M. Kennedy, "Methods of Assessment of Water Losses in Water Supply Systems: a Review," *Water Resour. Manag.*, vol. 30, no. 14, pp. 4985–5001, 2016.

[143] N. Samir, R. Kansoh, W. Elbarki, and A. Fleifle, "Pressure control for minimizing leakage in water distribution systems," *Alexandria Eng. J.*, vol. 56, pp. 601–612, dec 2017.

[144] Worldbank, "Electric power transmission and distribution losses," 2014.

[145] N. B. Jacobsen, "Industrial symbiosis in Kalundborg, Denmark," *J. Ind. Ecol.*, vol. 10, no. 1-2, pp. 239–255, 2006.

[146] A. B. Birchfield, T. J. Overbye, and K. R. Davis, "Educational Applications of Large Synthetic Power Grids," *IEEE Trans. Power Syst.*, vol. 34, no. c, pp. 765–772, 2019.

[147] A. Layton, B. Bras, and M. Weissburg, "Ecological Principles and Metrics for Improving Material Cycling Structures in Manufacturing Networks," *J. Manuf. Sci. Eng.*, vol. 138, no. 10, 2016.

[148] J. D. Glover, M. S. Sarma, and T. Overbye, *Power System Analysis & Design, SI Version*. Cengage Learning, 2012.

[149] S. Jain and S. Krishna, "Emergence and growth of complex networks in adaptive systems," *Computer Physics Communications*, vol. 121, pp. 116–121, 1999.

[150] S. R. Borrett, B. D. Fath, and B. C. Patten, "Functional integration of ecological networks through pathway proliferation," *Journal of Theoretical Biology*, vol. 245, no. 1, pp. 98–111, 2007.

[151] J. T. Finn, "Measures of ecosystem structure and function derived from analysis of flows," *Journal of Theoretical Biology*, vol. 56, no. 2, pp. 363–380, 1976.

[152] M. K. Lau, D. E. Hines, P. Singh, and S. R. Borrett, "enaR: Ecological Network Analysis with R," 2017.

[153] G. Simbolotti and R. Kempener, "Electricity Storage: Technology Brief," tech. rep., 2012.

[154] D. Lindley, "Smart grids: The energy storage problem," *Nature News*, vol. 463, no. 7277, pp. 18–20, 2010.